2014

Atmospheric Mercury Species In Northern Mississippi: Concentrations, Sources, Temporal Patterns, And Soil-Air Exchange

Yi Jiang
University of Mississippi

ATMOSPHERIC MERCURY SPECIES IN NORTHERN MISSISSIPPI:

CONCENTRATIONS, SOURCES, TEMPORAL PATTERNS, AND SOIL-AIR EXCHANGE

A Dissertation
presented in partial fulfillment of the requirements
for the degree of Doctor of Philosophy
in the Department of Chemistry & Biochemistry
The University of Mississippi

by

YI JIANG

August 2014

ABSTRACT

Mercury is a highly toxic element that is found both naturally and as an introduced contaminant in the environment. The majority of mercury released to the environment is into the atmosphere, where because of its high volatility and long residence time is dispersed globally. In order to better understand the factors controlling the distribution and temporal patterns of atmospheric mercury species, as well as the sources of airborne mercury in the mid-south region, concentrations of gaseous elemental mercury (GEM), gaseous oxidized mercury (GOM), and particulate-bound mercury (PBM), along with meteorological parameters and other ancillary data, were collected for more than a year in Oxford Mississippi. Mean levels of GEM were 1.54 ± 0.32 $ng \cdot m^{-3}$ and were lower and more stable in the winter and spring compared with summer and fall. Mean levels for GOM and PBM were 3.87 $ng \cdot m^{-3}$ and 4.58 $ng \cdot m^{-3}$, respectively; levels tended to be highest in the afternoon and lowest in the early morning hours. Precipitation events greatly reduce GOM and PBM levels but have little effect on GEM. GOM exhibited diurnal patterns characteristic of photochemical oxidation. Atmospheric modeling revealed that higher levels of plume events for airborne Hg often occur with air masses from the northern USA.

Gaseous mercury exchange between terrestrial surfaces and the atmosphere was also investigated. Mercury fluxes over four landscapes representative of north Mississippi were studied. Mercury emissions were higher during the summer than the winter. The influence of environmental variables, including temperature, solar radiation, humidity, wind speed, soil

moisture, and pressure, on mercury fluxes and ambient levels of atmospheric mercury were evaluated.

Analytical methods were also developed to measure wet and dry deposition of mercury, and estimates were made for deposition to Enid Lake and the Yocona River watershed. The data was incorporated into a mercury mass-balance model for Enid Lake, which currently has a mercury-based fish consumption advisory. Finally GEM concentrations were determined within an academic chemistry building and levels were compared to occupational safety permissible and recommended exposure limits.

LIST OF ABBREVIATIONS AND SYMBOLS

GEM	Gaseous Elemental Mercury
GOM	Gaseous Oxidized Mercury
PBM	Particulate-Bound Mercury
PCA	Principal Component Analysis
DMM	Dimethyl Mercury
CFPPs	Coal-Fired Power Plants
USEPA	United States Environmental Protection Agency
Model 2537A/B	GEM Analyzer
Model 1130	GOM Collecting Module
Model 1135	PBM Collecting Module
CVAFS	Cold Vapor Atomic Fluorescence Spectrometry
RPF	Regenerable Particulate Filter
EMEP	European Monitoring and Evaluation Programme
NOAA	National Oceanic and Atmospheric Administration
HYSPLIT	Hybrid Single-Particle Lagrangian Integrated Trajectory
CMAQ	Community Multiscale Air Quality Modeling System
CAM	Chemistry of Atmospheric Mercury
MCM	Mercury Chemistry Model
ADOM	Acid Deposition and Oxidants Model

MSCE-HM	MSC-E Heavy Metal
GRAHM	Global/Regional Atmospheric Heavy Metals Model
EMAP	Eulerian Model for Air Pollution
DEHM	Danish Eulerian Hemispheric Model
MSCE-HM-Hem	MSC-E Heavy Metal Hemispheric Model
SD	Standard Deviation
EDAS	Eta Data Assimilation System
SMOKE	Sparse Matrix Operator Kernel Emissions Model
WRF	Weather Research and Forecast Model
RRTM	Rapid Radiation Transfer Model
PBL	Planetary Boundary Layer
RMSE	Root-Mean-Squared Error
ANB	Average Normalized Bias
UPA	Unpaired Peak Accuracy
WDD	Wind Direction Degree
TGM	Total Gaseous Mercury
LOI	Loss-On-Ignition
DFC	Dynamic Flux Chamber
Tekran 1110	Tekran Automated Dual Switching Unit
Tekran 2505	Mercury Vapor Calibration Unit

Vaisala WXT 520	Automatic Weather Station
THg	Total Mercury
MDN	Mercury Deposition Network
NADP	National Atmospheric Deposition Program
REMAP	Regional Environmental Monitoring and Assessment Program
DMA	Direct Mercury Analyzer
AAS	Atomic Absorption Spectrometry
CRC	Chemical Rubber Company
OSHA	Occupational Safety & Health Administration
NIOSH	National Institute for Occupational Safety and Health
ACGIH	American Conference of Governmental Industrial Hygienists
ATSDR	Agency for Toxic Substances and Disease Registry

ACKNOWLEDGMENTS

It would not have been possible to write this doctoral dissertation without the help and support of the kind people around me. Above all, I would like to express the deepest appreciation to my research advisor, Dr. James V. Cizdziel, who has the attitude and the substance of a true professional. His wisdom, knowledge, and commitment to the highest standards inspired and motivated me. Without his guidance, support, and persistent help this dissertation would not have been possible. I also would like to thank Cizdziel group members: Pragya Chakravarty, Lorlyn Reidy, Garry Brown, Ryan Bu, Derek Bussan, Divya Nallamothu, Jingjing Chen and all undergraduate research students who worked with me in the past few years for their kindness, friendship and support.

I thank our research collaborator Dr. Lu (Jackson State University) for his contribution in mercury modelling. I thank Mae Gustin from University of Nevada, Reno and Anthony Carpi from City University of New York for providing dynamic flux chambers. I thank Lucas Hawkins and Eric Prestbo (Tekran® Corp.) for instrumentation training and troubleshooting. I also thank Southern Company for offering a spare mercury analyzer and Zhen Guo from Geology Department of University of Mississippi for his help in meteorological variables measurement. I am also grateful to my committee members: Dr. Steven Davis, Dr. Jason Ritchie, Dr. Randy Wadkins, and Dr. Qingying Bu for their encouraging words, thoughtful criticism, and attention during busy semesters.

I would like to thank my family and friends for their love, support and understanding during the long years of my education.

I also would like to acknowledge the financial, academic and technical support from USEPA, The University of Mississippi Graduate Student Council, and Department of Chemistry and Biochemistry.

TABLE OF CONTENTS

LIST OF TABLES

LIST OF FIGURES

INTRODUCTION AND ORGANIZATION OF THE DISSERTATION

Mercury is a persistent and widespread toxic environmental pollutant that is dispersed globally through atmospheric pathways. Airborne mercury comes from both natural and anthropogenic sources, and emissions appear to be leading to a general increase in mercury on local, regional and global scales. The atmosphere serves as an important route for mercury transfer into- and out of- aquatic ecosystems. Mercury deposits to terrestrial and aquatic systems through wet and dry mechanisms where it can undergo biotic and abiotic transformation to mono-methyl-mercury, which in-turn readily bioaccumulates and concentrates in food webs. Humans are exposed to methylmercury primarily through consumption of seafood. Methylmercury is a neuro- and cardiovascular- toxin, and exposure in-utero has been linked to subtle developmental deficits such as decreased performance in tests of language skills and memory function, and attention deficits.

Unfortunately, mercury is increasing in the atmosphere despite emission controls, primarily implemented in the western world. Recognizing that the problem requires a global effort, 92 nations, including the U.S., signed the Minamata Convention on Mercury in 2013, which is a legally-binding treaty aimed at reducing mercury pollution. Key to implementation of the treaty is monitoring, modeling, and scientific interpretation of airborne mercury. Together, this has motivated intensive research on mercury as a pollutant. Yet, there remains much that is not fully understood about the sources, distribution, cycling, and transformation of airborne mercury species.

The dissertation focuses on atmospheric mercury in northern Mississippi. It is believed to be the first study of atmospheric mercury species in the mid-south United States. Several projects were undertaken. The motivation, objectives, and results are best described in separate chapters, three of which were published in *Chemosphere*, *Air Quality, Atmosphere and Health*

and *Bulletin of Environmental Contamination and Toxicology*, and another is being prepared for submission. Each project used mercury instrumentation based on cold vapor atomic fluorescence, and each required different degrees of method development.

The first chapter provides background information on atmospheric mercury. Mercury has one of the most complex biogeochemical cycles of the elements and the atmosphere plays a critical role. This chapter also introduces the theory and fundamentals of the instruments and techniques used throughout this work. The remaining five chapters have their own abstract, introduction, objectives, materials and methods, results and discussion, and conclusion sections.

In chapter two, atmospheric mercury species, including gaseous elemental mercury (GEM), gaseous oxidized mercury (GOM), and particle-bound mercury (PBM) were measured on the University of Mississippi campus for more than a year. Temporal patterns were studied including the effect of meteorological conditions and relatively large swings in population. Atmospheric modeling was conducted to investigate potential sources of the mercury.

Chapter three is a study which examined the characteristics of Hg gas exchange over several different soils in the mid-south region, including a forest floor, and soils from agricultural and wetland areas. Unlike mercury point sources, which have been studied extensively, emissions from natural non-point are relatively uncertain. Data is critically needed for global models.

Chapter four involves measurement of mercury deposition to the region. The primary purpose was to estimate wet and dry deposition to Enid Lake, which has relatively high levels of mercury and a fish consumption advisory. The data feeds into an ongoing mercury mass-balance study of the reservoir and tests a hypothesis that levels are higher in precipitation from convective thunderstorms. Total-Hg was determined in rain water during eight separate months.

For dry deposition, direct measurement was carried out using a modified version of the surrogate surface method, and modeling of atmospheric mercury species measurements.

Lastly, chapter five brings our study indoors. For decades elemental mercury has been widely used in academic chemistry laboratories for a variety of purposes, most notably barometers, thermometers, electrical switches, and atomic line lamps. Here GEM concentrations were determined within an academic chemistry building by cold vapor atomic fluorescence spectrometry under different use scenarios.

MOTIVATION, RATIONALE AND PRIOR WORK

MOTIVATION AND RESEARCH QUESTIONS

Motivation

Mercury (Hg) is a widespread and persistent pollutant that poses a serious risk to humans and wildlife. The element has a complex biogeochemical cycle in which the atmosphere plays a critical role. It is deposited to terrestrial and aquatic ecosystems through wet and dry deposition mechanisms where inorganic mercury (Hg^{+2}) can be transformed to methylmercury by microorganisms. Methylmercury is a known human neurotoxin that can bioacculmulate in fish tissue and biomagnify up aquatic food chains. Consumption of contaminated fish is the primary route of human exposure to methylmercury.

The research described in this dissertation is focused on determining the distribution and cycling of atmospheric mercury species in the mid-south United States. **So why conduct this work?** To answer specific research questions, several of which are highlighted below along with the rationale for asking them in the first place; further details and background these research problems are given in the individual project chapters that follow. Whereas it is not the only reason for this work, it is emphasized that there has been little to no study of mercury in the region despite the presence of a number of large anthropogenic sources (e.g. coal-fired power plants) and conditions that favor methylation of mercury (e.g. numerous wetlands with anoxic sediments).

Research Questions

What is the atmospheric contribution of mercury to Enid Lake? Finding the answer to this question is what drove our initial research and is why we measured atmospheric mercury species in north Mississippi. To improve our understanding of mercury distribution and cycling in mercury-impaired water bodies, Dr. Cizdziel's research group has been developing a mass-balance for mercury in Enid Lake (Figure 1). The present work feeds into that mass-balance

model by estimating wet and dry deposition rates to both the lake and the Yocona River watershed. Enid Lake is a large (~surface area of 6,100 acres) reservoir in northern Mississippi which is routinely used by recreational and sustenance fishers despite their being a fish consumption advisory due to high levels of mercury in fish tissue. The lake is typical of many reservoirs in the region in that the source of the high levels of mercury is unknown. Identifying the fate and transport of Hg in water bodies is critical to improving water quality and ecosystem health (Fulkerson and Nnadi. 2006).

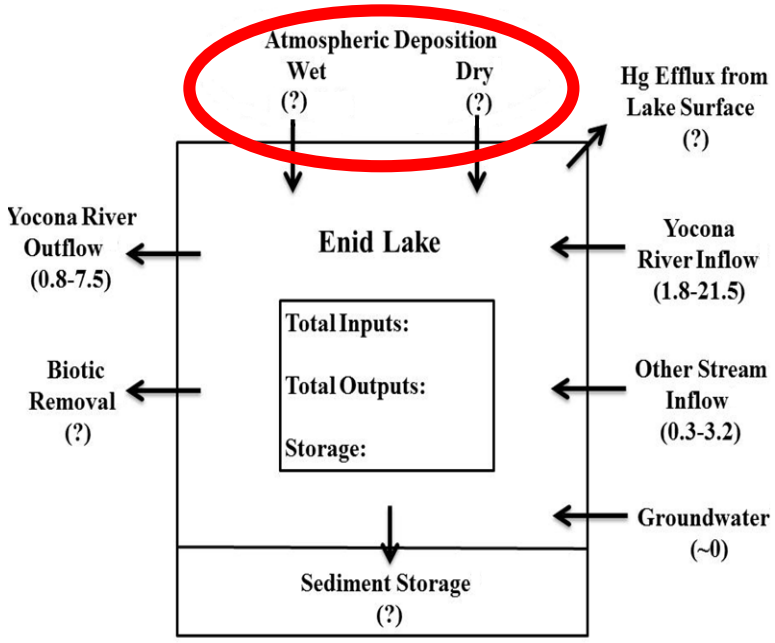

Figure 1. Estimated Hg mass balance (kg/yr) for Enid Lake. Atmospheric deposition was addressed in the current study

A summary of prior work and relevant background on mercury deposition to lakes.

The atmosphere is often the most significant source of Hg to lakes and other water bodies (Sprovieri et al. 2010). As noted mercury enters aquatic and terrestrial ecosystems through wet and dry deposition. Based on model predictions and depending on location, the dry deposition can be from 0.25 to 3 times the rate of wet deposition (Lin et al. 2006). Previous work has

concluded that if the concentrations of GOM and PBM are higher than 100 pg/m^3, they contribute the most to the deposition of mercury. If the air contains less than that, wet deposition will dominate. In forested areas, dry deposition is more important than wet deposition (Cohen et al. 2004).

Estimating wet and dry deposition to Enid Lake is the subject of Chapter 5. Briefly, wet deposition is relatively straightforward and requires collecting and analyzing multiple precipitation events. Compared with wet deposition, currently there is no standard method for determining dry deposition of mercury. While all operationally defined forms of atmospheric mercury (elemental, oxidized, and particulate) can be dry deposited, oxidized forms are of particular concern due to high deposition velocities, water solubility, and reactivity (Lyman et al. 2009). Direct measurements of dry deposition of mercury have only been developed in the past few years, and include the use of a surrogate surface for characterizing potential dry deposition of GOM. Another approach to measuring dry deposition is to quantify airborne mercury species and apply deposition velocities from the literature (Zhang et al. 2012). In the present work we used both approaches to get our deposition values.

Are mercury levels higher in convective thunderstorms compared to other precipitation events? Nair et al. (2013) suggests that thunderstorms increase mercury deposition because they reach higher levels in the atmosphere and can scavenge gaseous oxidized mercury that accumulates in the upper troposphere**.** Others have shown that the wet deposition of mercury is high in the southeast US (Figure 2). Although the data shown is for a single year (2009), the pattern is relatively consistent year after year. Our work estimating wet deposition to Enid Lake offers an opportunity to test that hypothesis. In the present work we

collected and analyzed rain for mercury over the course of nearly a year, including thunderstorm and non-thunderstorm events. Results are presented in Chapter 4.

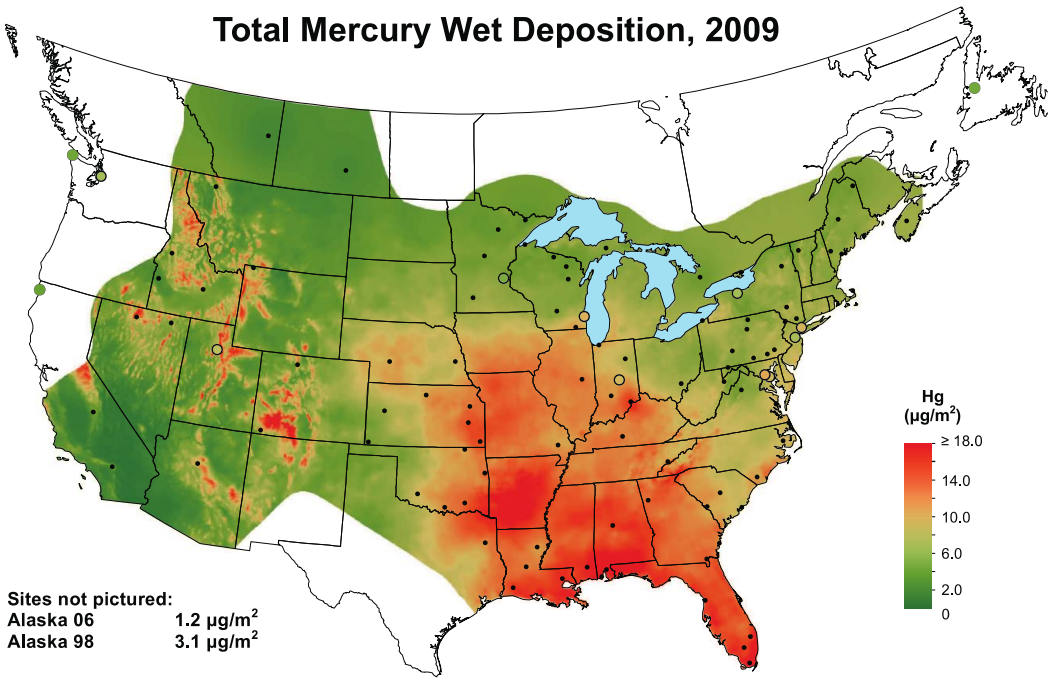

Figure 2. Mercury wet deposition map for USA, 2009 (NADP), the high levels of deposition in the southeast US is discussed in detail in Chapter 4

What is novel about our dry deposition measurements? We devised a new scheme to measure dry deposition of atmospheric mercury using a surrogate surface (cation exchange membrane) for capturing airborne GOM and a thermal decomposition atomic absorption spectrometer for measuring the adsorbed mercury. Details and background are given in Chapter 4.

So why measure atmospheric mercury species mercury in north Mississippi? In order to determine dry deposition rates for the Enid Lake model. However, there are more reasons. Currently it is difficult to evaluate atmospheric mercury trends due to the lack of continuous and complete mercury speciation data sets. Regional differences, temporal trends, and potential sources can only be determined by monitoring. Thus, in addition to estimating atmospheric mercury deposition to the region, our published data can be used by others in

atmospheric mercury models. *Moreover, since we are measuring atmospheric mercury species, and since there is no information on atmospheric mercury in the region, it was of great interest to examine temporal trends and conduct atmospheric modelling to study possible sources and the atmospheric chemistry of airborne mercury species for the mid-south region.* To that end, GEM, GOM, and PBM were monitored for about a year. A few of the specific research questions that were addressed in this part of the work follow.

What is the influence of sudden population swings on the levels of airborne mercury species? *This is the first time that this question has been addressed with empirical data and it has resulted in a publication.* In addition, we evaluated the impact of meteorological variables airborne mercury, weekly and seasonal trends, and studied the potential sources of mercury in the region using atmospheric modelling. Details are provided in Chapter 2.

Why study Hg soil-air exchange in Mississippi soils?

We used a dynamic flux chamber to examine mercury fluxes from soils and evaluate the factors that impact evasion and deposition of mercury. Why? To fully understand the global biogeochemical cycling of Hg it is necessary to investigate Hg exchange between terrestrial surfaces and the atmosphere. First a little background. Prior research shows that the magnitude of Hg emissions from natural sources and anthropogenic sources are similar (Pirrone et al. 2010). Among natural sources, soils have been implicated as major contributor of mercury to the atmosphere (Kim et al. 1995). Mercury can be deposited to- and emitted from- terrestrial surfaces (Zhang et al. 2012; Gustin. 2003). Evasion of Hg from soils appears to be driven by multiple factors, such as solar radiation, soil temperature, soil moisture content, and wind speed (Poissant et al. 1998; Ericksen et al. 2006). Emissions from soils typically exhibit daily variability and can be quite high in areas of enriched substrates (Gustin et al. 2003).

Soils have large surface areas and agricultural fields which routinely turn-over soils may be introducing a relatively greater quantity of mercury to the global atmospheric budget. However, there are few measurements from soils in the mid-south US where agriculture is intensive. In the present work, we investigated, for the first-time, mercury emissions from soils from the mid-south region.

What soils were chosen for analysis and why? Soils from major ecoregions were selected including the Mississippi Alluvial Plain (representative agricultural soils from the Mississippi Delta), Southeastern Coastal Plain (both forested and agricultural areas). In addition, wetland sediment was selected because it is considered a hot-spot for mercury methylation. Further details and results are presented in Chapter 3.

LIST OF REFERENCES

Cohen, M., Artz, R., Draxler, R., Miller, P., Poissant, L., Niemi, D., Ratte, D., Deslauriers, M., Duval, R., Laurin, R., Slotnick, J., Nettesheim, T., and McDonald, J., **2004**. Modeling the atmospheric transport and deposition of mercury to the Great Lakes, *Environ. Res*. 95, 247–265.

Ericksen, A. J., Gustin, M. S., Xin, M., Weisberg, J. P., Fernandez, G. C. J., **2006**. Air-soil exchange of mercury from background soils in the United States. *Sci. Total Environ*. 366, 851-863.

Fulkerson, M., and Nnadi, F. N., **2006**. Predicting mercury wet deposition in Florida--A simple approach. *Atmos. Environ*. 40, 3962-3968.

Gustin, M. S., **2003**. Are mercury emissions from geologic sources significant? A status report. *Sci. Total Environ*. 304, 153-167.

Kim, K. H., Lindberg, S. E., Meyers, T. P., **1995**. Micrometeorological measurements of mercury vapor fluxes over background forest soils in eastern Tennessee. *Atmos. Environ*. 29, 267-282.

Lin, C., Pongprueksa, P., Lindberg, E. S., Pehkonen, O. S., Byun, D., Jang, C., **2006**. Scientific uncertainties in atmospheric mercury models 1: Model science evaluation. *Atmos. Environ.* 40(16), 2911-2928.

Lyman, S. N., Gustin, M. S., Prestbo, E. M., Kilner, P. I., Edgerton, E., Hartsell, B., **2009**. Testing and Application of Surrogate Surfaces for Understanding Potential Gaseous Oxidized Mercury Dry Deposition. *Environ. Sci. & Technol*. 43, 6235-6241.

Nair, S. U., Wu, Y., Holmes, D. C., Schure, A., Kallos, G., Walters, T. J., **2013**. Cloud-resolving simulations of mercury scavenging and deposition in thunderstorms. *Atmos. Chem. Phys. Discuss.* 13, 3575-3611.

Pirrone, N., Cinnirella, S., Feng, X., Finkelman, R. B., Friedli, H. R., Leaner, J., Mason, R., Mukherjee, A. B., Stracher, G. B., Streets, D. G., and Telmer, K., **2010**. Global mercury emissions to the atmosphere from anthropogenic and natural sources, *Atmos. Chem. Phys.* 10, 5951–5964.

Poissant, L., Casimir, A., **1998**. Water–air and soil–air exchange rate of total gaseous mercury measured at background sites. *Atmos. Environ*. 32, 883–893.

Sprovieri, F., Pirrone, N., Ebinghaus, R., Kock, H., Dommergue, A., **2010**. A review of worldwide atmospheric mercury measurements. *Atmos. Chem. Phys*. 10, 8245-8265.

Zhang, L., Blanchard, P., Johnson, D., Dastoor, A., Ryzhkov, A., Lin, J. C., Vijay, K., Gay, D., Holsen, M. T., Huang, J., Graydon, A. J., St. Louis, L. V., Castro, S. M., Miller, K. E., Marsik, F., Lu, J., Poissant, L., Pilote, M., Zhang, M. K., **2012**. Assessment of modeled mercury dry deposition over the Great Lakes region. *Environ. Pollut.* 161, 272-283.

CHAPTER ONE

1. FUNDAMENTALS OF ATMOSPHERIC MERCURY

1.1 MERCURY SPECIES IN THE ATMOSPHERE

1.1.1 The importance of determining speciation of atmospheric mercury

Mercury has three oxidation states: 0, +1 and +2. The "elemental" form (oxidation state 0) and the oxidized form (oxidation state +2) are the predominant forms in the atmosphere. Airborne mercury species are generally classified into three primary forms (species): gaseous elemental mercury (GEM), gaseous oxidized mercury (GOM), and particulate-bound mercury (PBM). GEM is the predominant form of atmospheric mercury and only slowly converts to GOM through photochemical reactions. It is also relatively inert and thus has a long residence time (estimated at 6-12 months) in the atmosphere, allowing it to circulate globally. The other two forms (GOM and PBM) have significantly higher surface reactivity with atmospheric particles/aerosols and have greater water solubility. Thus they have much shorter residence times (hours to months) in the atmosphere, being removed through wet and dry deposition mechanisms. The current global "background" (far-removed from point sources) level of atmospheric mercury is considered to be around 1.6 $ng \cdot m^{-3}$ in the Northern Hemisphere and 1.2 $ng \cdot m^{-3}$ in the Southern Hemisphere (Lindberg et al. 2007). Selected physical and chemical properties of some environmentally relevant mercury species are summarized in Table 1 (Schroeder et al. 1998).

Table 1. Physical/chemical properties of mercury and some of its compounds

Property	Hg^0	$HgCl_2$	HgO	HgS	CH_3HgCl	$(CH_3)_2Hg$
Melting Point (°C)	-39	277	decomp. @ +500°C	584 (sublim.)	167 (sublim.)	------
Boiling Point (°C)	357 @1 atm	303 @ 1 atm	------	------	------	96 @ 1 atm
Vapor Pressure (Pa)	0.180 @ 20°C	$8.99*10^{-3}$ @ 20°C	$9.20*10^{-12}$ @ 25°C	------	1.76 @ 25°C	$8.30*10^{3}$ @ 25°C
Water Solubility (g/l)	$49.4*10^{-6}$ @ 20°C	66 @ 20°C	$5.3*10^{-2}$ @ 25°C	~ 2*10-24	~ 5-6 @ 25°C	2.95 @ 24°C
Henry's law coefficient in water ($Pa \cdot m^{-3} \cdot mol^{-1}$)	729 @ 20°C	$3.69*10^{-5}$ @ 20°C	$3.76*10^{-11}$ @ 25°C	------	$1.6*10^{-5}$ @ 15°C and pH=5.2	646 @ 25°C

Before the 1980s, researchers didn't pay much attention to either physical or chemical speciation of the mercury emissions. Later it became known that, because of their significant different atmospheric behavior, GEM, GOM and PBM must be considered in emission inventories. An example highlighting the importance of atmospheric Hg speciation is occurred in the early 1990's in the Florida Everglades. The Everglades were severely contaminated by mercury, with top predators dying of mercury poisoning. However, years of sampling "total mercury" did not reveal causes of problem. Measurements of GOM (using a prototype of the 1130 instrument which was used in our study) confirmed that virtually all mercury deposition in the Florida Everglades was due to GOM from nearby sources (primarily waste incinerators) (Dvonch et al. 1998). Subsequently, GOM emission controls were placed on Florida sources. Follow-up studies have produced convincing evidence that controls on emissions from waste incinerators, combined with a reduction in the use of mercury in household items, have resulted in a sharp decline of mercury levels in the Everglades (Atkeson et al. 2005).

In another example, Peterson et al (1995) demonstrated the importance of mercury speciation on mercury transport and deposition in a modeling study. In the study, two areas were selected and modeled for the atmospheric deposition of mercury. The model was run using two different emission scenarios: 1) with all emissions as GEM, and 2) with a given fraction of the emissions in the form of GOM. The total emissions of mercury were the same in both cases. The local and regional deposition was increased by more than a factor of 2 in the scenario with GOM emissions corresponding to 10-60% of the total mercury emitted, indicating the importance of mercury speciation on local and regional deposition.

More recently, atmospheric mercury species have been shown to play a vital role in identifying the sources of mercury emissions elsewhere. Multivariate statistical receptor models,

such as principal component analysis (PCA), have been successfully used to apportion the sources of Hg deposited in South Florida (Dvonch et al. 1999) and the sources of other chemical compounds elsewhere (Anderson et al. 2002). Air mass transport to sampling sites is considered by using the hybrid single-particle lagrangian integrated trajectory (HYSPLIT) (Draxler et al. 1997); back-trajectories are calculated using input data from the National Weather Service.

Swartzendruber et al (2006) observed GOM in the free troposphere at the Mt. Bachelor Observatory using Tekran system and found that high concentrations of GOM are present in the free troposphere because of in situ oxidation of GEM to GOM (Figure. 3)

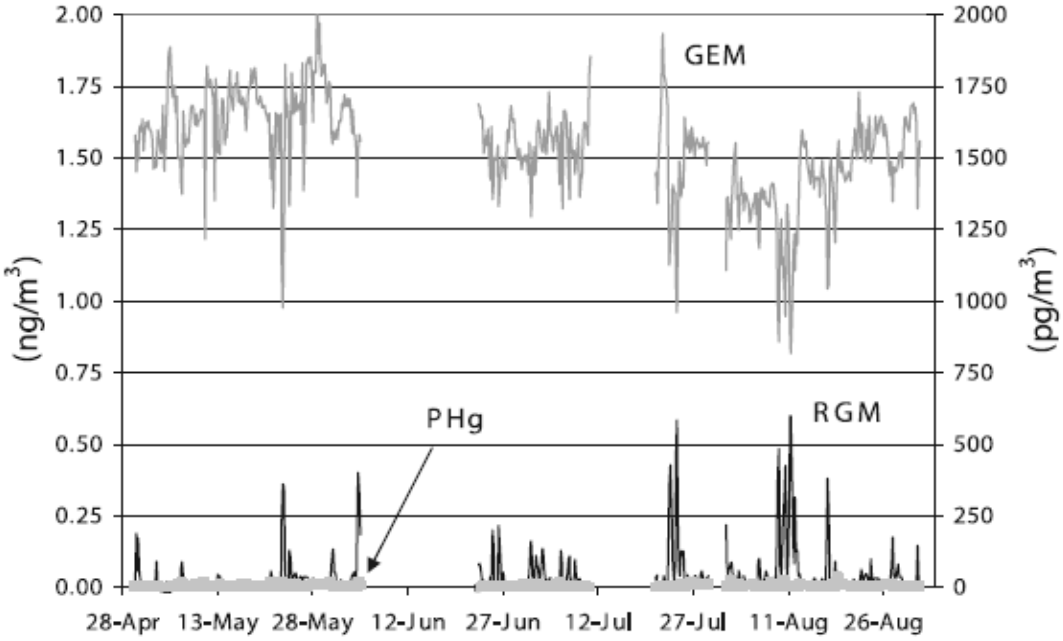

Figure 3. Time series of GEM, GOM (RGM), and PBM (PHg) from 30 April to 30 August 2005 at the Mt. Bachelor Observatory

1.2 MERCURY SOURCES AND EMISSIONS

To determine the spatial and long-term temporal variability of atmospheric mercury concentrations and deposition fluxes, it is important to understand the global or regional Hg emission sources and the chemical and physical processes in the atmosphere. Recent study suggest that mercury emissions from anthropogenic sources and natural sources have been estimated at 5207 ton/year and 2320 ton/year, respectively (Pirrone et al. 2010).

1.2.1 Mercury emissions from natural sources

The mercury emissions from natural sources include (wildfires, volcanoes, and geothermal sources) and re-emission processes of historically deposited mercury over land, vegetation, and water surfaces. Mason et al (2009) estimated mercury emissions from volcanoes and geothermal activities at about 90 Mg/year, which accounts for about 2% of the total contribution from natural sources. The emissions from volcanoes varies whether they are in a degassing or eruption phase, and Hg/SO_2 mass ratios have been used to estimate emissions worldwide (Nriagu and Becker. 2003; Pyle and Mather. 2003).

Evasion from water bodies, land, and vegetation accounts for a large portion of natural sources (Pirrone et al. 2010). Mercury evasion from the surface of natural water bodies was estimated at 2778 Mg/year, which would account for about 37% of net gaseous mercury evasion to the atmosphere (Mason et al. 2009). Generally the evasion of mercury from fresh water bodies is higher than that observed over the oceans (Mason et al. 2009). Mercury fluxes from soils and vegetation are vary depending on top soil concentrations, meteorological conditions, type of vegetation, and historical atmospheric deposition to the region (Pirrone et al. 2010). By summing up all the net emissions from the soils and vegetation, the total net global mercury evasion is

estimated at 1464 Mg/year (Mason et al. 2009). Global mercury emissions by natural sources is summarized in Table 2.

Table 2. Global mercury emissions by natural sources in 2008 (Pirrone et al. 2010)

Source	Mercury ($Mg\ yr^{-1}$)	Contribution (%)
Oceans	2682	52
Lakes	96	2
Forests	342	7
Tundra/Grassland/Savannah/ Prairie/Chaparral	448	9
Desert/Metalliferous/Non-vegetated Zones	546	10
Agricultural areas	128	2
Evasion after mercury depletion events	200	4
Biomass burning	675	13
Volcanoes and geothermal areas	90	2
TOTAL	5207	100

Hg^0 vapor is the primary species released from natural sources, although other volatile inorganic Hg compounds, such as dimethyl mercury (DMM), may also be emitted (Nelson et al. 2009). If DMM is released into the atmosphere, it is expected to be rather short-lived due to rapid oxidation by ubiquitous hydroxyl radials. Mercury bound to particulate matter may also originate from some types of natural sources or processes.

1.2.2 Mercury emissions from anthropogenic sources

Before the 1970's, chlor-alkali plants were considered to be the single largest source category of anthropogenic Hg emissions to the environment in many industrialized countries. Since then, changes in the mix of fossil fuels used to generate power and heat for industrial, commercial and residential use has substantially changed the ranking among the remaining source categories. Currently the major source categories include coal combustion, waste

incineration, medical and industrial wastes as well as metal smelting, refining and manufacturing facilities (Pirrone et al. 2010).

In the U.S., coal-fired power plants (CFPPs) are the largest unregulated source of mercury emissions and are responsible for approximately 45 percent of the country's industrial emissions (Figure 4). This is in part because other large domestic sources of mercury emissions are already subject to federal and more stringent state regulations. Coal is mined in about 27 states in the USA. However, more than 90% of US coal reserve is contained within 10 states: Montana, Illinois, Wyoming, West Virginia, Kentucky, Pennsylvania, Ohio, Colorado, Texas, and Indiana. Maps showing the distribution of coal-fired power plants and associated Hg emissions is given in Figures 5 and 6, respectively.

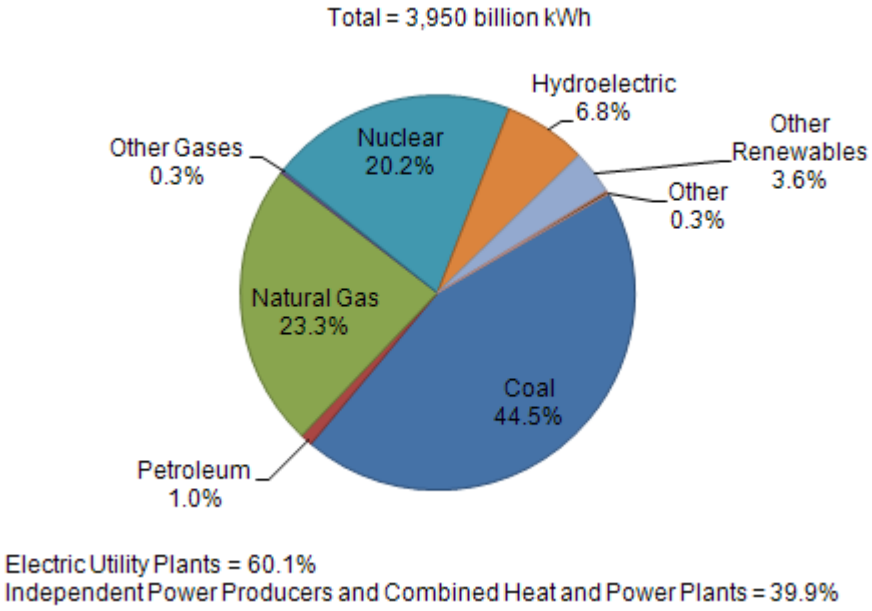

Figure 4. U.S. Electric Power Industry Net Generation, 2009 (U.S. Energy Information Administration. 2009)

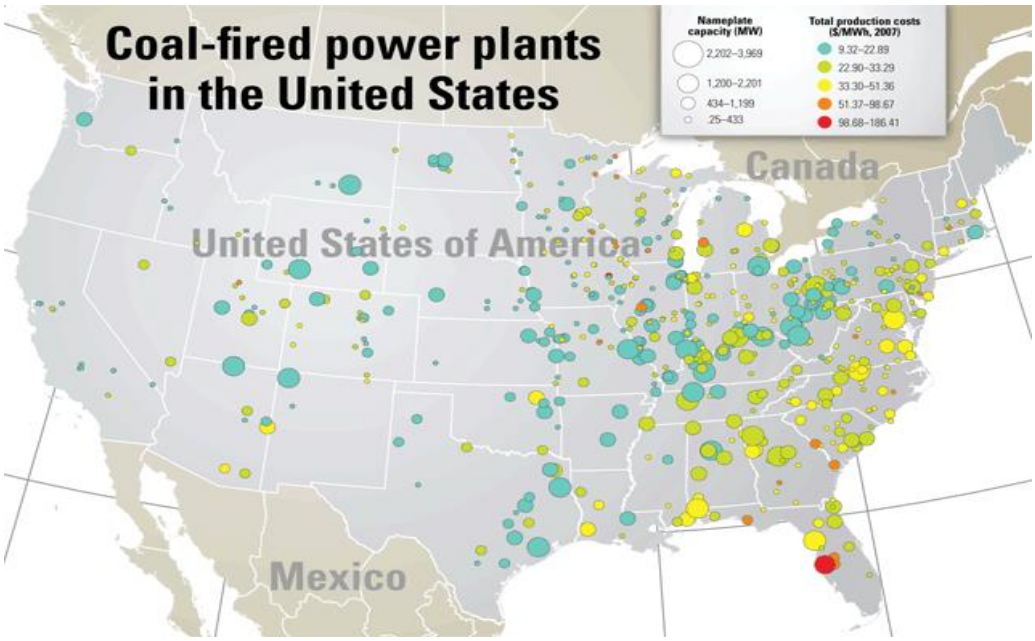

Figure 5. The distribution of CFPPs in USA. (United State Environmental Protection Agency (USEPA). 2007)

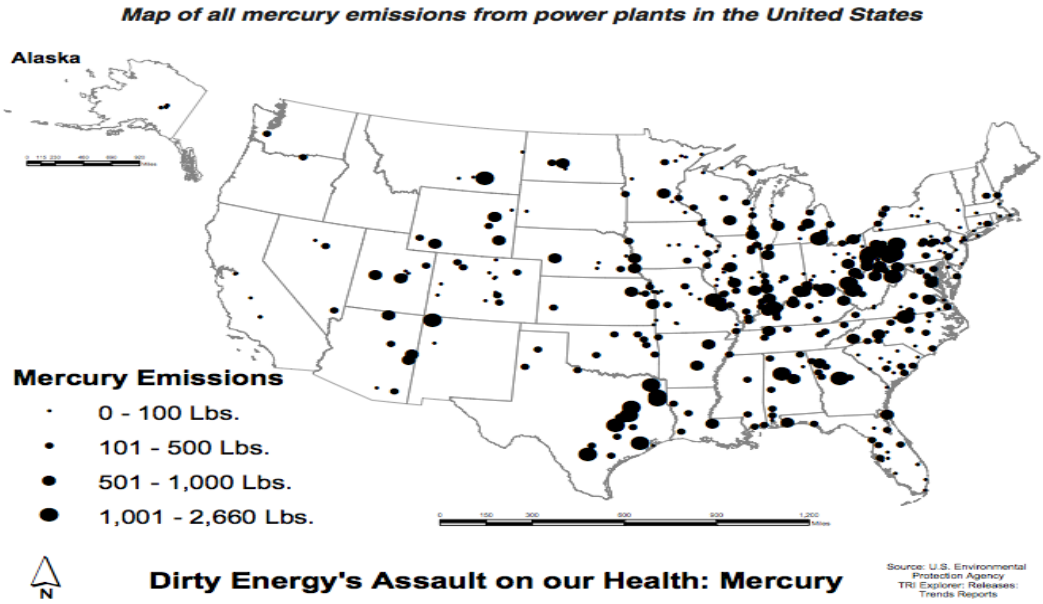

Figure 6. Map of mercury emissions from power plants in USA. (U.S. Energy Information Administration. 2009)

World coal consumption in 2006 was 6118 Tg, representing the primary fuel used in electrical power generation facilities (42%) and accounting for about 27% of world's energy consumption (Energy Information Administration. 2009). Pirrone summarized mercury concentrations ($\mu g \cdot g^{-1}$) in coals from different regions all over the world in Table 3 (Pirrone et al. 2010), and estimated mercury emission from fossil fuels (primarily coal) is about 810 Mg/year. Mercury emissions from other anthropogenic sources are also summarized in Table 4 (Pirrone et al. 2010).

Table 3. Mercury levels ($\mu g \cdot g^{-1}$) in coal from different countries/regions (Pirrone et al. 2010)

Country/region	Hg in coal	Hg in coal fly ash
Australia	0.01–1.0	0.34
China	0.19–1.95	–
Guizhou Province	0.52	–
Europe	0.01–1.5	0.23
India	0.11–0.80	0.007-0.28
Japan	0.045	-
Korea	0.012–0.048	–
Russia	0.02–0.9	
South Africa	0.01–1.0	0.56–0.64
Argentina	0.021–0.96	
Brazil	0.041–0.778	
Colombia	0.020–0.17	
Peru	0.041–0.63	
Venezuela	0.030–0.280	0.268
USA	0.17 (mean)	
World	0.02–1.0	0.62

Table 4. Hg emissions from major anthropogenic sources (Mg/year) (Pirrone et al. 2010) SC=Stationary Combustion; NFMP=Non-Ferrous Metal Production; PISP=Pig Iron and Steel Production; CP=Cement Production; CSP=Caustic Soda Production; MP=Mercury Production; WD=Waste Disposal; CB=Coal-Bed Fires; VCM=Vinyl Chloride Monomer Production; O=other; T=Total

	SC[a]	NFMP	PISP	CP	CSP	MP	GP	WD	O	T	Reference year
S. Africa	32.6	0.3	1.3	3.8	0.0	0.0	0.3	0.6	1.3	40.2	2004
China	268.0	203.3	8.9	35.0	0.0	27.5	44.7	14.1	7.6	609.1	2003
India	124.6	15.5	4.6	4.7	6.2	0.0	0.5	77.4	7.5	240.9	2004
Australia	2.2	11.6	0.8	0.9	0.0	0.0	0.3	0.2	0.6	16.6	2005
Europe	76.6	18.7	0.0	18.8	6.3	0.0	0.0	10.1	14.7	145.2	2005
Russia	46.0	5.2	2.6	3.9	2.8	0.0	4.3	3.5	1.5	69.8	2005
N. America	65.2	34.7	12.8	15.1	10.3	0.0	0.0	13.0	1.7	152.8	2005
S. America	8.0	13.6	1.8	6.4	2.2	0.0	16.2	0.0	1.5	49.7	2005
Total	623.2	302.9	32.8	88.6	27.8	27.5	66.3	118.9	36.4	1324.3	
Rest of the world	186.8	7.1	10.4	147.1	135.1	22.5	333.7	68.5	28.2	939.4	2006
Total	810.0	310.0	43.2	235.7	162.9	50.0	400.4	187.4	64.6	2319.7[c]	

1.3 MEASURING AIRBORNE MERCURY SPECIES

An automated system from Tekran Corporation (Toronto, Canada) is commonly used for measuring mercury species in the air, and was employed in the present study (Figure 7). The gaseous elemental mercury analyzer (model 2537B) is combined with module for collecting GOM (model 1130) and a module for collecting PBM (module 1135). Together they provide "continuous" measurements of the three mercury species, with data on 5 minute intervals for GEM, and 2-3 hour intervals (for GOM and PBM). The model 2537B determines mercury only in the GEM form; thus GOM and PBM samples are converted to GEM immediately prior to analysis by thermal desorption/reduction to Hg^0. The 2537B contains two parallel gold traps to alternately adsorb and desorb GEM immediately before detection by Cold Vapor Atomic Fluorescence Spectrometry (CVAFS). The thermal-desorption step cleans the gold trap part for re-use. The 1130 module uses a KCl-coated quartz annular denuder to capture GOM samples and the 1135 module uses a quartz regenerable particulate filter (RPF) to capture PBM.

This system runs automatically and produces 5-minute integrated GEM values, while concurrently collecting GOM and PBM species. The analytical steps associated with the ambient air Hg speciation instrument are given in Table 5. Briefly, upon completion of the 2 hour collection period for GOM and PBM (Table 5, step 1), the sample train stops collecting ambient air (valve closes) and the system is flushed with "zero" air (Hg-free air). Next the RPF containing PBM collected over the prior 3 hours is heated to 800ºC which releases this Hg fraction as GEM. The mercury is carried by high-purity argon to the 2537B analyzer for measurement. Subsequently, the denuder is heated to 500 ºC which also releases the Hg fraction as GEM and is carried to the 2537B as before. Thus, the speciation system reports twelve GOM

and twelve PBM values from each 24-hour period. The system is designed to be coupled to a computer and a data logger for data archive, telemetry and remote retrieval of instrument status.

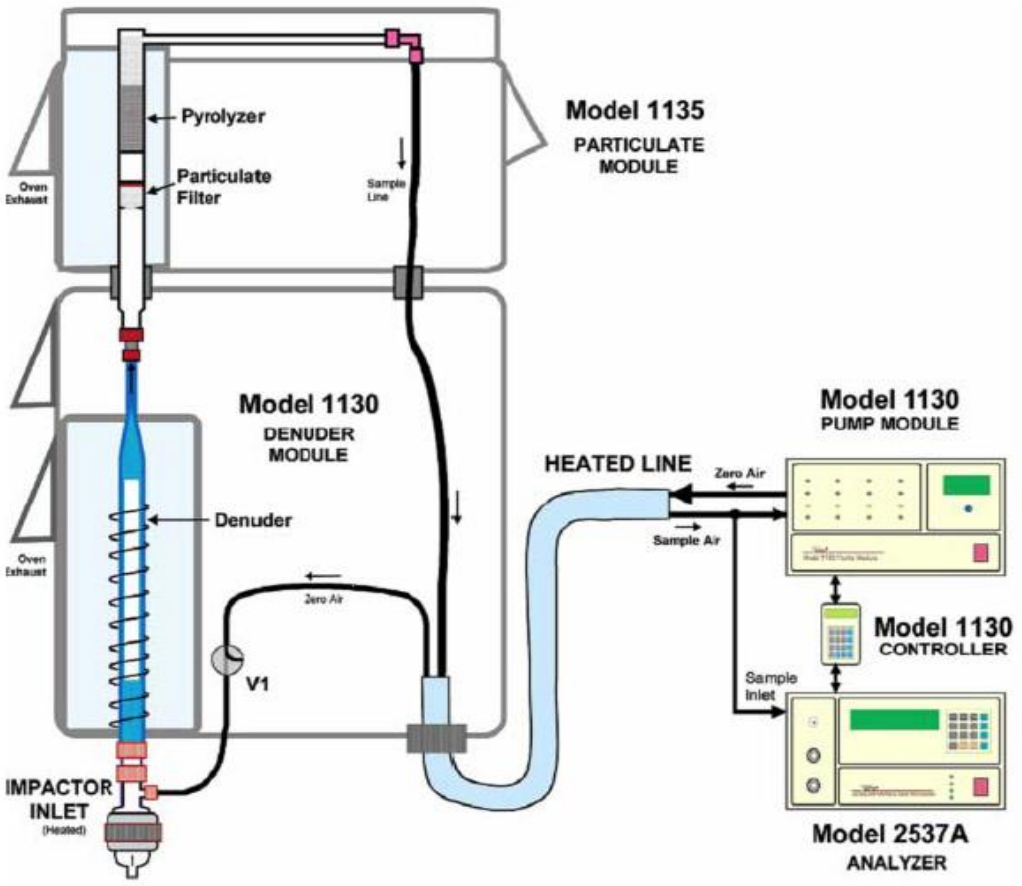

Figure 7. Schematic of the automated system for measuring atmospheric Hg species

Table 5. Atmospheric mercury speciation instrument analytical steps

Steps	Function	Duration(S)	Event Flags
Sample Duration (1)	Measure GEM every five minutes	3600	0
Zero Air Flush (2)	The sampling system is flooded with zero air which acts as a carrier	890	1
Pyrolyzer Preheat (3)	The pyrolyzer is heated PBM converted to GEM	290	2
Particulate Filter Desorption (4)	Desorbs PBM, The Model 2537 quantities the mercury released during this step	890	2
Annular Denuder Desorption (5)	The denuder is heated, releasing GOM that was trapped during the previous sampling period	890	3
Zero Air/Cool Down (6)	The sensing elements are cooled and post-analysis zero levels are determined	590	1

GEM

The Model 2537B performs continuous measurement of total gaseous mercury (GEM) in ambient air with an update rate as low as 2.5 minutes and a detection limit of <0.1 ng/m^3. Figure 8 shows the instrument samples air and traps mercury vapor into a cartridge containing an ultra-pure gold adsorbent. The amalgamated mercury is thermally desorbed and detected using CVAFS. A dual cartridge design allows alternate sampling and desorption, resulting in continuous measurement of the air stream.

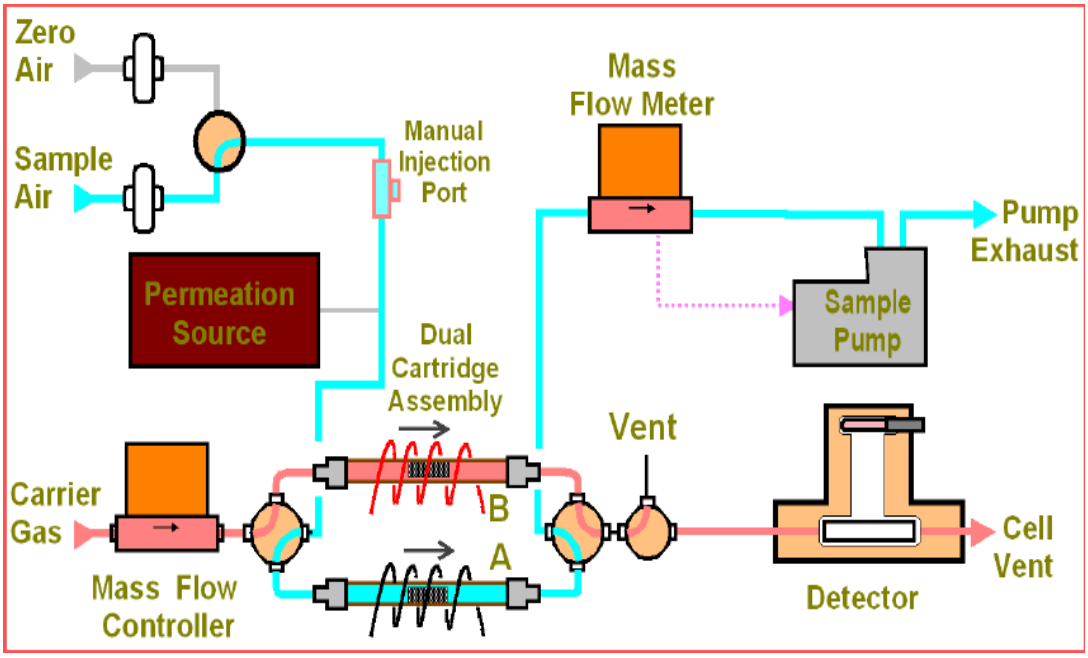

Figure 8. Flow diagram of Tekran 2537 mercury analyzer

GOM

The Tekran 1130 contains a KCl-coated annular denuder which serves to capture reactive mercury (GOM species) while allowing elemental mercury to pass through. It is synchronized with the operations of the GEM (Model 2537B) analyzer and the PBM 1135 module. Programmable timing parameters allow automatic GOM readings to be taken at specified intervals, once every two hours in our study.

PBM

The Tekran model 1135 is used to trap the fine fraction particulate bound mercury with a unique quartz regenerable filter. One of the greatest problems with conventional particulate mercury measurement methods is that GOM will be trapped on the filter medium along with the PBM. This can result in large measurement artifacts. Here this is not a problem because GOM is removed by the denuder prior to PBM collection.

1.4 MODELING AIRBORNE MERCURY

The complex species-dependent behavior of atmospheric mercury makes studying it a challenge. Measuring atmospheric mercury species reliably is costly. It requires expensive equipment and bi-weekly maintenance. Moreover, deploying equipment in remote areas is logistically challenging. In such a case, numerical modelling becomes a powerful tool for investigation. Many numerical models of different types have been developed in the past decade to evaluate the atmospheric transport and deposition of mercury on local, regional and global scales. Models vary depending on their complexities and their purpose.

An inter-comparison study for evaluation of numerical models of Hg long-range atmospheric transport and deposition was conducted by European Monitoring and Evaluation Programme (EMEP). Three stages were included in the project: (1) Comparison of chemical schemes for a cloud environment (Ryaboshaplo et al. 2002); (2) Air concentrations in short term episodes (Ryaboshaplo et al. 2007); (3) Long-term deposition and source-receptor budgets (Ryaboshaplo et al. 2007). Models used in the intercomparison study are summarized in Table 6.

Describing each of these models is beyond the scope of this study. Here is presented a brief introduction of the two models used in this study: Hybrid Single Particle Lagrangian Integrated Trajectory (HYSPLIT) model and the Community Multi-Scale Air Quality (CMAQ) model. A more detailed description for both is given in chapter 2.

Briefly, for the HYSPLIT model, hypothetical puffs of pollutant are considered to be emitted from each given source location. Advection and diffusion calculations are made in a Lagrangian framework while mercury concentrations are calculated on a fixed grid. The model has evolved over several stages during the last decade (Draxler and Hess. 1998). The initial version of the model (Draxler and Taylor. 1982) used only in rawinsonde (equipment used on

weather balloons to measure various atmospheric parameters) observations and the dispersion was assumed to consist of uniform mixing during the daytime and no mixing at night. Dispersion due to wind shear was introduced by splitting up the daytime mixed layer into smaller layers each night. In the next revision (Draxler and Stunder. 1988), variable strength mixing was introduced based upon a temporally and spatially varying diffusivity profile. In the third version of the model (Draxler and Hess. 1997), the use of rawinsonde data was replaced by gridded meteorological data from either analyses or short-term forecasts from routine numerical weather prediction models. Particularly, the current version of the model updated the advection algorithms to include temporal interpolation and although the dispersion of a pollutant can still be calculated by assuming the release of a single puff, the puff can now be defined with either a Gaussian or top-hat horizontal distribution (Draxler and Hess. 1998).

The CMAQ model was developed by the USEPA and used in mercury policy development (Bullock and Braverman. 2007). It is a comprehensive, three-dimensional, multi-scale, Eulerian-based atmospheric chemistry, transport, and deposition model for multiple air pollutants.

Table 6. EMEP intercomparison study of numerical models for long-range atmospheric transport of mercury. Colors showing different models were used in each stage. M. Cohen (National Oceanic and Atmospheric Administration (NOAA))

Models Acronym	Model name	Institution	Stage I	Stage II			Stage III		
			Chemistry	GEM	GOM	PBM	Wet Dep	Dry Dep	Budgets
CAM	Chemistry of Atmospheric Mercury	Environmental Institute, Sweden							
MCM	Mercury Chemistry Model	Atmos. & Environmental Research, USA							
CMAQ	Community Multi-Scale Air Quality	US EPA							
ADOM	Acid Deposition and Oxidants Model	GKSS Research Center, Germany							
MSCE-HM	MSC-E Heavy Metal	EMEP MSC-E							
GRAHM	Global/Regional Atmospheric Heavy Metal	Environment Canada							
EMAP	Eulerian Model for Air Pollution	Bulgarian Meteo-service							
DEHM	Danish Eulerian Hemispheric Model	National Environmental Institute							
HYSPLIT	Hybrid Single Particle Lagrangian Integrated Trajectory	US NOAA							
MSCE-HM-Hem	MSC-E heavy metal hemispheric Model	EMEP MSC-E							

1.5 LIST OF REFERENCES

Anderson, M. J., Daly, E. P., Miller, S. L., Milford, J. B., **2002**. Source apportionment of exposures to volatile organic compounds: II. Application of receptor models to TEAM study data. *Atmos. Environ*. 36, 3643–58.

Atkeson, T. D., Pollman, C. D., and Axelrad, D. M., **2005**. Recent Trends in Hg Emissions, Deposition, and Biota in the Florida Everglades: A Monitoring and Modeling Analysis. *Human Exposure around the World*. Springer Publisher, Norwell, MA. 26, 637-656.

Bullock, O. R. J. and Braverman, T., **2007**. Application of the CMAQ mercury model for US EPA regulatory support. *Dev. Environm. Sci*. 6, 85–95, doi: 10.1016/S1474-8177(07)06022-6.

Draxler, R. R., and Taylor, A. D., **1982**. Horizontal dispersion parameters for long-range transport modeling. *J. Appl. Meteorol*. 21, 367-372.

Draxler, R. R., and Stunder, B. J. B., **1988**. Modeling the CAPTEX vertical tracer concentration profiles. *J. Appl. Meteorol*. 27, 617-625.

Draxler, R. R., Hess, G. D., **1997**. Description of the HYSPLIT_4 Modeling System. *NOAA Technical Memorandum ERL ARL-224*.

Draxler, R. R., Hess, G. D., **1998**. An overview of the HYSPLIT_4 modelling system for trajectories, dispersion and deposition. *Aust. Met. Mag*. 47, 295-308.

Dvonch, J. T., Graney, J. R., Marsik, J. F., Keeler, J. G., and Stevens, R. K., **1998**. An investigation of source-receptor relationships for mercury in South Florida using event precipitation data. *Sci. Total Environ.* 213, 95-108.

Dvonch, J. T., Graney, J. R., Keeler, G. J., Stevens, R. K., **1999**. Use of elemental tracers to source apportions mercury in south Florida precipitation. *Environ. Sci. & Technol*. 33, 4522-4527.

Lindberg, S., Bullock, R., Ebinghaus, R., Engstrom, D., Feng, X., Fitzgerald, W., Pirrone, N., Prestbo, E., and Seigneur, C., **2007**. A Synthesis of Progress and Uncertainties in Attributing the Sources of Mercury in Deposition. *AMBIO: J. Human Environ*. 36, 19–33.

Mason, R. P., **2009**. Mercury emissions from natural processes and their importance in the global mercury cycle. Springer, New York, USA, chap. 7, 173–191.

Nelson, F. P., Nguyen, H., Morrison, L. A., Malfroy, H., **2009**. Mercury sources, transportation and fate in Australia. Final report to the department of environment, Macquarie University.

Nriagu, J., Becker, C., **2003**. Volcanic emissions of mercury to the atmosphere: global and regional inventories. *Sci. Total Environ*. 304, 3-12.

Peterson, G., Iverfeldt, A., Munthe, J., **1995**. Atmospheric mercury species over central and northern Europe. Model calculations and comparison with observations from the Nordic air and precipitation network for 1987 and 1988. *Atmos. Environ*. 29, 47-67.

Pirrone, N., Cinnirella, S., Feng, X., Finkelman, R. B., Friedli, H. R., Leaner, J., Mason, R., Mukherjee, A. B., Stracher, G. B., Streets, D. G., and Telmer, K., **2010**. Global mercury emissions to the atmosphere from anthropogenic and natural sources, *Atmos. Chem. Phys.* 10, 5951–5964.

Pyle, M. D., and Mather, A. T., **2003**. The importance of volcanic emissions in the global atmospheric mercury cycle. *Atmos. Environ.* 37, 5115-5124.

Ryaboshaplo, A., Bullock, R., Ebinghaus, Rlk Ilyin, Ilk Lohman, K., Munthe, J., Petersen, G., Seigneur, C., WangBerg, I., **2002**. Comparison of mercury chemistry models. *Atmos. Environ*. 36, 3881-3898.

Ryaboshaplo, A., Bullock, R., Christensen, J., Cohen, M., Dastoor, A., Ilyin, I., Petersen, G., Syrakov, D., Artz, S. R., Davignon, D., Draxler, R. R., Munthe, J., **2007**. Intercomparison study

of atmospheric mercury models: 1. Comparison of models with short-term measurements. *Sci. Total Environ.* 376, 228-240.

Ryaboshaplo, A., Bullock, R., Christensen, J., Cohen, M., Dastoor, A., Ilyin, I., Petersen, G., Syrakov, D., Travnikov, O., Artz, S. R., Davignon, D., Draxler, R. R., Munthe, J., Pacyna, J., **2007**. Intercomparison study of atmospheric mercury models: 2. modelling results vs. long-term observations and comparison of country deposition budgets. *Sci. Total Environ.* 377, 319-333.

Schroeder, H. W., Munthe, J., **1998**. Atmospheric mercury–An overview. *Atmos. Environ.* 32(5), 809-822.

Swartzendruber, P. C., Jaffe, D. A., Prestbo, E. M., Weiss-Penzias, P., Selin, N. E., Park, R., Jacob, D. J., Strode, S. and Jaegl, L. **2006**. Observations of reactive gaseous mercury in the free troposphere at the Mount Bachelor Observatory. *J. Geophys. Res*. 111(D24): doi: 10.1029/2006JD007415. ISSN: 0148-0227.

CHAPTER TWO

2. TEMPORAL PATTERNS AND MODELING OF ATMOSPHERIC MERCURY SPECIES IN NORTHERN MISSISSIPPI

Portions of this chapter were published:

Yi J., Cizdziel J., Lu D. (2013) "Temporal patterns of atmospheric mercury species in northern Mississippi during 2011-2012: influence of sudden population swings", *Chemosphere* 93(9): 1694-1700.

Lu D., Yi J., Cizdziel J., White L., Reddy R. (2014) "Numerical Simulation of Atmospheric Mercury in the Mid-South USA", *Air Quality, Atmosphere and Health*, (online 28 March 2014).

2.1 ABSTRACT

Gaseous elemental mercury (GEM), gaseous oxidized mercury (GOM) and particulate bound mercury (PBM) were measured on the University of Mississippi campus from July 2011 through June 2012. It is believed to be the first time that levels of atmospheric mercury species have been documented in northern Mississippi, and at a location with relatively large and sudden swings in population. The mean level (± 1SD) of GEM was 1.54 ± 0.32 $ng \cdot m^{-3}$; levels were lower and generally more stable during the winter (1.48 ± 0.22) and spring (1.46 ± 0.27) compared with the summer (1.56 ± 0.32) and fall (1.63 ± 0.42). Mean levels for GOM and PBM were 3.87 $pg \cdot m^{-3}$ and 4.58 $pg \cdot m^{-3}$, respectively; levels tended to be highest in the afternoon and lowest in the early morning hours. During the fall and spring academic semesters concentrations and variability of GOM and PBM both increased, possibly from vehicle exhaust. There were moderate negative correlations with wind speed (all species) and humidity (GOM and PBM). Backward air mass trajectory modeling revealed that the majority of these events occurred from air masses that passed through the northern continental US region. CMAQ model overestimated GEM concentration in summer and slightly underestimated it in winter. The model exhibited good skill in capturing seasonal variability of GOM, while it produced a significant overestimate for PBM in both summer and winter. Sensitivity tests revealed that anthropogenic emissions had great influences on local/regional ambient levels of GEM, GOM, and PBM, with anthropogenic emissions, contributing 10–20 % of GEM, 20–40 % of GOM, and 40–60 % of PBM. The evident influence of anthropogenic sources on Hg concentration suggests that discrepancies between modeled and observed are partly attributable to the uncertainties in anthropogenic emission inventory used in the air quality modeling system. Overall, this study illustrates the complexity of temporal fluctuations of airborne mercury species, even in a small town environment.

2.2 INTRODUCTION

Mercury is a toxic environmental pollutant capable of long-range (global) transport through the atmosphere (Lin et al. 2006). Airborne mercury comes from both natural sources (e.g., evasion from soils, vegetation, volcanoes, forest fires, and mineral deposits) and anthropogenic sources (e.g., coal combustion, waste incineration, and certain industrial processes), and these sources have been estimated at 5207 Mg/year and 2320 Mg/year, respectively (Pirrone et al. 2010). Anthropogenic emissions appear to be leading to a general increase in mercury on local, regional and global scales (Pirrone et al. 2010). Mercury deposits to terrestrial and aquatic systems through wet and dry mechanisms where it can undergo biotic and abiotic transformation to methylmercury, which in-turn readily bioaccumulates and concentrates in food webs (Watras et al. 1998). This has motivated intensive research on mercury as a pollutant.

Airborne mercury is commonly classified as existing in three primary forms (species), gaseous elemental mercury (GEM), gaseous oxidized mercury (GOM) and particulate bound mercury (PBM), each with distinctive chemical and physical properties and environmental behavior. GEM is the predominant form of atmospheric mercury (often >95% of the total). Because it is relatively inert, sparingly soluble in water, and has low dry deposition velocity (i.e., 0.02–0.2 $cm \cdot s^{-1}$) (Seigneur et al. 2004), it has a long residence time (months to years), allowing it to circulate globally (Schroeder et al. 1998; Weiss-Penzias et al. 2003). The northern hemispheric background level of GEM is approximately 1.6 $ng \cdot m^{-3}$ (Lindberg et al. 2007). GEM is slowly converted to soluble GOM through various photochemical reactions, including reactions which may involve ozone (O_3), hydroxyl radical (OH), nitrate (NO_3), hydrogen peroxide (H_2O_2), and/or atomic bromine (Br) (Holmes et al. 2010). GOM and PBM have much

shorter residence times (hours to weeks) in the atmosphere, and are readily removed through wet and dry deposition mechanisms (Lyman et al. 2007). PBM is any form of mercury contained in- or associated with- aerosol particles, whose transport depends greatly on particle size and meteorological conditions (Keeler et al. 1995). Natural emissions are primarily in the gaseous elemental form, whereas anthropogenic emissions often include all three species (GEM, GOM and PBM) (Schroeder et al. 1998). Several studies have demonstrated the importance of determining mercury speciation, particularly for GOM which is often responsible for contamination near point sources (Peterson et al. 1995; Dvonch et al. 1998; Landis et al. 2002). Most studies of atmospheric mercury species in the United States have been conducted in the northeast (Sillman et al. 2007), in the south in Florida or along the Gulf of Mexico (Rolison et al. 2013), and in the far west in Nevada or California (Stamenkovic et al. 2007). Our work has been motivated in part by the lack of data for mercury in the mid-south environment, despite the region having several large-scale Coal-fired power plants (CFPPs), conditions that favor methylation of Hg^{+2} (e.g. wetlands and backwaters with high levels of natural organic matter, sulfate-reducing bacteria, and long-hot summers), and lakes with fish consumption advisories due to high-levels of mercury (Ullrich et al. 2001).

The aim of this study was to fill a data-gap for atmospheric mercury in the mid-south USA to aid regional mercury models and deposition studies. The study included monitoring airborne mercury species in northern Mississippi for a full year. Here, we report on their concentration, temporal variations, and sensitivity to meteorological parameters. Atmospheric Hg modeling efforts in the USA have been mainly focused on the regions of northeast (Sillman, et al. 2007), midwest (Holloway et al. 2012), or far west in Nevada or California (Stamenkovic et al. 2007). There is a lack of study for atmospheric Hg modeling in the mid-south USA, where

there are several CFPPs and where conditions favor methylation of Hg^{2+} (e.g., wetlands and backwaters with high levels of natural organic matter, sulfate-reducing bacteria, and long hot summers). To that end, we include backward trajectory air mass modeling and air quality modeling to investigate possible sources for mercury. The study also allowed us to evaluate the impact of a sudden doubling of a population center on airborne mercury, because it took place in a "college town" (Oxford, Mississippi), where the population about doubles from approximately 25,000 to 50,000 while school is in session.

2.3 MATERIAL AND METHODS

2.3.1 Sampling Site

Oxford is located in northern Mississippi at an elevation of ~150 m above sea level. This relatively small urban college town has a population that about doubles during the traditional academic year, starting in late August. The atmospheric mercury speciation system was situated about 20 m above the ground on a platform raised several meters above the roof of a building (34°21'50"N, 89°32'60"W) in the center of the University of Mississippi (Ole Miss) campus. The location on the top of the building is high enough to receive air masses unimpeded by trees and vegetation which can influence speciation via absorption and volatilization.

Major sources of anthropogenic airborne mercury in the region are shown in Figure 9. There are no major sources in the immediate study area. However, there are several within a 125 km radius, including two CFPPs. The Allen Fossil Plant is a 552 MW facility located near Memphis, Tennessee, a city with a population of about 650,000; it reported releases of 86.2 kg of mercury in 2010 (USEPA, 2010). The other CFPP is the 514 MW Red Hills generation facility located ~110 km to the south with 186 kg of mercury reported released in 2010 (USEPA, 2010). Further to the north and west are two additional CFPPs (Figure. 9), which together released 526 kg of mercury to the air in 2010, and two industrial steel facilities (347 kg), and a manufacturing facility (143 kg). In the surrounding region as a whole (defined here as Mississippi, Tennessee, Arkansas, Louisiana, Alabama, Georgia, Kentucky, Indiana, Illinois, and Missouri) anthropogenic sources were estimated to release a total of 13,085 kg to the air in 2010 (USEPA, 2010). Among the sources, CFPPs accounted for 70.1% of the emissions; steel and chemical companies yielded a total of 18.5%, waste incinerators 1.4%, and the remaining (other) 10%.

The emission from waste incinerators is notable because it represents a significant decline from earlier emission inventories.

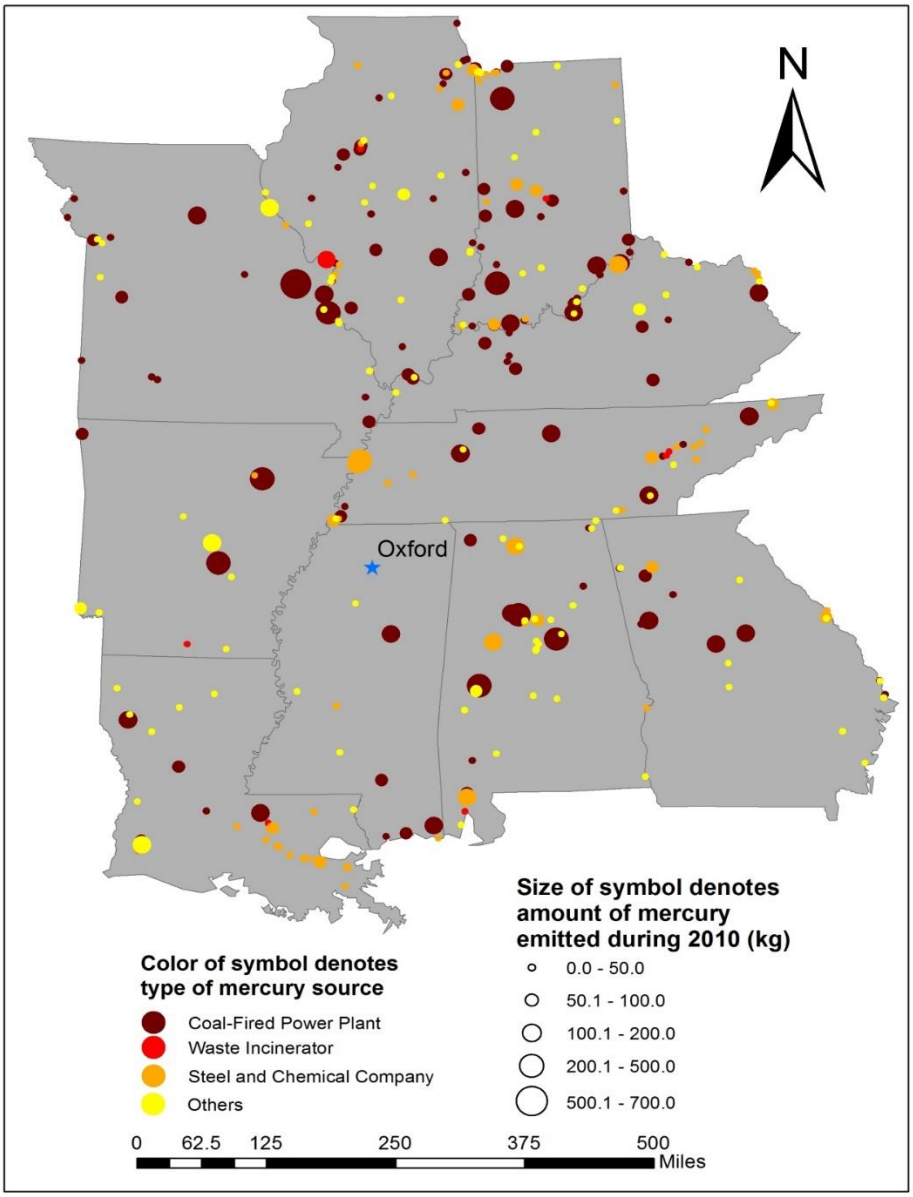

Figure 9. Map showing the sampling site (Oxford, MS) and major anthropogenic sources of airborne mercury in the region based on EPA 2010 Toxic Release Inventory

Emissions from natural sources in the region are complex and include evasion from agricultural fields, forests, and waterbodies. Moreover, evasion of mercury from surfaces includes re-emission of previously deposited mercury originating from both natural and anthropogenic sources. We are not aware of any studies evaluating the natural mercury emission inventory for the region.

2.3.2 Measuring Airborne Mercury Species

We measured mercury species in the ambient air from July 2011 – June 2012 using an automated system from Tekran Inc. (Toronto, Canada). The system uses a model 2537B mercury analyzer for GEM measurements based on cold vapor atomic fluorescence spectrometry (CVAFS), and is combined with a model 1130 GOM and model 1135 PBM speciation units, to sample and detect the three mercury species. The unit was operated with a total flow rate of 10 $L \cdot min^{-1}$ and 1 $L \cdot min^{-1}$ for analytical sampling, and an inlet with an impactor is used to remove coarse particle ($\geq$2.5μm) from the ambient air. In short, ambient air is sequentially passed through a KCl-coated quartz annular denuder which captures GOM, through a quartz regenerable particulate filter to sample PBM, and through one of two gold traps to collect GEM. The system uses two parallel gold traps to alternately adsorb and desorb (thermally) GEM every 5 minutes. High-purity argon carries the desorbed mercury atoms through the fluorescence cell of the analyzer. PBM and GOM are measured on a 2 hour basis after being thermally desorbed from the filter and denuder, respectively, a process that assures these operationally defined mercury species are converted to GEM for measurement with the 2537B. The speciation system reports twelve PBM and twelve GOM values for each 24 hour period.

For quality assurance, the system was set to perform an automatic calibration using an internal permeation source every 24 hours. In addition, an external calibration check was

performed regularly (~monthly) using a Tekran 2505 mercury vapor calibration unit and a digital gas-tight syringe. Injection recoveries were within 92-105%. During one period results for adjacent gold traps started to deviate from each other by >10%, possibly due to passivation of the gold surface. The gold traps were replaced and the deviation was eliminated. The suspect data (about 2 weeks' worth) associated with this event was removed from the data set. Bi-weekly maintenance included replacing the frit in the impactor, sodalime trap, sample filter and zero air filters, and re-coating the KCl-denuder. The regenerable particulate filter was replaced monthly.

2.3.3 Modeling and Data Analysis

To investigate potential source areas of mercury observed in Oxford, MS, the NOAA Hybrid Single-Particle Lagrangian Integrated Trajectory model (HYSPLIT) using Eta Data Assimilation System (EDAS) 40 km input data, was used to calculate backward air mass trajectories (Draxler et al. 1997). The HYSPLIT model was initially designed to help in case of atmospheric emergencies. It computes advection, dispersion and deposition using either puff or particle approaches. The dispersion rate is calculated by considering vertical diffusivity profile, wind shear, and horizontal deformation of the wind field. The concentrations are calculated at a specific grid point for puffs and as cell-average concentrations for particles, where a Lagrangian transport model is applied by considering the advection of the puff and calculating growth rate with the local mixing coefficients. Twenty-four hour back trajectory modeling was applied for starting heights of 200 m, 500 m and 1200 m above the ground surface when GEM concentrations exceeded 5.0 $ng \cdot m^{-3}$, GOM was greater than 35 $pg \cdot m^{-3}$, and PBM exceeded 15 $pg \cdot m^{-3}$; this represented the ten highest peaks for each species during the period of 1 July 2011 through 30 June 2012. In addition, the modeling was done for the 10 lowest GEM concentrations, and for 10 data periods when GOM and PBM were about 1 SD below the mean

and relatively stable (not impacted by rain events, etc.). Backward trajectories were merged for a specific starting height.

The following models were also applied in this study: Community Multi-scale Air Quality model (CMAQ, version 5.0), an air quality modeling system with a chemistry and transport model; the Sparse Matrix Operator Kernel Emissions model (SMOKE, version 3.0), an emission processing model; and the Weather Research and Forecast model (WRF, version 3.3), a mesoscale numerical meteorological model. Here we provide a brief description of the model system; details can be found elsewhere, including in Lu et al (2008, 2012), and Skamarock et al (2001). The WRF model was used to provide the meteorological background input for the air quality study. The parameterizations employed by WRF consisted of a level-1.5 order turbulence kinetic energy closure scheme, 5 layers in the land surface model microphysics (Ferrier et al. 2002), Rapid Radiation Transfer Model (RRTM) long wave radiation scheme (Mlawer et al. 1997), simple short wave radiation (Dadhia. 1989), YSU PBL scheme (Noh et al. 2003), and the modified version of the Kain-Fritsch (Kain and Fritsch. 1993) convective scheme. The SMOKE model is used to convert the source-level emissions (county total emissions) reported on a yearly basis to spatially resolved, hourly emissions, with detailed speciation information (Houyoux et al. 2001). It produced the basic model-ready emissions, including gases and PM from point, area, non-road, on-road, and biogenic sources. The CMAQ model was developed by the USEPA and is described by Byun and Ching (1999). It is a comprehensive, three-dimensional, multiscale, Eulerian-based, atmospheric chemistry, transport and deposition model for multiple air pollutants. The carbon-bond 2005 gas-phase chemistry module (Yarwood et al. 2005) was applied in the CMAQ model. Hg oxidation pathways were represented for both the gas and aqueous phases (Baker and Bash. 2012). The CB05 with Hg includes 56 chemical species (52 core species and 4 Hg species) and it

is an updated version of the earlier Carbon Bond 4 gas phase mechanism. In the version 5.0 of the CMAQ model a bi-directional flux model for GEM is applied. The flux of Hg is estimated as a function of its content in environmental media and redox reactions between elemental and oxidized Hg in soil and surface waters (Bash. 2010). The parameterization method was implemented on a regional scale depending upon various land-use, soil, and plant compensation points.

This off-line modeling system for air quality assessment with WRF-CMAQ runs over three nested domains centering Oxford, Mississippi. The spatial resolutions for coarse, middle and fine domains are 36-, 12- and 4-km respectively. In horizontal, the grid numbers are 97 x 85, 103 x 91, and 97 x 97 for coarse, middle, and fine domains respectively. Nested domains share the identical layers vertically. The vertical layers of WRF are 35 sigma levels with 15 layers within the planetary boundary layer (PBL) (less than 1500 m), in which the lowest sigma level is approximately at the height of 21 meter. In this paper, a layer averaging scheme was adopted for the CMAQ simulations whereby multiple WRF layers are combined into one CMAQ layer to reduce the air quality model computational time. The WRF 35 vertical layers were collapsed into 25 vertical layers in CMAQ where all layers within PBL remained. This approach helps resolve the emission and chemical reactions of pollutants occur within PBL. Such practice has been applied in other previous air quality modeling evaluations as well (Cheng et al. 2002; Lin et al. 2005). Figure 10 shows the domain configuration coverage. The 36-km domain used the default initial and boundary conditions from CMAQ as input, but the 12- and 4-km domains obtained their initial and lateral boundary conditions from 36-km domain. Table 7 shows the default initial and boundary conditions for each Hg forms within each sigma layer range.

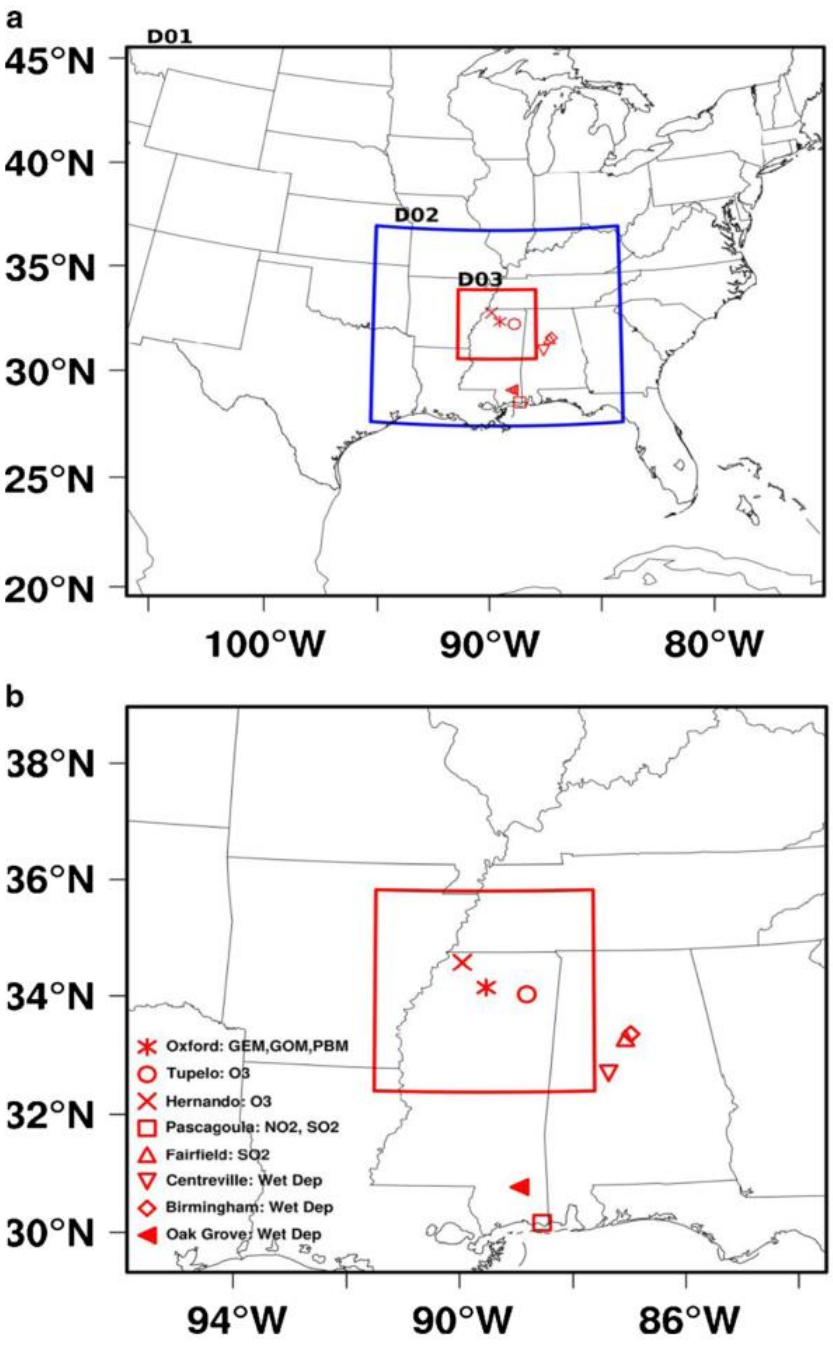

Figure 10. (a) Model domain configuration and monitoring sites domain. (b) Zoomed in map of the 12- and 4-km domains to display the detailed monitoring sites. O_3 measurements were from the sites of Hernando and Tupelo, NO_2 from the site of Pascagoula, and SO_2 from the sites of Pascagoula and Fairfield. Wet deposition measurements were obtained from three sites of Oak Grove, Birmingham and Centreville. Ambient concentrations of GEM, GOM, and PBM; surface temperature; and wind speed observations were obtained in Oxford, MS

Table 7. The default initial and boundary conditions for each Hg species for each sigma layer range in CMAQ model

Hg species	Sigma layer range					
	1.0–0.98	0.98–0.93	0.93–0.84	0.84–0.60	0.60–0.30	0.30–0.00
GEM (ppm)	1.78×10^{-7}	1.77×10^{-7}	1.76×10^{-7}	1.75×10^{-7}	1.74×10^{-7}	1.73×10^{-7}
GOM (ppm)	2.00×10^{-9}	3.00×10^{-9}	4.00×10^{-9}	5.00×10^{-9}	6.00×10^{-9}	7.00×10^{-9}
PBM ($\mu g/m^3$)	1.08×10^{-5}	1.026×10^{-5}	9.72×10^{-6}	7.558×10^{-6}	4.859×10^{-6}	1.62×10^{-6}

In this study, we applied some statistic parameters including the correlation coefficient (denoted as R), Root-Mean-Squared Error (RMSE), Average Normalized Bias (ANB) (West et al. 2004) and Unpaired Peak Accuracy (UPA) as the quantitative measures of model-observation agreement. The ANB is defined as the average residual divided by averaged observation:

$$\mathbf{ANB} = \frac{\frac{1}{N}\sum_{i=1}^{N}(x_m^i - x_o^i)}{\frac{1}{N}\sum_{i=1}^{N}x_o^i} = \frac{\sum_{i=1}^{N}(x_m^i - x_o^i)}{\sum_{i=1}^{N}x_o^i} \qquad (1)$$

where N is the total number of existing observation–prediction pairs at a monitoring site, x_0^i and x_m^i are the ith observation and corresponding model simulation. Negative ANB value indicates model underprediction, and positive value indicates model overprediction. UPA is defined as

$$\mathbf{UPA} = \frac{P_{\text{peak}}^u - O_{\text{peak}}}{O_{\text{peak}}} \qquad (2)$$

where P^u_{peak} is the maximum predicted concentration and O_{peak} is the maximum observed concentration. UPA measures model's ability to replicate the highest concentration observed (Wen et al. 2011).

In addition an interpolated emission inventory map was generated using 2010 Toxic Release Inventory data from the U.S. Environmental Protection Agency, the most recent data

available. The mercury contours were obtained from inverse distance weighted interpolation method that is based on the assumption that the interpolating surface is influenced most by the nearby points and less by the more distant points. The interpolated value is a weighted average of the scatter points and the weight assigned to each scatter point diminishes as the distance from the interpolation point to the scatter point increases. In this paper, there are total of 305 mercury emission sites within the region used to make interpolation contours.

Meteorological data was obtained from a monitoring station located <2 km from the mercury speciation system. Due to the similar altitude and surroundings, the weather conditions were considered to be the same between sites. Daily averages were obtained for temperature, dew point, humidity, ambient pressure, visibility, wind speed, and wind direction degree (WDD). Solar radiation measurements were not available for this study. Pearson Correlation coefficients were obtained between the weather parameters and the daily averages for the three mercury species (StatPlus Software). Relationships were considered significant at $p < 0.05$.

2.4 RESULTS AND DISCUSSION

2.4.1 Atmospheric Mercury Speciation

Summary statistics for atmospheric mercury species in Oxford, MS from July 2011 through June 2012 by month, season, and in total are given in Table 8. The table includes the number of plume "events", defined here as periods of time with consecutive data points 2 standard deviations above the mean. Total gaseous mercury (TGM) during the study period averaged 1.60 $ng \cdot m^{-3}$, with >98% of the total being GEM. Overall concentrations of GEM were relatively uniform at 1.54 ± 0.32 $ng \cdot m^{-3}$ (mean ± 1SD), although there was a slight decline in the winter months (1.48 ± 0.22) and spring months (1.46 ± 0.27). These levels are also close to the 1.65 $ng \cdot m^{-3}$ measured in the Great Smoky Mountains in neighbouring Tennessee (Valente et al. 2007), and are lower than measurements at urban sites or near point sources (Lyman et al. 2005; Friedli et al. 2009). The levels in our study are also higher than those found for "global background" (i.e., in very remote areas) which is about 1.2 ng m^{-3} (e.g., Soerensen et al. 2010). This is consistent with our contention that the site is impacted by local and regional sources (described below). It should be noted that because of the complexity of atmospheric mercury chemistry, meteorological patterns, and numerous other factors, a "global background" is clearly a generalization.

Table 8. Summary statistics for mercury species in Oxford, MS during 2011-2012

Month	GEM ($ng \cdot m^{-3}$)					PBM ($pg \cdot m^{-3}$)					GOM ($pg \cdot m^{-3}$)				
	n	range	mean±SD	median	events*	n	range	mean±SD	median	events*	n	range	mean±SD	median	events*
June	4196	0.8-4.7	1.40±0.24	1.39	18	343	0-19	5.30±3.30	4.95	9	343	0-31	2.78±4.46	1.23	7
July	4334	0.9-4.2	1.67±0.32	1.60	20	337	0-15	3.70±3.00	2.87	5	336	0-14	1.83±1.83	1.43	6
August	4231	0.9-6.1	1.59±0.33	1.51	22	338	0-14	3.92±2.10	3.54	9	338	0-36	2.96±4.31	1.41	5
Summer	12761	0.8-6.1	1.56±0.32	1.49	60	1018	0-19	4.31±2.93	3.72	23	1017	0-36	2.54±3.79	1.38	18
September	4197	0.8-7.9	1.63±0.47	1.50	17	314	0-17	5.04±3.31	4.67	7	314	0-23	6.94±4.09	7.30	7
October	4347	0.8-5.9	1.69±0.44	1.57	16	335	0-18	5.22±2.43	5.23	6	326	0-82	8.04±11.51	3.71	6
November	2299	1.0-3.3	1.50±0.17	1.48	6	184	0-14	3.35±2.42	2.80	3	183	0-17	2.30±3.31	1.04	5
Fall	10843	0.8-7.9	1.63±0.42	1.51	39	851	0-18	4.74±2.88	4.53	16	841	0-82	6.34±8.25	4.34	18
December	4310	0.8-5.1	1.53±0.28	1.48	13	332	0-14	3.59±2.77	3.00	5	332	0-20	2.59±3.72	1.13	8
January	2540	1.0-3.3	1.46±0.19	1.44	9	138	0-16	3.84±3.44	2.88	3	136	0-84	8.16±11.86	4.01	3
February	4068	1.1-4.3	1.45±0.17	1.43	18	319	0-24	5.60±4.77	4.36	5	319	0-41	4.14±5.10	2.54	6
Winter	10918	0.8-5.1	1.48±0.22	1.45	40	789	0-24	4.44±3.92	3.56	13	787	0-84	4.18±6.66	1.91	17
March	2389	0.9-3.5	1.53±0.21	1.52	9	179	0-23	3.82±3.86	2.85	4	179	0-24	3.97±4.65	2.26	4
April	1485	0.8-2.2	1.37±0.16	1.37	14	121	0-16	4.56±3.02	3.57	3	120	0-27	2.10±4.12	1.55	5
May	4332	0.8-6.0	1.46±0.31	1.41	18	353	0-33	5.64±4.07	4.84	4	353	0-26	1.75±3.53	1.89	7
Spring	8206	0.8-6.0	1.46±0.27	1.42	41	653	0-33	4.94±3.92	4.11	11	652	0-27	2.43±4.08	1.95	16
Total	42728	0.8-7.9	1.54±0.32	1.47	180	3311	0-33	4.58±3.40	3.98	63	3297	0-84	3.87±6.17	1.71	69

* "events" represent periods of time with data points that are two standard deviations above the mean.

2.4.2 Daily and Seasonal Fluctuations

For GEM, levels tended to decrease in the early daylight (~7:00-9:00) but rebounded as the day progressed, except during the winter when GEM was relatively stable throughout (Figure 11). The drop was surprising given that others have observed a rise at sunlight, presumably due to solar-induced re-emission of GEM deposited on surfaces overnight (Peterson et al. 2009). However, GEM is also converted to GOM by various oxidants generated by solar irradiation and indeed we observed a rise in GOM as the day progressed (Figure 11). We also observed a slight rise in GEM which may be due to increased flux of mercury from soil and other surfaces due to increasing intensity of solar radiation. Choi and Holson (2009) showed that whereas mercury emission flux from a forest floor was correlated with both temperature and solar radiation, the flux was better correlated with solar radiation (during leaf-off periods). Another potential contribution to increase levels of GEM during the day is mixing of GEM stored in the nocturnal residual layer back to the surface (Stamenkovic et al. 2007; Peterson et al. 2009). In the current study, GEM was higher in the summer than in the winter (Figure 11); the mean temperature in Oxford is 25.5º C in the summer and 7.7 ºC in the winter. Whereas overall GEM concentrations are consistent with rural and remote sites, there were, however, occasional transient spikes of GEM, ten of which exceeded 5 $ng \cdot m^{-3}$. These "plume events" will be discussed later under back-trajectory results.

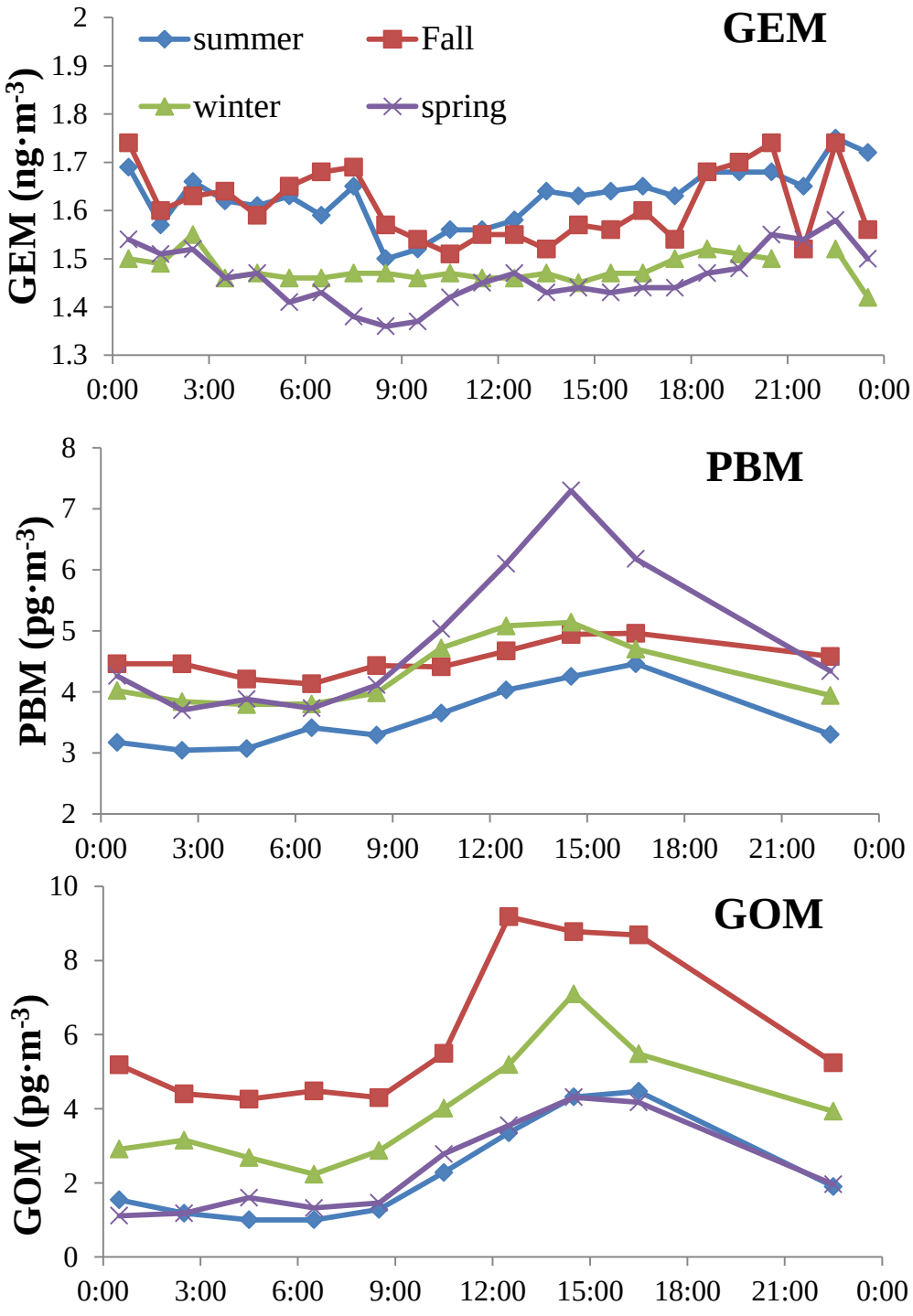

Figure 11. Hourly mean of GEM, PBM and GOM concentrations for the four seasons during 2011-2012 in Oxford, MS. Data gap stems from 24 hour calibration period; the calibration cycle has since been changed to a 25 hour period to rotate timing of data loss

For GOM and PBM, which on average accounted for <2% of the total mercury, there were also daily and seasonal trends. GOM was highest in the fall and winter while PBM was highest in the spring. Both species had peak levels in the afternoon. There are several factors that are likely contributing to these trends, including a greater number of sources during the period, and changing ecological or meteorological conditions (the latter is discussed in the weather section below). As for the increased sources, we note that the university (student population ~25,000) commences the fall semester in late August, and that during periods when school is not in session (e.g., summer and winter break) most students leave the town. Thus, there is a tremendous rise in vehicular traffic in and around campus during the academic year. Indeed, GOM and PBM increased in both intensity and variability while the university was in session and decreased between semesters (Table 9). For example, the total number of GOM data points per spike event (defined as a period of time when the level exceeded two standard deviations of the mean) decreased significantly during the fall (40) and spring (48) semesters and increased during the summer (92) and winter break (52). Note: in this case the smaller the number the more the spike events there are during the period. Given the timing it is plausible that some of the spikes in GOM and PBM may be attributed to vehicle exhaust associated with increased traffic during the semester, and possibly other population-related sources. Hoyer et al (2004) investigated mercury emissions from motor vehicles and found that gasoline and diesel motor vehicles indeed contribute to airborne mercury. Emission for GEM plus PBM for the light-duty gasoline vehicles and diesel vehicles ranged from 0.31 to 1.4 $ng \cdot mile^{-1}$ and 6.3 to 11.0 $ng \cdot mile^{-1}$, respectively. Mercury levels in vehicular fuel was studied by Liang et al (1996); concentrations ranged from 0.22–1.43 $ng \cdot g^{-1}$ for regular gasoline, and 0.40 $ng \cdot g^{-1}$ for diesel fuel. There may be other transient sources of mercury. For example, we found increased GOM and

PBM during a college football game which attracts thousands of people; the monitoring station is adjacent to the stadium. We also seen a small rise in GEM with students returning to campus but this increase was not prevalent in the longer term; it may have been overwhelmed by the seasonal effect discussed earlier.

Table 9. Fluctuations of atmospheric mercury species during periods of increased activity on the campus of the University of Mississippi

Time period	GEM ($pg \cdot m^{-3}$)				
	n	range	mean±SD	median	n/event*
Summer break	14099	785-6100	1548±328	1481	198
Fall semester	13395	809-7859	1609±400	1503	291
Winter break	4762	1059-3870	1506±223	1470	280
Spring semester	10437	844-4342	1451±202	1422	227
Time period	**PBM ($pg \cdot m^{-3}$)**				
	n	**range**	**mean±SD**	**median**	**n/event***
Summer break	1126	0-33	4.63±3.37	3.86	43.3
Fall semester	1040	0-18	4.65±2.84	4.48	43.3
Winter break	311	0-13	3.28±2.63	2.57	104
Spring semester	814	0-25	4.90±4.16	3.92	54.0
Time period	**GOM ($pg \cdot m^{-3}$)**				
	n	**range**	**mean±SD**	**median**	**n/event***
Summer break	1113	0-31	2.27±3.43	1.22	55.6
Fall semester	1029	0-82	5.94±7.83	3.52	39.6
Winter break	310	0-53	2.66±4.93	1.02	51.7
Spring semester	812	0-84	3.91±6.37	1.37	47.8

* "n/event" represents the number of data points between "plume" events, such that the lower the number the more frequent the anomalous peaks.

2.4.3 An example of mercury fluctuations for a typical week during the semester

Figure 12 illustrates temporal patterns and the influence of meteorological conditions on airborne mercury speciation for a typical week during the academic semester. GEM temporarily spiked to above 3 $ng \cdot m^{-3}$ for short periods on September 2 and 3; the sources of these events are

unknown. A spike in GOM and a slight increase in PBM happened to coincide with a college football game (and associated barbeques, vehicular traffic, foot traffic disturbing the ground, etc.); the stadium is adjacent to the monitoring station. GEM seemed to decrease during the game compared to immediately before and after the event, possibly due to limited traffic (foot and vehicular) around the sampling station. A rain event on September 4 caused the GOM and PBM to decrease dramatically. A spike in PBM coincided with a wind event from the north with an average speed of 9.2 mph. Finally, another peak in GOM and PBM occurred during the day on 6 September, the day after the Labor Day holiday when the university resumed session. Overall, this illustrates that the levels of mercury species in the atmosphere on any given day depend on a number of factors including the environmental behaviour/chemistry of the individual species, local activities/sources, meteorological conditions, time of day, and seasonal trends (discussed earlier).

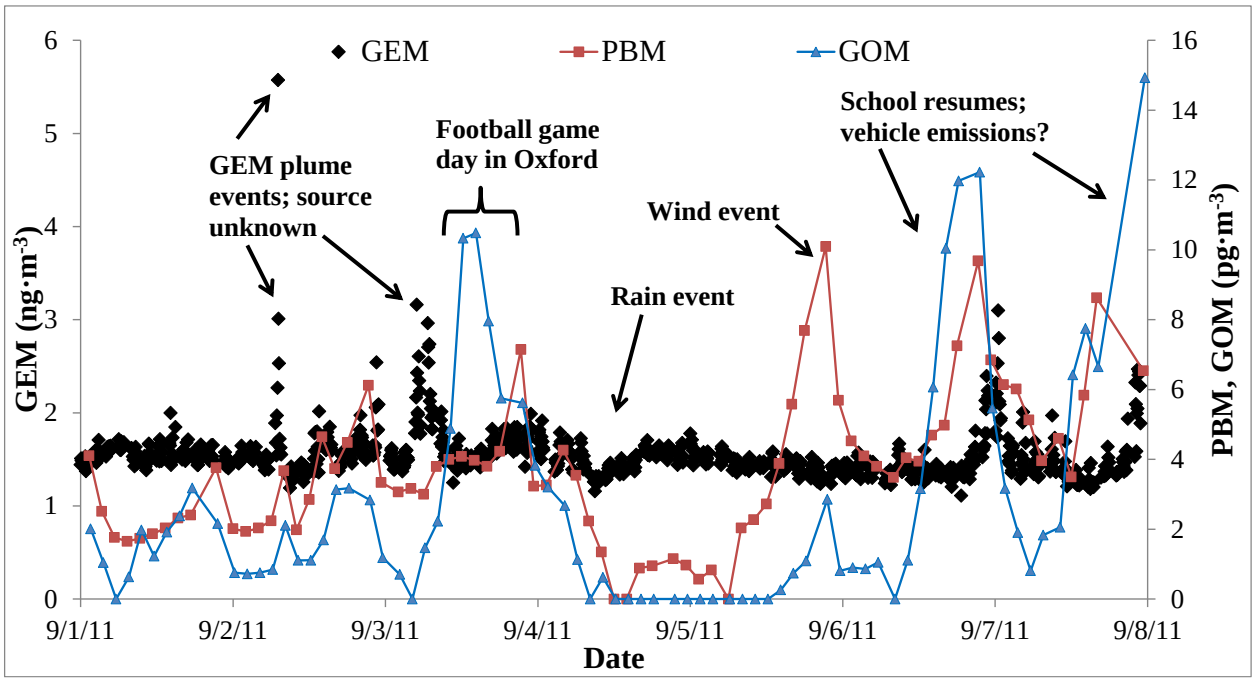

Figure 12. Temporal fluctuations of airborne mercury species during a typical school week at the University of Mississippi

2.4.4 Correlation between mercury species and weather

Pearson correlation coefficients between daily averages for mercury species and select meteorological parameters were determined on a seasonal basis and for the year-long dataset (Table 10). GEM concentrations were relatively insensitive to weather conditions, with no significant correlations for the total results. This was expected because GEM is relatively inert and is sparingly soluble in water. For spring and summer, there was a moderate negative correlation for GEM and wind speed. Wind speed also was negatively correlated with GOM and PBM for several seasons. Indeed, wind speed has been shown to be a major factor in mercury concentration variation, with lower wind increasing residence time in the boundary layer leading to higher levels in certain sampling hours (Liu et al. 2002), and this is likely a factor in the current data as well.

Table 10. Pearson correlation coefficients for mercury species and meteorological variables based on daily averages. Numbers in bold and italic represents r values with $p<0.05$. WDD=Wind Direction Degree

Season	Species	Temp.	Dew Point	Humidity	Pressure	Visibility	Wind Speed	WDD
Spring	GEM	0.29	0.25	0.23	-0.17	-0.08	***-0.55***	-0.10
	PBM	***-0.79***	***-0.62***	-0.19	0.06	0.10	-0.34	***0.75***
	GOM	***-0.52***	***-0.68***	***-0.76***	***0.81***	0.24	***-0.72***	***-0.52***
Summer	GEM	0.48	0.49	0.13	-0.12	-0.12	***-0.53***	-0.09
	PBM	-0.35	***-0.63***	***-0.54***	0.09	0.13	0.09	-0.31
	GOM	0.10	-0.40	***-0.64***	-0.13	0.12	0.09	-0.06
Fall	GEM	-0.21	-0.30	-0.14	-0.31	0.37	0.02	0.18
	PBM	-0.39	***-0.62***	-0.43	-0.10	0.16	-0.10	0.29
	GOM	-0.39	-0.30	0.07	***0.50***	-0.02	-0.34	0.10
Winter	GEM	-0.49	-0.42	-0.05	***0.59***	-0.02	-0.32	-0.12
	PBM	-0.43	***-0.71***	***-0.67***	***0.64***	0.25	***-0.58***	-0.10
	GOM	-0.17	***-0.52***	***-0.77***	0.42	0.29	-0.50	-0.02
Total	GEM	0.29	-0.12	-0.42	-0.20	0.13	-0.27	-0.14
	PBM	-0.19	***-0.62***	***-0.51***	0.05	0.26	-0.12	***-0.55***
	GOM	0.34	-0.45	***-0.68***	-0.24	0.15	0.01	0.03

For GOM, which is soluble in water, there was a significant correlation (r=-0.68) with humidity and sometimes dew point (r=-0.68, spring; r=-0.52, winter). Indeed, precipitation events clearly have a large impact on GOM (and PBM) because of their solubility and capability to be washed from the air (see Figure 12 for example). During the spring, GOM was moderately to highly correlate with all meteorological variables except visibility. PBM was also significantly correlated with a number of parameters; for example, during the winter PBM was significantly negatively correlated with humidity (r=-0.67), dew point (r=-0.71), and wind speed (r=-0.58) and highly positively correlated with pressure (r=0.64). PBM was highest in the spring, a season when pollen is highest; though the relationship between pollen events and PBM needs further investigation.

With regard to wind direction, we observed that major spikes in GOM and PBM, species which often have anthropogenic sources, tended to occur when the wind direction was generally from the north. This was further confirmed through back-trajectory calculations, the results of which are provided below.

2.4.5 Back-trajectory HYSPLIT results

Backward trajectories indicated that the air masses during plume events generally originated either from northern continental (dominated by terrestrial sources) or, less frequently, from the south (e.g., the Gulf of Mexico) (Figure 13). Air masses originating from northern continental region accounted for the majority of the highest plume events. At least 7 of the 10 highest events for each mercury species occurred when air masses originated from north or west, passing directly over urban and industrial areas in western Tennessee and eastern Arkansas. Moreover, examining backward trajectories for the 10 lowest GEM events, and 10 separate days when GOM and PBM averaged about one standard deviation below the mean, showed the

opposite trend with lines generally stemming from the south or with short lines indicating stable air masses during the period (Figure 13). This was most evident with PBM where at least 7 of the 10 events occurred with air masses from the south. This finding, along with other data collected from a Gulf coast site (Malcolm et al. 2003), suggests that air masses from the Gulf of Mexico are generally low in mercury relative to air masses travelling over continental (terrestrial) locations.

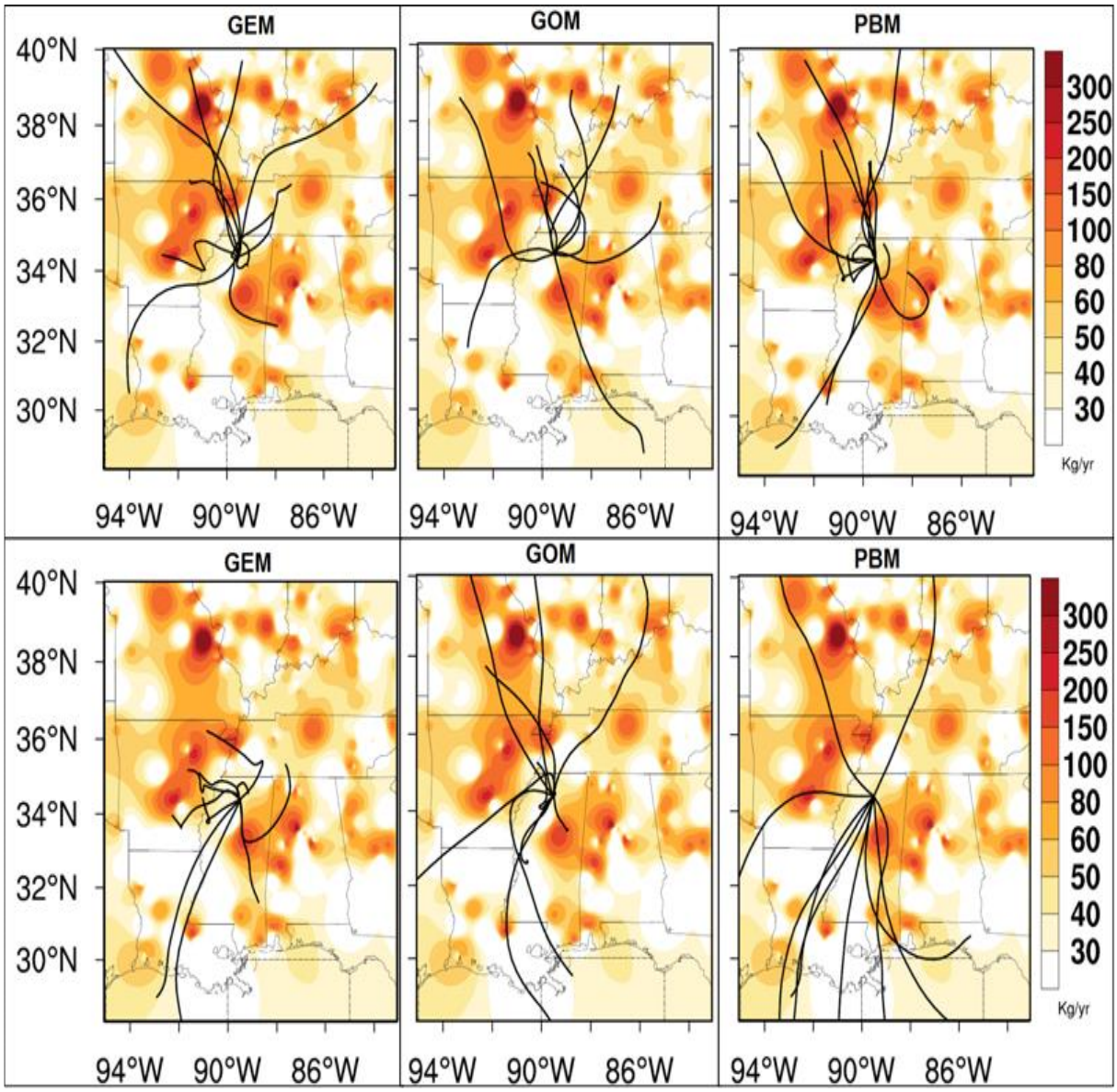

Figure 13. Mercury emission distribution (shaded contours) and 24 hour HYSPLIT backward air mass trajectories (dark lines) for the ten highest events for each species (top row) and the ten lowest cases of GEM and when GOM and PBM were about one standard deviation below the mean and relatively stable (bottom row) in Oxford, MS from July 2011-June 2012. A travelling height of 500 m was used in the calculation (see text for other modeling details)

2.4.6 CMAQ modelling work

Also we conducted a sensitivity study where all anthropogenic Hg emission within a radius of 500 km from Oxford, Mississippi was removed for simulation in order to separate the influence on ambient concentration of regional anthropogenic Hg emissions from background contributions. The air quality model runs for both summer and winter seasons by inputting the modified Hg emission while keeping other inputs identical with standard simulations. Figure 14 shows the percent contributions for ambient GEM, GOM, and PBM. The contribution percentages were obtained by the difference between modified emission simulations and the standard simulations. As expected, the ambient concentrations of GEM, GOM, and PBM are decreased over the whole domain area in the modified emission simulation. For GEM (Fig. 14a), ambient concentrations dropped by approximate 10–20 % over most areas within 500 km from Oxford, Mississippi. Beyond these areas, concentrations fell by less than 10 %. On the other hand, ambient GOM concentration decreased by 20–40 % in most areas while PBM dropped by 40–60 %. For both GOM (Fig. 14b) and PBM (Fig. 14c), the greatest decrease in concentrations appeared over the region from south-western Tennessee, Arkansas to eastern Louisiana, which is consistent with the locations of large anthropogenic emissions (Figure 9).

Our results suggest that anthropogenic Hg sources significantly impact the local/regional ambient Hg concentrations, especially for GOM and PBM. This conclusion agrees well with other studies. By investigating North American anthropogenic Hg emission influence on deposition, Zhang et al (2012) found that anthropogenic sources account for 22 % of the Hg wet deposition flux and 20 % of the dry deposition flux in the contiguous USA but 30–60% in the industrial areas. Seigneuret al (2004) also presented a similar conclusion about the anthropogenic Hg impact on North American deposition. They found that anthropogenic emissions are

responsible for 24 % of wet deposition and 43 % of dry deposition flux. After studying the impact of a CFPP shutdown over 4 months in Rochester, New York, Huang et al (2010) found that the CFPP significantly influenced local Hg concentrations. When the CFPP was closed, median concentrations of GEM, GOM, and PBM apportioned to the CFPP factor decreased significantly by 25, 74, and 67 %, respectively, compared to those measured when the CFPP was still in operation (Wang et al. 2013).

The great influence of anthropogenic sources in Hg concentration implies that modeled errors are highly sensitive to the uncertainties associated with the anthropogenic emission inventory used in the air quality modeling system. In addition, anthropogenic sources seem to have a greater impact on GOM and PBM than GEM. This is because the emission speciation of Hg has a profound impact on the Hg deposition, especially near the emission sources. GEM has a long lifetime in the atmosphere, and its ambient concentration is mainly subject to long-range transport while GOM and PBM concentrations have a significant contribution from local/regional emission sources. Since the natural emission speciation is dominated by GEM, the speciation of anthropogenic emission of Hg has particularly strong implications for ambient GOM and PBM concentrations.

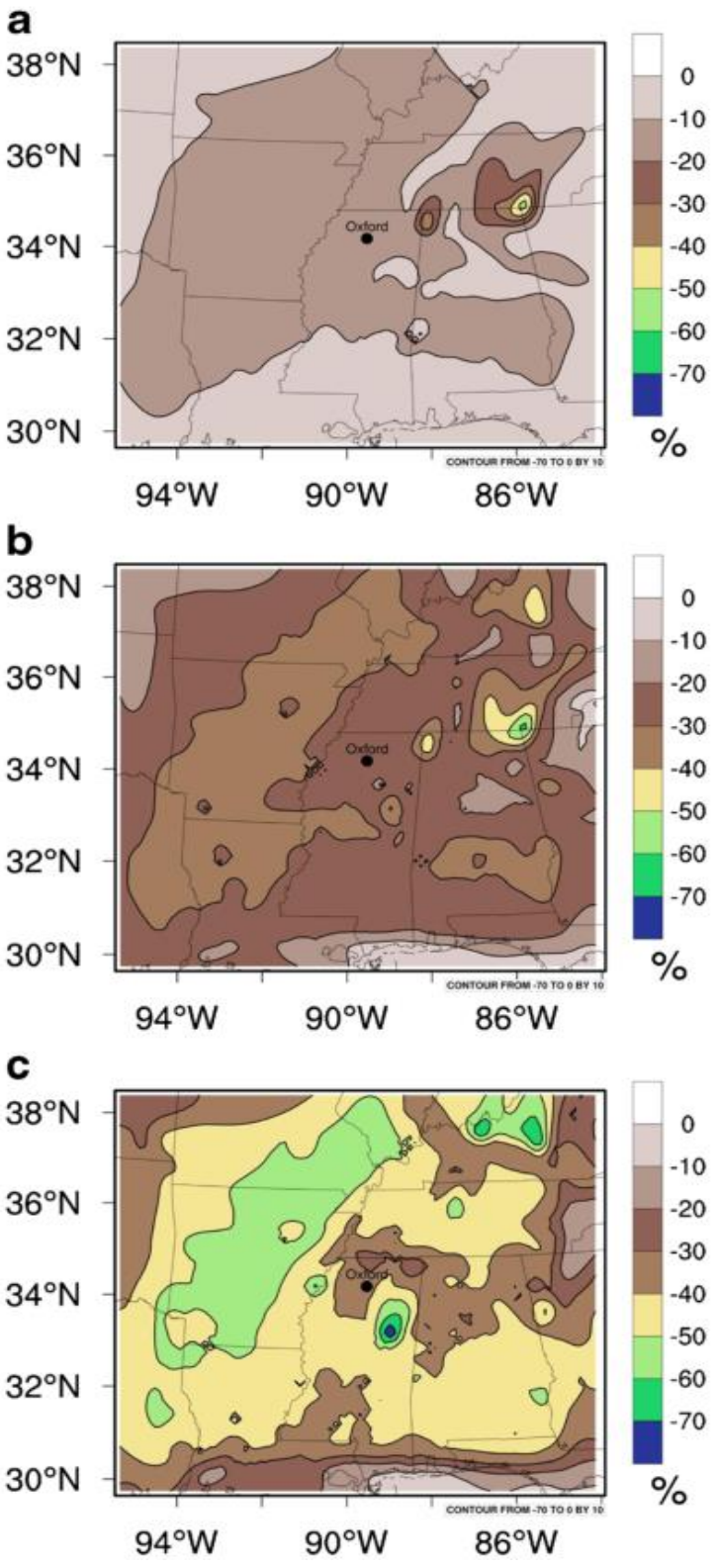

Figure 14. Percent decreases for ambient concentrations of **a** GEM, **b** GOM, and **c** PBM after conducting the sensitivity test

2.4.7 Comparison between observed and modelled ambient Hg concentrations

To compare modeled results for speciated atmospheric with measured ambient levels, Hg concentrations from the lowest model layer (σ=0.997) were extracted from the corresponding grid box of 4-km resolution domain. Observed GEM levels averaged about 1.51 $ng \cdot m^{-3}$ during the summer and 1.63 $ng \cdot m^{-3}$ in the winter. This is consistent with other published measurements of global GEM background levels over the US (Seigneur et al. 2006), reflecting that the background levels used in model boundary and initial conditions for Hg are reasonable. Higher Hg levels in winter can be partly attributable to coal and natural gas combustion, increased wood burning, weakened sinks due to the lower atmospheric oxidative capacity, and poor vertical mixing caused by a decreased boundary layer height during the cold season (Lan et al. 2012).

The CMAQ model overestimated GEM concentration during summer (Fig. 15a) but underestimated it during winter (Fig. 15b). The model seems to lack the ability to capture observed variations, especially during winter. This is in agreement with other modeling studies focusing on urban areas (Lin et al. 2010). Most regional photochemical models cannot capture GEM peaks observed at ground levels caused by emissions, because of model assumptions for instantaneous emission dilution in grid cells (Pongprueksa et al. 2008).

Compared to GEM, the model had a better performance in GOM simulations with relatively high R values of 0.32 and 0.36 during summer and winter. The GOM concentrations were significantly high biased in summer and decreased levels in the winter (Fig. 16a and Fig. 16b). Lin et al (2010) suggested that the overestimate of reactive Hg could be attributed to the production of GOM from oxidation of GEM, uncertainty in emission speciation, low deposition velocity of reactive species, and/or the possible of residual photochemistry activities off the continent. GEM is relatively unreactive species of Hg. Relatively little GEM gets deposited

through deposition. GOM dominates in the wet deposition of Hg. Possible errors could exist in the model chemical mechanism; for example, the removal process (i.e., through dry deposition), lack of particle to gas partitioning of atmospheric Hg, and/or important missing chemical relationships were not yet incorporated into CMAQ.

For PBM concentration, CMAQ model produced a significant overestimate in both summer and winter. The ANB values are 225% and 99% for summer and winter respectively. For both months, CMAQ model overestimated daily peak and lowest concentrations for most cases (Fig. 17a and Fig. 17b). Observed mean PBM concentrations were higher in the winter (7.2 $pg \cdot m^{-3}$) than in the summer (5.1 $pg \cdot m^{-3}$). Rutter et al (2008) explained that increased PBM concentrations in the winter are due to fewer particles for gas partitioning of reactive Hg because of lower ambient temperatures during the winter.

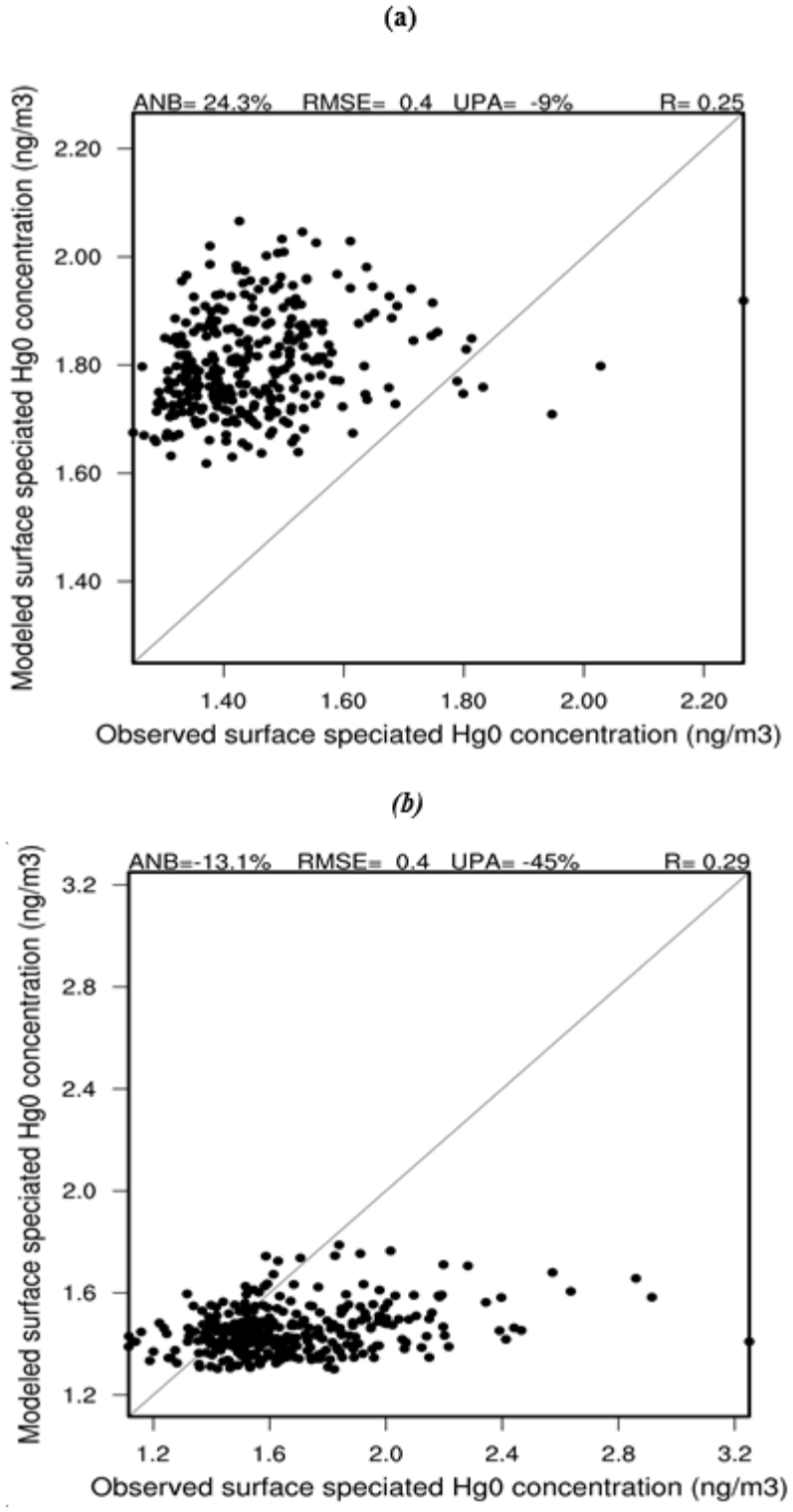

Figure 15. Hourly atmospheric ambient GEM concentration from model and observations in July 2011 (**a**) and February 2012 (**b**)

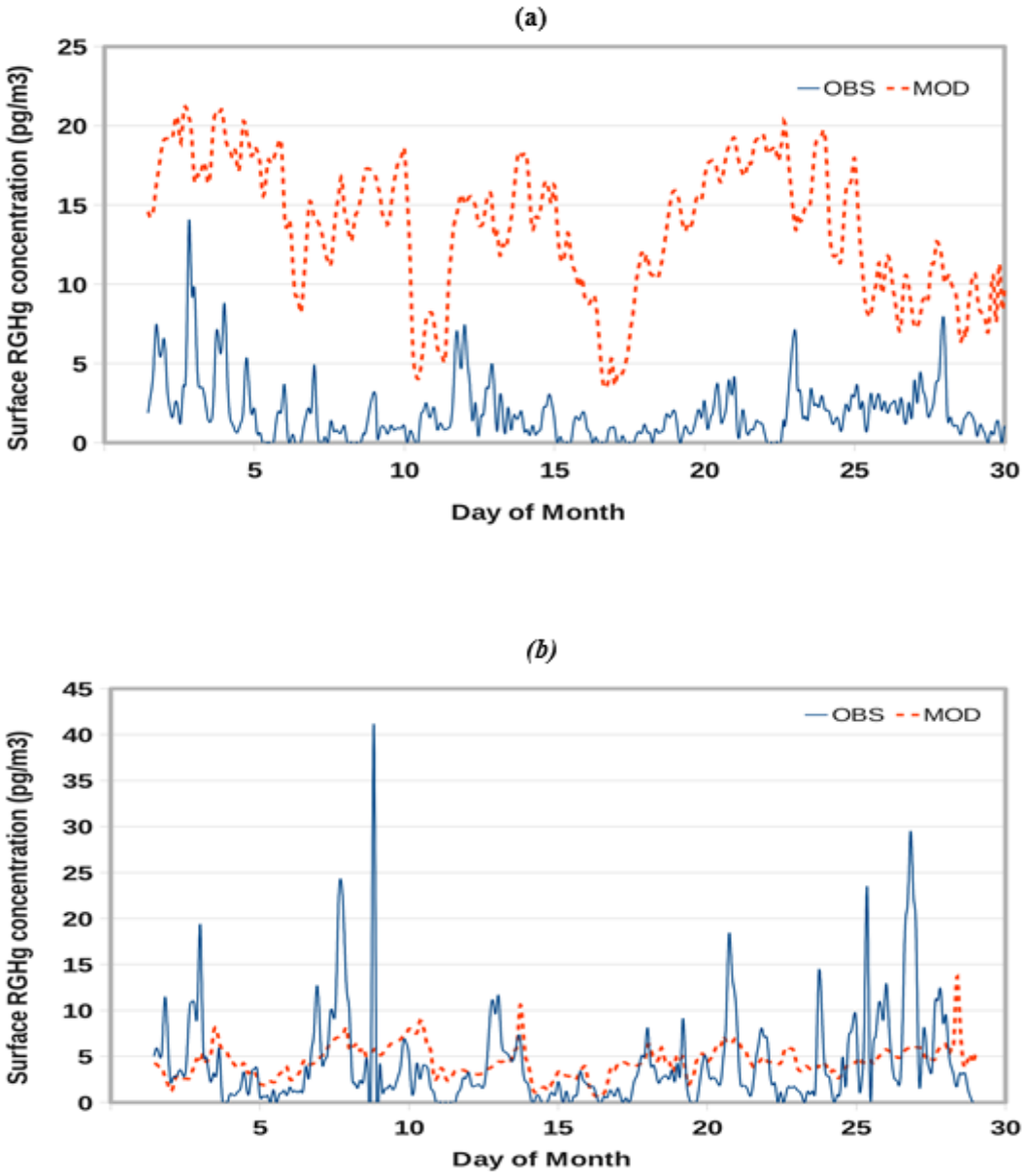

Figure 16. Time series of GOM from model and observed are displayed in **a** and **b** for July 2011 and February 2012, respectively

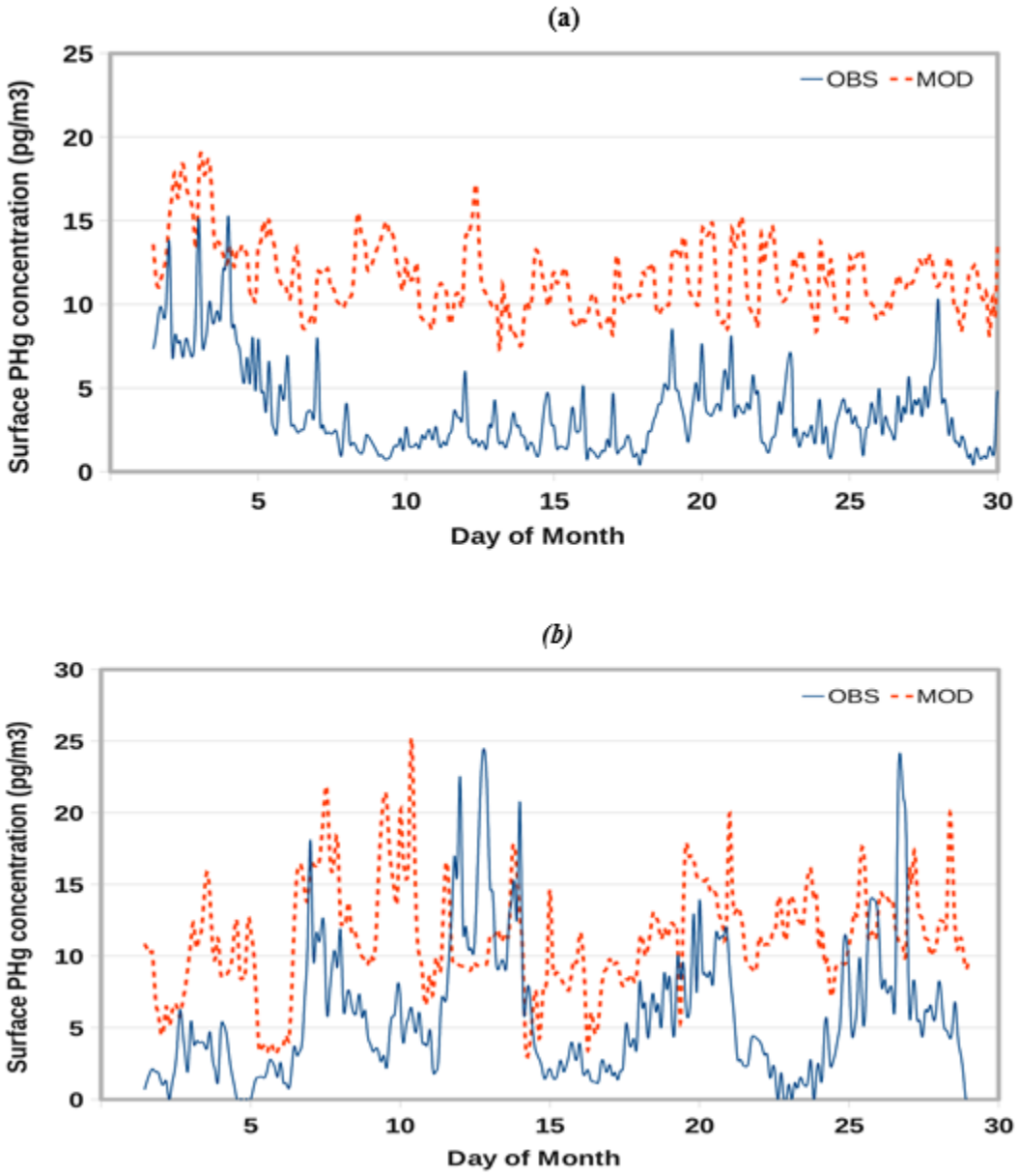

Figure 17. Time series of PBM from model and observed are displayed in **a** and **b** for July 2011 and February 2012, respectively

2.5 CONCLUSIONS

Measurements of airborne mercury species measured in Oxford, Mississippi indicate that GEM levels are 1.54 ± 0.32 ng·m^{-3} with occasional spikes in concentration, the largest of which tend to occur during air mass transport from the north, including industrial areas around Memphis, TN, the closest large city. For GOM and PBM, there appears to be additional localized sources because their concentrations and variability increased during the fall and winter semesters and decreased when students were not on campus. Thus, an influx of a mere 25,000 people or so is sufficient to influence local concentrations of airborne Hg species in a small town environment. Snapshots of airborne Hg data during the fall semester illustrate temporal patterns and the influence of local sources and meteorological conditions on Hg species.

The CMAQ model reproduced reasonable background concentrations for GEM, though slightly overestimating it in the summer and slightly underestimating it in the winter. Compared to GEM, the model performed better for the GOM simulations, effectively capturing seasonal variability. For PBM, the CMAQ model significantly overestimated the levels in both the summer and winter. We conducted a sensitivity test where all anthropogenic Hg emissions within a radius of 500 km from the site were removed from the simulation. Ambient levels of GEM, GOM, and PBM decreased over the whole domain area in both the summer and winter. Anthropogenic emissions accounted for~10–20% of GEM concentrations. Anthropogenic Hg sources had a relatively greater impact on the local/regional ambient GOM (~20-40%) and PBM (~40-60%). The relatively large influence of anthropogenic sources in Hg concentration implies that errors in the model results are highly sensitive to the uncertainties in anthropogenic emission inventories. Thus, the model would greatly benefit from more up-to-date emission data (i.e., release of inventory data by the government in a more-timely manner).

2.6 ACKNOWLEDGMENTS

Duanjun Lu, Loren White, and Remata Reddy, all from Jackson State University, were responsible for the numerical modelling work. We thank L. Hawkins and E. Prestbo (Tekran Inc.), M. Olson (National Atmospheric Deposition Program), and M. Cohen for advice on using the speciation system and for discussion of ambient mercury measurements. We also thank Zhen Guo (Geology Department of the University of Mississippi) for his support of mapping the mercury emission sources. Funding granted by U.S. Environmental Protection Agency (#CD-95450510-0).

2.7 LIST OF REFERENCES

Baker, K. R., Bash, J. O., **2012**. Regional scale photochemical model evaluation of total mercury wet deposition and speciated ambient mercury. *Atmos. Environ.*, 49, 151–162, doi:10.1016/j.atmosenv.2011.12.006.

Bash, J. O., **2010**. Description and initial simulation of a dynamic bidirectional air-surface exchange model for mercury in Community Multiscale Air Quality (CMAQ) model. *J. Geophys. Res.* 115, 1–15. doi:10.1029/2009JD012834.

Byun, D. W., Ching, J. K. S., **1999**. Science algorithms of the EPA Models-3 Community Multiscale Air Quality Model (CMAQ) modeling system. EPA/600/R-99/030, US Environmental Protection Agency, Office of Research and Development, Washington, DC, 20460.

Cheng, C. J., Tonnesen, G. S., Wang, B., Wang, Z. S., Omary, M., **2002**. Evaluation and Intercomparison of N_2O_5 Chemistry in Two Versions of CMAQ, Model-3 User Workshop.

Choi, H. D., Holsen, T. M., **2009**. Gaseous mercury fluxes from the forest floor of the Adirondacks. *Environ. Pollut.* 157, 592–600.

Dadhia, J., **1989**. Numerical study of convection observed during the Winter Monsoon Experiment using a mesoscale two-dimensional model. *J. Atmos. Sci.* 46, 3077-3107.

Draxler, R. R., Hess, G. D., **1997**. Description of the HYSPLIT_4 modeling system. NOAA Technical Memorandum, ERL, ARL-224, http://www.arl.noaa.gov/ready/hysplit4.html.

Dvonch, J. T., Graney, J. R., Marsik, F. J., Keeler, G. J., and Stevens, R. K., **1998**. An investigation of source-receptor relationships for mercury in South Florida using event precipitation data. *Sci. Total Environ.* 213, 95-108.

Ferrier, B. S., Jin, Y., Black, T., Rogers, E., DiMego, G., **2002**. Implementation of a new grid-scale cloud and precipitation scheme in NCEP Eta model. Preprints, 15th Conf. on Numerical Weather Prediction, San Antonio, TX, *Amer. Meteor. Soc.*, 280–283.

Friedli, H. R., Arellano Jr, A. F., Geng, F., Cai, C., and Pan, L., **2009**. Measurement of atmospheric mercury in Shanghai during September 2009. *Atmos. Chem. Phys*. 11, 3781-3788.

Holloway, T., Voigt, C., Morton, J., Spak, S. N., Rutter, A. P., Schauer, J. J., **2012**. An assessment of atmospheric mercury in the Community Multiscale Air Quality (CMAQ) model. *Atmos. Chem. Phys. Discuss.* 12, 2131–2166.

Holmes, D. C., Jacob, D. J., Corbitt, S. E., Mao, J., Yang, X., Talbot, R., Slemr, F. **2010**. Global atmospheric model for mercury including oxidation by bromine atoms. *Atmos. Chem. Phys*. 10, 12037-12057.

Houyoux, M. R., Vukovich, J. M., Coats, C. J., **2001**. Emission inventory development and processing for the Seasonal Model for Regional Air Quality (SMRAQ) project. *J. Geophys. Res*. 105, 9079-9090.

Hoyer, M., Baldauf, W. R., Scarbro C., Barres, J., Keeler, G. J., **2004**. Mercury emissions from motor vehicles. International Emissions Inventory Conference, *Air Toxic Session*, Clearwater, FL. http://www.epa.gov/ttn/chief/conference/ei13/toxics/hoyer.pdf

Huang, J., Choi, H.-D., Hopke, P. K., and Holsen, T. M., **2010**. Ambient mercury sources in Rochester, NY: results from principle components analysis (PCA) of mercury monitoring network data. *Environ. Sci. Technol*. 44, 8441–8445.

Kain, J, S., Fritsch, J. M., **1993**. Convective parameterization for mesoscale models: The Kain-Fritsch scheme. The Representation of Cumulus Convection in Numerical Models. *Meteor. Monogr.* 46, Amer. Meteor. Soc., 165-170.

Keeler, G., Glinsorn, G., Pirrone, N., **1995**. Particulate mercury in the atmosphere: its significance, transport, transformation and sources.Water, *Air and Soil Pollut.* 80, 159–168.

Lan, X., Talbot, R., Castro, M., Perry, K., Luke, W., 2012. Seasonal and diurnal variations of atmospheric mercury across the US determined from AMNet monitoring data. *Atmos. Chem. Phys.* 12, 10569–10582.

Landis, M. S., Stevens, R. K., Schaedlich, F., Prestbo, E. M., **2002**. Development and characterization of annular denuder methodology for the measurement of divalent inorganic reactive gaseous mercury in ambient air. *Environ. Sci. Technol.* 36, 3000-3009.

Liang, L., Horvat, M., Danilchik, P., **1996**. A Novel Analytical Method for Determination of Picogram Levels of Total Mercury in Gasoline and Other Petroleum Based Products. *Sci. Tot. Environ.* 187, 57-64.

Lin, C. J., Ho, T. C., Chu, H., Yang, H., Mojica, M. J., Krishnarajanagar, N., Chandru, S., Chiou, P., Hopper, J. R., **2005**. Sensitivity analysis of ground-level ozone concentration to emission changes in two urban regions of southeast Texas. *J. of Environ Manag*. 75, 315-323.

Lin, C. J., Pongprueksa, P., Lindberg, S. E., Pehkonen, S. O., Byun, D., and Jang, C., **2006**. Scientific uncertainties in atmospheric mercury models I: Model science evaluation. *Atmos. Environ.* 40, 2911–2928.

Lin, C. J., Pan, L., Streets, D. G., Shetty, S. K., Jang, C., Feng, X., Chu, H. W., Ho, T. C., **2010**. Estimating mercury emission outflow from East Asia using CMAQ-Hg. *Atmos. Chem. Phys*. 10, 1853–1864, doi:10.5194/acp-10-1853-2010.

Lindberg, S., Bullock, R., Ebinghaus, R., Engstrom, D., Feng, V., Fitzgerald, W., Pirrone, N., Prestbo, E., Seigneur, C., **2007**. A synthesis of progress and uncertainties in attributing the sources of mercury in deposition. *Ambio.* 36, 19–32.

Liu, S., Nadim, F., Perkins, C., Carley, J. R., Hoag, E. G., Lin, Y., Chen, L., **2002**. Atmospheric mercury monitoring survey in Beijing, China. *Chemosphere*. 48, 97-107.

Lu, D., Reddy, R. S., Fitzgerald, R., Stockwell, W. R., Williams, Q. L., Tchounwou, P. B., **2008**. Sensitivity modeling study for an ozone occurrence during the 1996 Paso del Norte ozone campaign. Int. *J. Environ. Res. Public Health*. 5, 181-203.

Lu, D., Fitzgerald, R., Stockwell, W. R., Reddy, R. S., White, L., **2012**. Numerical Simulation for a Wind Dust Event in the US/Mexico Border Region, *Air Quality. Atmosphere and Health*, DOI 10.1007/s11869-012-0174-7.

Lynam, M. M., Keeler, G. J., **2005**. Automated speciated mercury measurements in Michigan. *Environ. Sci. Technol.* 39, 9253–9262.

Lyman, N. S., Gustin, S. M., Pretsbo, M. E., Marsik, J. F., **2007**. Estimation of Dry Deposition of Atmospheric Mercury in Nevada by Direct and Indirect Methods. *Environ. Sci. Technol.* 41, 1970-1976.

Malcolm, E. G., Keeler, G. J., Landis, M. S., **2003**. The effects of the coastal environment on the atmospheric mercury cycle. *J. Geophys. Res.* 108, 4357. DOI:10.1029/2002JD003084.

Mlawer, E. J., Taubman, S. J., Brown, P. D., Iacono, M. J., Cloμgh, S. A., **1997**. Radiative transfer for inhomogeneous atmosphere: RRTM, a validated correlated-k model for the long-wave. *J. Geophys. Res.* 102 (D14), 16663-16682.

Nair, U. S., Wu, Y., Holmes, C. D., Ter Schure, A., Kallos, G., Walters, J. T., **2013**. Cloud-resolving simulations of mercury scavenging and deposition in thunderstorms. *Atmos. Chem. Phys.* 13, 10143–10157.

Noh, Y., Cheon, W. G., Hong, S. Y., Raasch, S., **2003**. Improvement of the K-profile model for the planetary boundary layer based on large eddy simulation data. *Bound.-Layer Meteor.* 107, 401–42.

Peterson, C., Gustin, M., Lyman, S., **2009**. Atmospheric mercury concentrations and speciation measured from 2004 to 2007 in Reno, Nevada, USA. *Atmos. Environ.* 43, 4646-4654.

Peterson, G., Iverfeldt, A., Munthe, J., **1995**. Atmospheric mercury species over central and northern Europe. Model calculations and comparison with observations from the Nordic air and precipitation network for 1987 and 1988. *Atmos. Environ.* 29, 47-67.

Pirrone, N., Cinnirella, S., Feng, X., Finkelman, R. B., Friedli, H. R., Leaner, J., Mason, R., Mukherjee, A. B., Stracher, G. B., Streets, D. G., and Telmer, K., **2010**. Global mercury emissions to the atmosphere from anthropogenic and natural sources. *Atmos. Chem. and Phys.* 10, 5951-5964.

Pongprueksa, P., Lin, C. J., Lindberg, S. E., Jang, C., Braverman, T., Bullock, O. R., Ho, T. C., Chu, H. W., **2008**. Scientific uncertainties in atmospheric mercury models III: Boundary and initial conditions, model grid resolution, and Hg(II) reduction mechanism. *Atmos. Environ.*, 42(8), 1828-1845.

Rolison, J. M., Landing, W. M., Luke, W., Cohen, M., Salters V. M., **2013**. Isotopic composition of species-specific atmospheric Hg in a coastal environment. *Chem. Geol.* 336, 37-49.

Rutter, A. P., Schauer, J. J., Lough, G. C., Snyder, D. C., Kolb, C. J., Von Klooster, S., Rudolf, T., Manolopoulos, H., Olson, M. L., **2008**. A comparison of speciated atmospheric mercury at an urban center and an upwind rural location. *J. Environ. Monit.* 10(1), 102-108.

Schroeder, W. H., Munthe, J., **1998**. Atmospheric mercury – an overview. *Atmos. Environ.* 32, 809–822.

Seigneur, C., Vijayaraghavan, K., Lohman, K., Karamchandani, P., Scott, C., **2004**. Global source attribution for mercury deposition in the United States. *Environ. Sci. Technol.* 38, 555–569.

Seigneur, C., Vijayaraghavan, K., Lohman, K., **2006**. Atmospheric mercury chemistry: Sensitivity of global model simulations to chemical reactions. *J. Geophys. Res.-Atmos*. 111(D22), 2006.

Sillman, S., Marsik, F. J., Al-Wali, K. I., Keeler, G. J., Landis, M. S., **2007**. Reactive mercury in the troposphere: model formation and results for Florida, the northeastern United States, and the Atlantic Ocean. *J. Geophys. Res*. 112, D23305.

Skamarock, W. C., Klemp, J. B., Dudhia, J., **2001**. Prototypes for the WRF (Weather Research and Forecasting) model. Reprints, Ninth Conf. on Meso-scale Processes, Fort Lauderdale, FL. *Amer. Meteor. Soc*. J11-J15.

Soerensen, A. L., Skov, H., Jacob, D. J., Soerensen, B. T., Johnson, M. S., **2010**. Global concentrations of gaseous elemental mercury and reactive gaseous mercury in the marine boundary layer. *Environ. Sci. Technol.* 44, 7425-30.

Stamenkovic, J., Lyman, S., Gustin, M. S., **2007**. Seasonal and diel variation of atmospheric mercury concentrations in the Reno (Nevada, USA) airshed. *Atmos. Environ*. 41, 6662–6672.

Ullrich, M. S., Tanton, W. T., Abdrashitova, A. S., **2001**. Mercury in the aquatic environment: a review of factors affecting methylation. *Environ. Sci. Technol*. 31, 241-293.

US EPA. **2010**. Toxics Release Inventory. http://www.epa.gov/tri/.

Valente, R. J., Shea C., Humes K. L., Tanner R. L., **2007**. Atmospheric mercury in the Great Smoky Mountains compared to reginal and global levels. *Atmos. Environ*. 41, 1861-1873.

Wang, Y., Huang, J., Hopke, P. K., Rattigan, O. V., Chalupa, D. C., Utell, M. J., Holsen, T., **2013**. Effect of the shutdown of a large coal-fired power plant on ambient mercury species. *Chemosphere*, http://dx.doi.org/10.1016/j.chemosphere.2013.01.024.

Watras, J. C., Back, C. R., Halvorsen, S., Hudson, J. R., Morrison, A. K., Wente. P. S., **1998**. Bioaccumulation of mercury in pelagic freshwater food webs. *Sci. Total Environ*. 219, 183-208.

Wen, D., Lin, J. C., Meng, F., Gbor, P. K., He, Z., Sloan, J. J., **2011**. Quantitative assessment of upstream source influences on total gaseous mercury observations in Ontario. Canada, *Atmos. Chem. Phys*. 11, 1405–1415, doi:10.5194/acp-11-1405-2011.

Weiss-Penzias, P., Jaffe, D. A., McClintick, A., Prestbo, E. M., Landis, M. S., **2003**. Gaseous elemental mercury in the marine boundary layer: evidence for rapid removal in anthropogenic pollution. *Environ. Sci. Technol*. 37, 3755-3763.

West, J. J., Zavala, M. A., Molina, M. J., San Martini, F., McRae, G. J., Sosa-Iglesias, G., Arriaga-Colina, J. L., **2004**. Modeling ozone photochemistry and evaluation of hydrocarbon emissions in the Mexico City metropolitan area. *J. Geophys. Res.* 109, D19312.

Yarwood, G., Rao, S., Tocke, M., Whitten, G. Z., **2005**. Updates to the Carbon Bond Mechanism: CB05. ENVIRON International Corporation, Novato. Report to the U.S. EPA. http://www.camx.com/publ/pdfs/CB05_Final_Report_120805.pdf.

CHAPTER THREE

3. GASEOUS MERCURY EXCHANGE OVER SOILS FROM THE MISSISSIPPI DELTA AND NORTH MISSISSIPPI

3.1 ABSTRACT

To fully understand the global biogeochemical cycling of Hg it is necessary to investigate Hg exchange between terrestrial surfaces and the atmosphere. In this study, gaseous mercury exchange fluxes were determined over landscapes representative of northern Mississippi (agriculture, forest, and wetland) as well as residential lawns. Environmental variables, including air temperature, solar radiation, humidity, wind speed, and pressure were monitored concurrently with the air-surface Hg exchange measurements. Ambient total gaseous mercury (TGM), soil temperature, and soil moisture content were also monitored for select studies. Mercury fluxes were seasonally dependent with net emission during the summer (mean 1.65 ± 1.58 $ng \cdot m^{-2} \cdot h^{-1}$) and lower emission rates (or deposition) during the winter (-0.13 ± 0.15 $ng \cdot m^{-2} \cdot h^{-1}$). Total-Hg levels in the soil ranged from 17.1 $ng \cdot g^{-1}$ for agricultural soil from Lafayette County to 62.7 $ng \cdot g^{-1}$ for wetland sediment, and were correlated (r=0.66) with loss-on-ignition (an estimate of organic matter content). Mean ambient levels of TGM ranged between 0.93-1.48 $ng \cdot m^{-3}$ in the warm season and between 1.13-1.48 $ng \cdot m^{-3}$ in the cold season. Mercury emission fluxes were found to vary diurnally, similar to previous investigations, with higher fluxes during daytime (mostly emissions) and lower but stable mercury fluxes during nighttime. Soil Hg fluxes were significantly lower in dark conditions than in the light for all but the grass. Methods were developed and evaluated to study Hg fluxes under light and dark conditions, and Arrhenius relationships revealed associated activation energies. One of the goals of this work is to scale up emissions from these landscapes (geographically-associated land use areas) but our preliminary work only allows crude estimates due to large uncertainties.

3.2 INTRODUCTION

Gaseous elemental mercury (GEM) consists of over 95% of the mercury in the air, has a residence time of 0.5-2 years, and undergoes long distance transport after emission from the sources (Schroeder et al. 1998). Mercury emission sources include anthropogenic and natural sources. Unlike mercury near point sources which have been studied intensively throughout the world (Estrade et al. 2011; Streets et al. 2005; Pacynaa et al. 2010), non-point sources of mercury are still under-characterized. Natural non-point sources include geologically enriched substrates and active geothermal areas, biomass burning, soil/substrates, lakes, and wetlands (Engle et al. 2006); anthropogenic non-point sources include urban surfaces, industrial landfills, sewage sludge amended soils, and mine wastes (Xin et al. 2006).

In order to understand the global biogeochemical cycling of Hg in the environment it is necessary to investigate its exchange between terrestrial surfaces and the atmosphere. Indeed, measurement of Hg emissions from representative surfaces are crucial to evaluate the role of terrestrial environments in the cycling of Hg on both regional and global scales (Gustin et al. 2003). However, there are relatively few such studies and none in the mid-south USA.

A variety of factors have been shown to influence Hg emissions from soils. Mercury fluxes from natural surfaces (typically reported as ng of Hg emitted or deposited per m^2 per hour) are largely influenced by substrate Hg concentration, sunlight, temperature, atmospheric turbulence, relative humidity, soil moisture content, and vegetation cover (Gustin et al. 2008). Another important factor is reduction of oxidized divalent mercury (Hg^{2+}) in soil and aquatic environments to Hg^0 which is often catalyzed by solar radiation (Fitzgerald et al. 1998).

The present study focused on the characteristics of Hg gas exchange over different types of soil from the mid-south US, including three agricultural fields, a loblolly pine forest, wetland sediment, and grass from a residential lawn.

3.3 MATERIAL AND METHODS

3.3.1 Site description

We investigated mercury fluxes over agricultural soils, wetland sediment, a forest floor, and a residential lawn. The agricultural soils were from the Mississippi Delta and Lafayette County, MS; sediment was from a wetland located near the University of Mississippi; the forest was a commercial loblolly pine forest planted in the 1990's in Oxford, MS; and the lawn (fescue grass) was also in Oxford, MS (Table 11, Figure 18). Due to logistical issues and the difficulty deploying sophisticated instrumentation at remote field sites (e.g., power, security, access, proximity) the mercury flux system was setup at a single site and representative soil samples were brought to the site in large bins (Figure 19), except for the forest where measurements were conducted in-situ (Figure 20). It was important that we measured fluxes outside under natural conditions rather than in a laboratory setting. The system was deployed in the backyard of Dr. Cizdziel's home on the outskirts of town where there are no significant point sources of mercury. Shovels were used to gather soil to a depth of about 1 foot (~30 cm). The soil was placed into large plastic bins and mixed. The bins were covered and brought to the backyard testing site for analysis.

Table 11. Coordinates and description of soil sampling sites

Soil Type	Description	Location	Latitude	Longitude
Agriculture	Cotton field	Lafayette County, MS	34.272125	-89.522294
Grass	Lawn		34.379189	-89.601822
Wetland	Pond edge		34.351175	-89.555886
Forest	Loblolly Pine		34.379406	-89.601697
Agriculture	Dundee	Mississippi Delta	33.395056	-90.682278
Agriculture	Dowling		33.389972	-90.682028

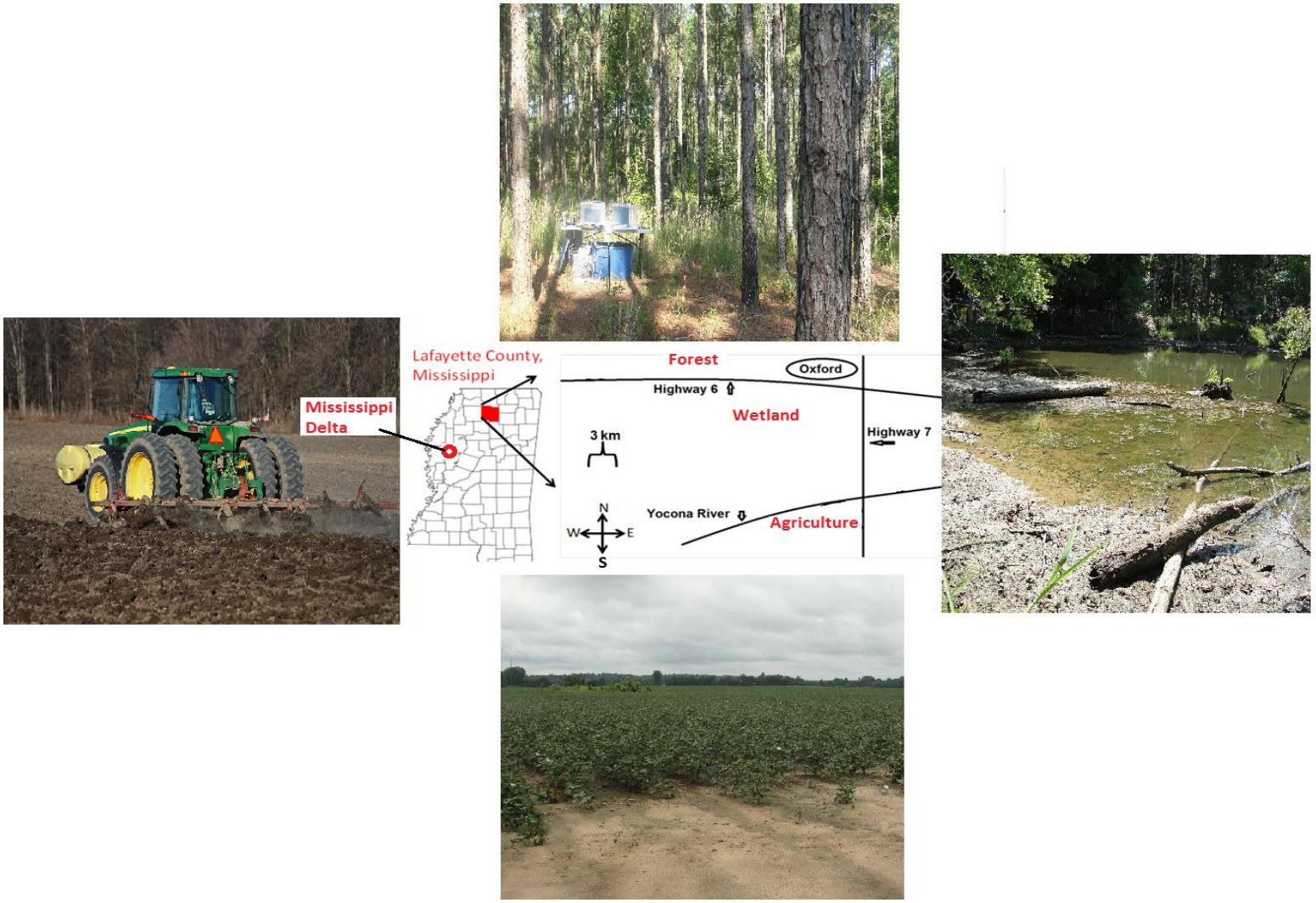

Figure 18. Locations of soil sampling sites in northern Mississippi

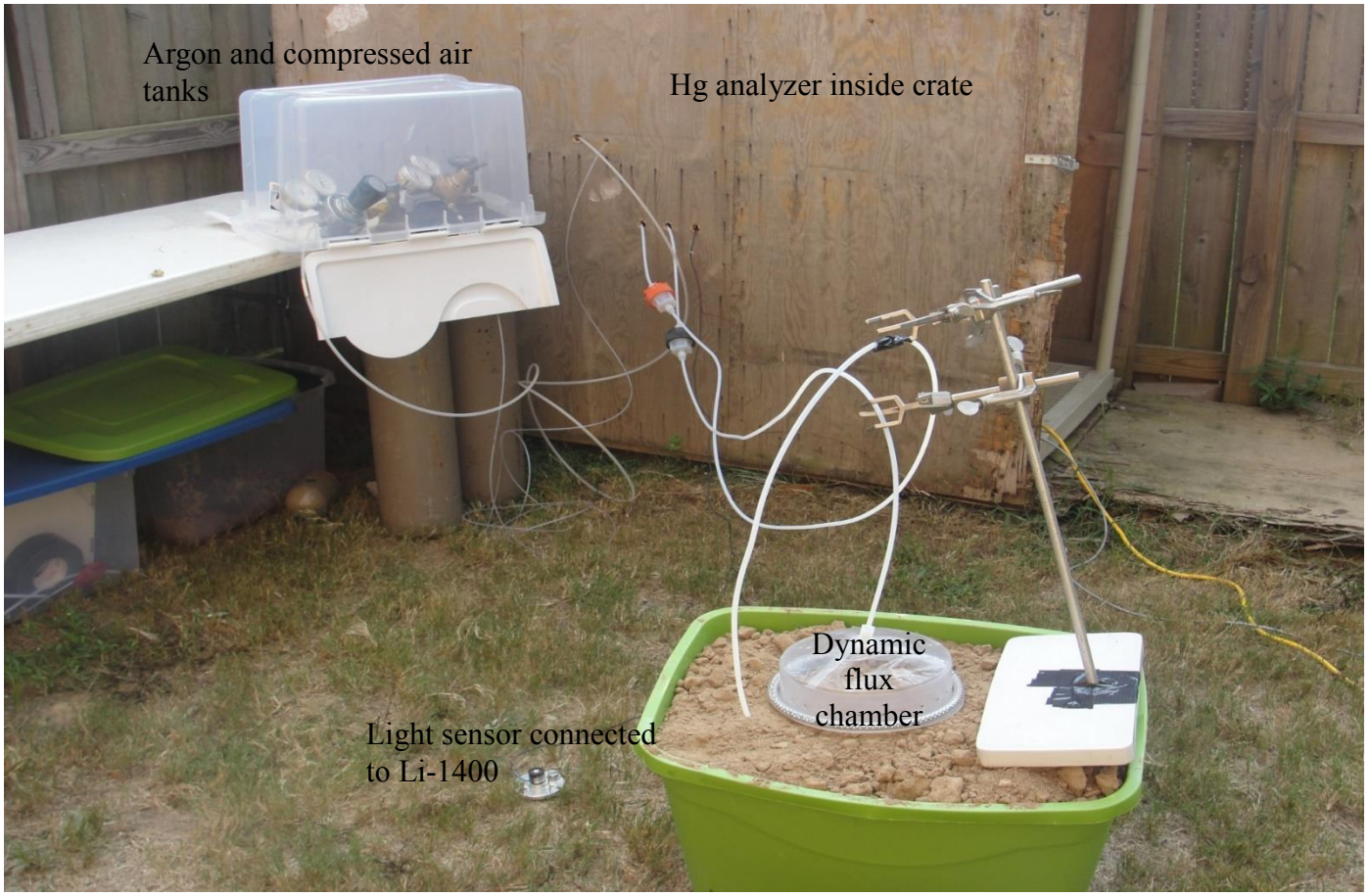

Figure 19. Experimental setup for measuring mercury flux over bare soils. The system was deployed in the backyard of Dr. Cizdziel's home

Figure 20. Measuring mercury flux from a forest floor. Experimental setup (top) and close-up of the dynamic flux chamber showing the air flow direction (bottom)

Three agricultural soils were tested. One of the agriculture fields is located about 8 miles south of Oxford and the University of Mississippi in Lafayette County, nestled in the gentle hills of north Mississippi (elevation 300-400 feet). The other two were from the Mississippi Delta and are classified as Dundee and Dowling soils. Dundee soils consist of poorly drained loamy soils that can be relatively deep. Dowling soils are poorly drained, strongly acid, fine-textured soils on flats or in depressions. Both soils were primarily deposited Mississippi River alluvium, washed in during flood events and deposited in slack-water areas, although some was washed from higher-soils (Soil Survey in Mississippi. 1953). Both of the soils are moderately slowly permeable, and relatively acidic.

3.3.2 Total-Hg and organic matter content measurements

The total-Hg concentration in the soils was determined using a Milestone Direct Mercury Analyzer following US EPA method 7473, which is based on thermal decomposition-atomic absorption spectrometry. The method has been described elsewhere (Fu et al. 2008). Sample boats were pre-heated to remove Hg and blanks were analyzed before testing the samples. Sample were run in triplicate. Loss-on-ignition (LOI) was determined by weighing the sample before and after the combustion analysis. LOI serves as an estimate of organic matter.

3.3.3 Mercury flux measurements

A Teflon dynamic flux chamber (DFC) was used for mercury flux measurements (Figure 19, 20). The DFC is the preferred method because they are portable, simple to deploy, and are not subject to the strict site constraints of the micrometeorological method. A detailed description of the DFC method has been reported elsewhere (Carpi et al. 1998; Lindberg et al. 1999; Eckley et al. 2010). In short, a pump draws air through the DFC (outlet) to a mercury

vapor analyzer. Air is also drawn through a second tube (inlet) outside the DFC for ambient air measurements. The Hg flux is then calculated as:

$$F = Q*(C_o-C_i)/A$$

where F is the Hg flux ($ng \cdot m^{-2} \cdot h^{-1}$), Q is the flushing flow rate through the chamber ($0.09\ m^3 \cdot h^{-1}$) and controlled by a mass flow controller inside the mercury analyzer, C_o is the air Hg concentration at the outlet ($ng \cdot m^{-3}$) and C_i is the air Hg concentration at the inlet, and A is the footprint area of the chamber ($0.036\ m^2$). We used a Tekran model 2537A elemental mercury vapor analyzer and a Tekran Automated Dual Switching Unit (Tekran model 1110) to sequentially sample the air at the DFC inlet and outlet in 10-min intervals providing a data point for Hg flux every 20 min. The inlet sampling tube was placed at the same height as inlet holes on the flux chamber. The inlet measures the concentration of atmospheric mercury, the outlet measures the sum of atmospheric mercury and any mercury either emitted from- or deposited on-the soil surfaces. When the outlet concentration is higher than the inlet concentration, mercury is being emitted from the soil; when the outlet concentration is lower than the inlet concentration, mercury is being deposited on the soil.

The turnover time for the chamber was 1.3 min (less than the 5 min sampling interval). The outlet sampling tube was connected to the top center of the chamber. The Tekran analyzer was routinely calibrated using injections of gaseous elemental mercury in ambient air using a Tekran 2505 Mercury Vapor Calibration Unit; replicate injections of known amounts of mercury produced recoveries > 90%.

Prior to the field measurements, all tubing, fittings and the chamber cover were rinsed with D.I. water and methanol. The mercury flux measurement system was tested before measuring soil samples to ensure that the concentration difference between inlet and outlet was

less than 5% when placed on a clean impermeable Teflon sheet. The system blank was tested before flux measurements were made by using a Teflon sheet, served as the bottom surface for the DFC. The blank results were negligible (mean=0.08 $ng \cdot m^{-2} \cdot h^{-1}$) for the study period, so the flux results are reported without correction for the chamber blanks. The detection limits for the mercury analyzer was 0.1 $ng \cdot m^{-3}$.

3.3.4 Meteorological and solar radiation measurements

Meteorological conditions, including ambient air temperature, wind speed, wind direction, relative humidity, pressure and precipitation, were measured using Vaisala WXT 520 automatic weather station located near the flux chamber (Figure 20). Solar radiation was measured by using Li-1400 Datalogger. Data logging for both systems were programmed to record data at 5 minute intervals to match the analysis interval of the mercury vapor analyzer.

3.4 RESULTS AND DISCUSSION

3.4.1 Total-Hg concentrations in the soils

Mercury concentration in the soil from the different sampling sites is given in Table 12. Concentrations varied between 62.7 ppb for the wetland soil and 17.1 ppb for agricultural soil from a cotton field in Lafayette County, MS. Concentrations were correlated with LOI (organic matter) (Table 12). Total-Hg concentrations in the soil in this study are comparable to other soils in the U.S and Canada (Poissant et al. 1998; Zhang et al. 2001; Nacht et al. 2004; Kuiken et al. 2008), but are lower than soils in China or over naturally enriched terrestrial landscapes (Fu et al., 2008; Fu et al. 2012; Edwards et al. 2013).

Table 12. Total-Hg and loss-on-ignition (LOI) data for soils used in flux measurements

Soil Type	Mercury (ng/g)	SD	LOI (%)
Ag. Lafayette Co.	17.1	0.9	1.27
Grass	26.6	0.2	1.65
Wetland	62.7	0.6	3.05
Forest	40.9	2.9	3.21
Ag. Delta Dundee	21.8	0.9	2.18
Ag. Delta Dowling	42.4	0.7	2.38

3.4.2 Total gaseous mercury concentrations in the ambient air

Total gaseous mercury concentrations in the ambient air (as measured by the inlet tube outside the flux chamber) are summarized in Table 13. Mean TGM concentrations ranged from 0.93 ± 0.40 ng·m^{-2}·h^{-1} to 1.48 ± 0.21 ng·m^{-2}·h^{-1} in the warm season. The mean TGM concentrations were higher in winter season, ranged from 1.13 ± 0.14 ng·m^{-2}·h^{-1} to 1.48 ± 0.19 ng·m^{-2}·h^{-1}. The TGM concentrations were consistent with background levels for the northern hemisphere, which is believed to be ~1.5 ng·m^{-3} (Ericksen et al. 2006). The lowest TGM levels were for grass during the warm season at night. We speculate that the low levels are due to localized deposition of Hg on the vegetation (grass surface). To test this hypothesis, we removed the grass from an area exposing the soil below and alternatively measured the fluxes from the grass and bare soil areas. The mean TGM concentration for the bare soil increased from 0.63 ng·m^{-3} to 1.32 ng·m^{-3}, suggesting that the grass indeed influencing the ambient air Hg levels. In the cold season the ambient levels of TGM over grass were the highest of all the soils (1.48 ± 0.19 ng·m^{-3}) but the fluxes were the lowest (-0.32 ± 0.25 ng·m^{-2}·h^{-1}), again suggesting that vegetation can play an important role on Hg gas exchange.

Table 13. Summary of inlet air total gaseous mercury (TGM) concentrations

Site	Warm Season			Cold Season		
	TGM Concentration (ng·m^{-3})			TGM Concentration (ng·m^{-3})		
	Range	Median	Mean±SD	Range	Median	Mean±SD
Forest	0.44-2.28	1.02	1.06±0.31	1.16-1.37	1.26	1.26±0.05
Grassland	0.20-1.66	0.94	0.93±0.40	1.18-1.99	1.45	1.48±0.19
Agriculture	0.17-1.59	1.08	0.94±0.40	0.90-1.42	1.19	1.19±0.16
Wetland	0.22-1.50	1.18	1.04±0.32	1.13-1.79	1.31	1.32±0.12
Delta(Dundee)	0.69-2.29	1.47	1.48±0.21	1.36-1.61	1.45	1.45±0.06
Delta(Dowling)	0.18-1.89	1.28	1.17±0.47	0.88-1.42	1.12	1.13±0.14

Pearson correlations were conducted between TGM concentrations and surface mercury emission fluxes (Table 14). Significant positive correlations between TGM and mercury fluxes, indicating that the soils are sources of Hg to the air, were observed for forest (warm season), agriculture (warm and cold season), wetland (warm season), Delta Dowling (warm season) soils. The positive correlations are highly influenced by the strong diurnal variations for TGM and Hg emission fluxes (Fu et al. 2012). Significant negative correlations, indicating that the soils are serving as sinks (Hg being deposited from the air), were only found in the winter, and occurred for grass, wetland, and Delta Dundee soils. Negative correlations (deposition) is common in winter with relatively low temperatures. When TGM and Hg emission fluxes were not significantly correlated, other meteorological parameters are likely controlling the Hg exchange rates (discussed below).

Table 14. Pearson correlations for Hg fluxes with meteorological parameters and TGM. Red indicates r values with p<0.05 *Power failure prevented measurements

	Sites	Temperature	Pressure	Humidity	Wind Speed	Solar Radiation	TGM
Warm Season	Forest	0.66	-0.15	-0.69	0.53	0.90	0.61
	Grass	0.25	0.08	-0.34	0.07	0.76	0.18
	Agriculture	0.77	0.32	-0.80	0.67	0.90	0.63
	Wetland	0.69	0.12	-0.68	0.54	0.87	0.50
	Delta (Dundee)	0.77	-0.06	-0.71	0.28	0.77	0.29
	Delta (Dowling)	0.81	-0.08	-0.80	0.62	0.92	0.62
Cold Season	Forest	-0.09	0.08	-0.06	0.05	N/A*	-0.47
	Grass	0.58	0.26	-0.26	0.30	0.40	-0.64
	Agriculture	0.80	-0.35	-0.80	0.47	0.75	0.69
	Wetland	-0.11	0.09	0.13	-0.12	-0.03	-0.74
	Delta (Dundee)	-0.15	0.30	-0.36	-0.11	0.36	-0.56
	Delta (Dowling)	0.52	-0.07	-0.55	0.05	0.53	0.43

3.4.3 Hg fluxes over forest floor

Results for Hg soil/air exchanges at a forest site are summarized in Table 15. During the warm season, there were 139 data points, of which 73 were net emissions. The mean Hg flux from the forest floor was 0.50 ± 1.20 $ng \cdot m^{-2} \cdot h^{-1}$ (Table 15). Most of the net Hg depositions were observed during the winter sampling campaign. The forest flux was generally lower than that measured from other (bare) soils, presumably because the canopy limits the solar radiation reaching the ground. Relationships between mercury fluxes and four main meteorological parameters (temperature, wind speed, humidity, and solar radiation) are plotted in Figure 21. The highest Hg flux (5.63 $ng \cdot m^{-2} \cdot h^{-1}$) was observed at maximum solar radiation, suggesting that thermal and/or photochemical reactions are involved. Indeed, strong correlations were observed in the warm season for mercury emission fluxes with solar radiation ($r=0.90$, $p<0.05$) and temperature ($r=0.66$, $p<0.05$), suggesting that solar radiation has an immediate and predominant effect on mercury emission fluxes from forest soils.

Other parameters that were correlated with Hg emission flux in the summer were humidity ($r=-0.69$, $p<0.05$), wind speed ($r=0.53$, $p<0.05$), and TGM (0.61 $p<0.05$). In contrast, there were no significant correlations observed between mercury emission fluxes and meteorological parameters in cold season, which is likely due to relatively cold temperatures and low levels of solar radiation reaching the ground.

Table 15. Summary statistics for air/soil mercury fluxes over Mississippi soils

Site	Warm Season					Cold Season				
	Sampling period	Hg Flux ($ng \cdot m^{-2} \cdot h^{-1}$)			n for Emission (Deposition)	Sampling period	Hg Flux ($ng \cdot m^{-2} \cdot h^{-1}$)			n for Emission (Deposition)
		Range	Median	Mean±SD			Range	Median	Mean±SD	
Forest	22-25 Aug 2013	(-0.93)-6.71	0.04	0.50±1.20	73(66)	18-19 Dec 2013	(-0.50)-0.12	-0.17	-0.19±0.14	6(69)
Grassland	25-27 Aug 2013	1.34-11.41	4.18	4.38±1.71	125(0)	13-14 Dec 2013	(-0.94)-0.22	-0.32	-0.32±0.25	9(64)
Agriculture	27-29 Aug 2013	0.08-5.46	1.10	1.58±1.37	157(0)	17-18 Dec 2013	(-0.52)-0.50	-0.09	-0.11±0.26	27(50)
Wetland	29-31 Aug 2013	0.63-11.81	1.82	2.54±2.10	140(0)	16-17 Dec 2013	(-0.69)-0.41	0.13	0.10±0.20	58(16)
Delta(Dundee)	17-18 Sep 2013	(-0.58)-2.47	0.18	0.32±0.57	54(31)	14-15 Dec 2013	(-0.43)-0.30	-0.03	-0.03±0.14	33(45)
Delta(Dowling)	18-19 Sep 2013	(-0.52)-4.87	-0.07	0.55±1.48	33(36)	12-13 Dec 2013	(-0.64)-0.24	-0.2	-0.20±0.23	17(54)

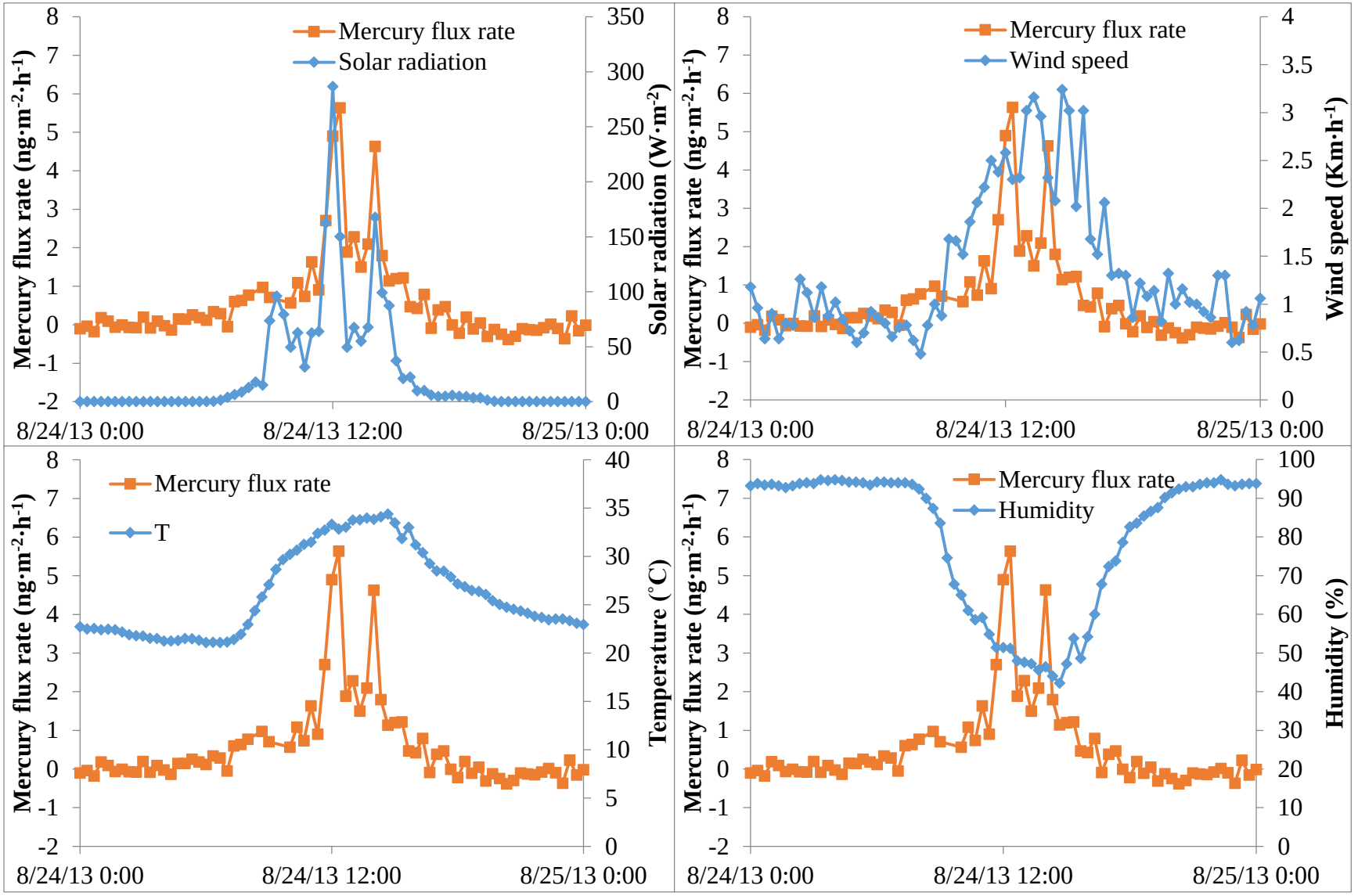

Figure 21. Relationships between Hg flux and solar radiation (top left), wind speed (top right), air temperature (bottom left), and humidity (bottom right) at forest sampling site in warm season.

3.4.4 Hg fluxes over grass

Summary statistics for Hg fluxes between air and grass covered soil is given in Table 15. In the summer, net Hg emission was observed with an average Hg flux of 4.38 ± 1.71 $ng \cdot m^{-2} \cdot h^{-1}$. The difference for Hg fluxes between light and dark conditions was lowest for grass compared to other soils, suggesting that Hg emissions from blades of grass may be contributing to the flux during night under warm conditions. To test this hypothesis, we removed the grass from an area exposing the soil below, and alternatively measured the fluxes from the grass and bare soil areas during the night (Figure 22). The data clearly shows that Hg flux was higher for the grass covered soil. It is unclear why the flux rates increased for the same area during the second test, but in both cases removing the grass lowered the flux rate.

Ericksen et al (2006) proposed that the relatively high fluxes over grassland during night (daytime mean: 4.69 ± 2.38 $ng \cdot m^{-2} \cdot h^{-1}$; nighttime mean: 4.10 ± 0.58 $ng \cdot m^{-2} \cdot h^{-1}$) are unrelated to the decreasing soil temperatures, and rather the high Hg fluxes are the result of the soil Hg pool replenishing in the absence of light. In our study, the Hg emission fluxes from grass ranged from -0.94-0.22 $ng \cdot m^{-2} \cdot h^{-1}$ with an average of -0.32 ± 0.25 $ng \cdot m^{-2} \cdot h^{-1}$ in cold season. These fluxes were lowest among all our measured soils, even with the highest mean solar radiation (Table 16). This implies that other factors (e.g., vegetation surfaces) were dominate.

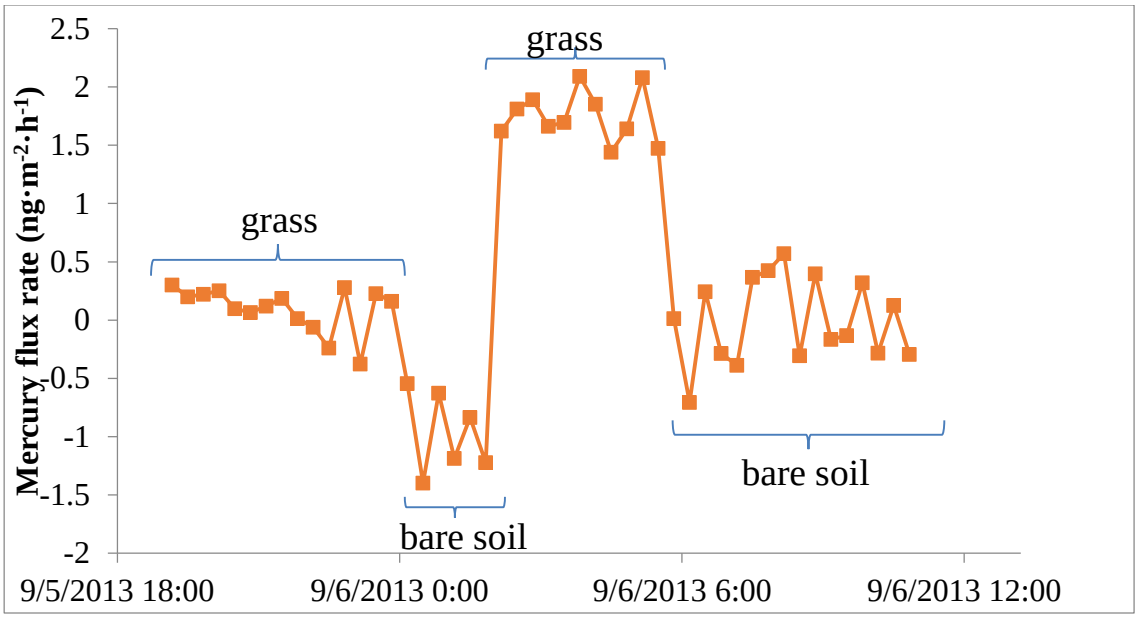

Figure 22. Hg fluxes from covered soil and bare soil at the grassland site

Table 16. Mercury emission/deposition fluxes over soils and meteorological parameters for summer and winter

Site	Warm Season					Cold Season				
	Hg Flux ($ng \cdot m^{-2} \cdot h^{-1}$)	Solar Radiation	Air Temp.	Relative Humidity	Wind Speed	Hg Flux ($ng \cdot m^{-2} \cdot h^{-1}$)	Solar Radiation	Air Temp.	Relative Humidity	Wind Speed
	Mean±SD	($W \cdot m^{-2}$)	ºC	(%)	($m \cdot h^{-1}$)	Mean±SD	($W \cdot m^{-2}$)	ºC	(%)	($m \cdot h^{-1}$)
Forest	0.50±1.20	25±52	26.45±4.25	79±18	1.54±0.79	-0.19±0.14	N/A*	10.40±2.11	63±7	1.84±0.50
Grassland	4.38±1.71	33±70	23.84±4.80	78±18	1.82±0.97	-0.32±0.25	66±124	6.78±1.59	74±24	2.02±0.84
Agriculture	1.58±1.37	84±134	24.91±5.66	70±22	1.90±0.89	-0.11±0.26	36±45	5.66±7.08	71±23	1.40±0.91
Wetland	2.54±2.10	62±111	26.78±5.36	73±21	1.79±1.06	0.10±0.20	39±52	8.18±4.43	62±18	2.21±1.07
Delta(Dundee)	0.32±0.57	59±88	24.54±3.07	77±12	2.72±1.20	-0.03±0.14	45±77	3.26±1.77	77±5	1.63±0.47
Delta(Dowling)	0.55±1.48	53±100	24.54±4.58	77±19	2.16±1.14	-0.20±0.23	35±50	0.34±4.10	70±24	1.92±0.51

3.4.5 Hg fluxes over agriculture soils

Lafayette County Soil. Mercury fluxes for the cotton field soil ranged from 0.08-5.46 $ng \cdot m^{-2} \cdot h^{-1}$ with an average of 1.58 ± 1.37 $ng \cdot m^{-2} \cdot h^{-1}$ in warm season (Table 15). Evasion was observed in the summer only. In contrast deposition dominated in the winter, with an average of -0.11 ± 0.26 $ng \cdot m^{-2} \cdot h^{-1}$. The corresponding substrate Hg content (17.1 $ng \cdot g^{-1}$) was lowest among all soil samples. Our results are generally similar to Hg emission fluxes reported for agricultural fields in Canada (1.1-2.9 $ng \cdot m^{-2} \cdot h^{-1}$) (Schroeder et al. 2005) and North Dakota (-1.4-5.0 $ng \cdot m^{-2} \cdot h^{-1}$) (Ericksen et al. 2006). However, the fluxes are lower than those measured in Guangzhou, China (135 $ng \cdot m^{-2} \cdot h^{-1}$) and Sichuan, China ((-4.1)-132 $ng \cdot m^{-2} \cdot h^{-1}$) (Fu et al. 2008, 2012).

The agriculture Hg air/surface exchange exhibited a clear seasonal variation. Figure 23 shows the air/surface exchange data distributions on different seasons. Higher fluxes were found in warm season compared to the fluxes in winter season. The appearance of higher fluxes in warm season was probably associated with the higher solar radiation, temperature, TGM, and wind speed (Table 16).

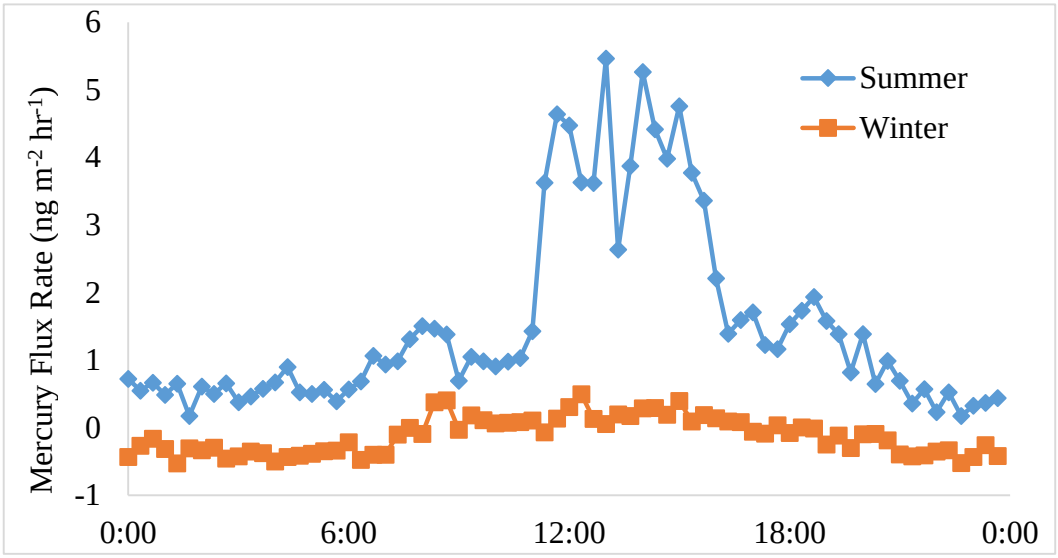

Figure 23. Mercury fluxes over agriculture soil in warm and cold seasons

3.4.6 Hg fluxes over wetland soil

Wetlands are very rich in biodiversity and crucial in the natural environment (Poissant et al. 2004). In addition to human health concerns, mercury has been reported to affect the reproductive health of birds and fish (Spalding et al. 1994). Wetlands are usually considered as shelters, nesting and feeding grounds for birds and fish. In order to evaluate and understand the mercury exchange and transformation processes in wetlands, the mercury emission fluxes from wetland were measured during both warm and cold seasons.

Summary statistics for mercury exchange fluxes from wetland sediment are given in Table 15. In warm season, the Hg fluxes over wetland soil ranged from 0.63-11.81 $ng \cdot m^{-2} \cdot h^{-1}$. The predominant flux of mercury over wetland was emission, averaging 2.54 ± 2.10 $ng \cdot m^{-2} \cdot h^{-1}$. The flux diminished in the winter season with an average of 0.10 ± 0.20 $ng \cdot m^{-2} \cdot h^{-1}$, but was the only soil among those tested that remained positive (still emitting Hg). In summer, mercury fluxes over wetland were strongly correlated with a number of parameters, including solar radiation ($r=0.87$, $p<0.05$), temperature ($r=0.69$, $p<0.05$), humidity ($r=-0.68$, $p<0.05$), wind speed

(r=0.54, $p<0.05$), and TGM (r=0.50, $p<0.05$). In contrast, fluxes in winter were only significantly correlated with TGM (r=-0.74 $p<0.05$).

3.4.7 Hg fluxes over delta agriculture soils

During the summer, mean mercury emission fluxes over Dundee soil and Dowling soils were 0.32 ± 0.57 ng·m^{-2}·h^{-1} and 0.55 ± 1.48 ng·m^{-2}·h^{-1}, respectively. For the Dowling soil, about half (36 out of 69) flux data points were net deposition, and the median flux was slightly negative (the only soil to have a net deposition in the summer), indicating the texture and structure of the soils could be important factors governing the variations of mercury emission fluxes. In the winter, fluxes for both soils were lower than the summer, with the majority of the data net deposition. It should be noted that these soils are only moderately permeable and are relatively acidic. These characteristics may be influencing the fluxes as follows. Acidic soil strongly binds Hg^{+2} reducing volatilization and photoreduction to Hg^0 (Fleck et al. 2007). Also, soil high permeability facilitates soil-air Hg gas exchange.

3.4.8 Comparison with other studies worldwide

Mercury emission fluxes between the air and various surfaces have been reported in several areas worldwide. This study constitutes the first study of mercury fluxes over Mississippi soils. Here we compare our data with that of other studies in the literature (Table 17). Only summer fluxes from this study were compared because of such low emission fluxes in the winter. In general, the mercury flux measured from the loblolly forest floor is comparable to other measurements on forest soils: ~1.0 ng·m^{-2}·h^{-1} (Choi et al. 2009), 0.9 ± 0.2 ng·m^{-2}·h^{-1} (Ericksen et al. 2006), and ~2.2 ng·m^{-2}·h^{-1} (Schroeder et al. 2005). Mercury fluxes from Mississippi agriculture soils are similar to the value of 1.1-2.9 ng·m^{-2}·h^{-1} (Schroeder et al. 2005), but are lower than measurements from Guangzhou and Sichuan, China (Fu et al. 2008, 2012). For grass,

our mean mercury flux was higher than reported by Ericksen et al (2006), but lower than the 1-8.3 $ng \cdot m^{-2} \cdot h^{-1}$ reported by Poissant et al (1998) and -18.7-13.4 $ng \cdot m^{-2} \cdot h^{-1}$ reported by Fu et al (2008), though it should be noted that the species of grass varied between studies. Mercury flux from our wetland soil was higher than the measurement from Katriina et al (2012). Overall, the mercury emission fluxes were found to vary diurnally, similar to previous investigations, with higher mercury fluxes during daytime (mostly emissions) and lower but stable mercury fluxes during nighttime.

Table 17. Mercury fluxes and ancillary data for natural landscapes worldwide. Bold numbers represent significant correlation ($p<0.05$) between mercury fluxes and corresponding parameters

Location	Classification	Time	Hg flux ($ng \cdot m^{-2} \cdot h^{-1}$)	Hg inlet conc. ($ng \cdot m^{-3}$)	Substrate Hg content ($ng \cdot g^{-1}$)	Substrate temp. (°C)	Air temp. (°C)	Solar radiation ($W \cdot m^{-2}$)	Reference
USA, MS	Forest	22-25 Aug 2013	(-0.93)-6.71	0.44-2.28	40.9		26.45	25	This Study
	Grassland	25-27 Aug 2013	1.34-11.41	0.20-1.66	26.6		23.84	33	
	Agriculture	27-29 Aug 2013	0.08-5.46	0.17-1.59	17.1		24.91	84	
	Wetland	29-31 Aug 2013	0.63-11.81	0.22-1.50	62.7		26.78	62	
	Delta Dundee	17-18 Sep 2013	(-0.58)-2.47	0.69-2.29	21.8		24.54	59	
	Delta Dowling	18-19 Sep 2013	(-0.52)-4.87	0.18-1.89	42.4		24.54	53	
Canada	Aquatic	Summers 1997 to 2000	0 - 5.0		0.3-6.5 ng/L(**0.47**)	16.7-26.1	14.9-28.0		Schroeder et al., 2005
	Forest	Summer 1997 and 1999	-0.4 - 2.2		0.15-0.33	14.0-17.5	15.6-19.6		
	Agriculture	July 1995, Sep 1999, June 2000	1.1 - 2.9		0.006-0.100		10.1-12.7		
	Sand	Aug 2001	0.44				14.8		
	Background rock/till	Summers 1997 to 2000	-0.03 - 1.7		0.005-0.25		17.3-19.7		
	Shales	July 1997 and 2001	9.1 - 213.5		0.358 - 1.6		11.9-20.1		
	Cinnabar	July 1997	91.8		179.5		16.6		
	Mineralized soil	June 1996	1760		124.6(**0.49**)		17.1		
USA	Agriculture		-1.4-5.0	1.4-3.7(-0.34)	29-35	r(0.15)	r(0.44)	r(**-0.71**)	Ericksen et al., 2006
	Desert	May 2003 to May 2004	-1.5-4.2	0.2-4.0(**0.50**)	12-30	r(0.28)	r(**0.23**)	r(**0.67**)	
	Grassland	July 2003 to August 2004	-0.9-9.7	0.5-3.2(**0.25**)	10-55	r(**0.14**)	r(0.20)	r(0.46)	
	Mixed forest		-0.2-3.8	1-2.3(**-0.56**)	32-60	r(N/A)	r(**0.39**)	r(**0.62**)	
	Pine forest		-0.3-3.7	0.7-1.4(**-0.55**)	40	r(**0.44**)	r(**0.51**)	r(**0.52**)	
Sweden	Forest lake	May 1988	0.19-19.5	1.59-4.16		0.5-23	0.4-24		Xiao et al., 1991
	Forest	Dec 1987 to June 1989	-2.0-1.4	2.06-3.01		-5-13	-10-20		
China. Guiyang	Landfill	Nov 2003	-72.48-308.7	175.22-1406.0					Feng et al., 2004
USA, NY	Forest	2005,2006	-2.5-27.2			r(**0.53**)	r(**0.44**)	r(**0.16**)	Choi et al., 2009
Finland	Wetland	May 2000	-0.3-0.6	1.3					Katriina et al., 2012
	Forest	August 2007	-1.0-3.5			11-15(**0.56**)	11-21(**0.86**)		
China, Sichuan	Agriculture	Dec 2005 to Sept 2006	-4.1-132	2.09-10.91	100		4.2-29	72.1	Fu et al., 2008
	Grassland	Dec 2005 to Aug 2006	-18.7-13.4	1.93-8.32	170		3.6-25.8	53.7	
	Bare soil	Aug 2006	-4.7-94.8	2.74-5.52	130		24.2	64.4	
	Broadleaf forest	Aug 2006	0.5-9.3	1.34-8.54	125		17.5-22.9	93.9	
	Pine forest	Aug 2006	-0.6-10.6	0-2.66	80		17.1	92.9	
USA, TN	Forest(Winter)	Jan, Feb 2004	-0.4-3.3	1.7-4.8	92	7	9	209	Kuiken et al., 2008
	Forest(Sprint)	March, April, May 2004	-1.2-1.2	1.3-3.3		17	19	110	
	Forest(Summer)	June, July, August 2004	-0.1-1.0	0.9-2.4		21	25	70	
	Forest(Fall)	Sep, Oct, Nov 2004	0-2.9	1.3-1.9		14	16	103	
USA, ME	Forest	27-29 May 2005	-0.1-2.5	1.4-2.4	69	10-15(0.16)	13-21(**0.72**)	26-844(**0.89**)	Kuiken et al., 2008
USA, NY		31 May to 2 June 2005	-0.5-0.5	1.1-1.6	50	11-14(**0.41**)	9-26(**0.18**)	17-8-129(0.11)	
USA, PA		4-5 June 2005	-1.3-1.8	1.4-3.6	33	14-16(**0.48**)	14-25(**0.32**)		
USA, NJ		18, 19, 21 May 2005	-0.3-0.7	1.5-2.2	13	11-13(**0.54**)	16-19(**0.65**)	17-	
USA, NC		14-15 May 2005	-4.4-1.5	2.1-9.5	21	16-18(0.32)	22-28(**0.74**)	37-	
USA, SC		11-12 May 2005	-5.1-1.9	1.5-13.2	47	18-21(**0.28**)	17-26(0.07)	6-317(0.09)	
USA, MI	Shaded forest	Summer 1998	-0.6-3.7	1.2-2.9		13.1-20.2		13-330	Zhang et al., 2001
	Open field		3.2-10.2	1.8-3.1		20.6-27.6		250-812	

3.4.9 Impact of soil temperature on Hg air/surface exchange

Clear diurnal patterns of mercury emission fluxes were observed for each soil (especially during warm season) with maximum flux rates at midday and minimum fluxes during the night. This cycle has been attributed to three primary meteorological parameters (solar radiation, soil temperature, and to a lesser extent humidity) (Poissant et al. 2004; Fu et al. 2008). Previous studies of mercury fluxes over soils have documented that a relatively strong exponential relationships exists between flux and soil temperature (Gustin. 2003; Feng et al. 2005). These phenomena have often been accounted for by physicochemical characteristics of elemental mercury (high vapor pressure and low water solubility) and photo-induced reactions. A laboratory-based study conducted on Hg enriched soil found that as soil temperature increased, Hg flux increased by a similar magnitude (Moore and Carpi. 2005). Gustin et al (2004) suggested that elevated temperature could accelerate Hg desorption from soil and movement up through the soil column. Schluter et al (2000) suggested that the rise of soil temperature would increase the activity of Hg^{+2}, facilitating the photoreduction of Hg^{+2} to Hg^{0}.

The Arrhenius equation to study the processes driving evasion of Hg from soils. One way to help understand the processes driving the evasion of Hg from soils is to calculate the apparent activation energy (E_a). This approach has been described elsewhere (Kocman and Horvat, 2010). Briefly, in this scenario E_a is considered the energy which the system must absorb in order to initiate a Hg flux increase (Gustin et al. 2003). Assuming that the transfer of Hg^{0} from soil to atmosphere is governed by a pseudo-first order reaction, the reaction rate of Hg flux over the soil surface can be described using the Arrhenius equation:

$$Ln(F) = Ln(A)-E_a/RT$$

Where F is Hg flux, R is the gas constant (1.9872 cal·k^{-1}), T is the soil temperature in degrees Kelvin, A is a pre-exponential factor (a frequency factor or the number of times mercury atoms gain sufficient energy to be thermally desorbed from the surface), and E_a is the apparent activation energy. The equation is used to show the effect of a change of temperature on the rate of flux reactions. Even though multiple mechanisms may be involved in Hg absorption/desorption over the soils, the approach is often used to describe the general temperature dependence of kinetic constants for various processes. Thus, E_a can be calculated by fitting the Arrhenius Equation to the data for the measured fluxes at different soil temperatures. When E_a is close to the enthalpy of volatilization (~14.5 kcal·mol^{-1} at 20 ºC) fluxes are likely controlled by direct emission of elemental mercury from the soil surface, whereas if the Ea is higher (~30 kcal·mol^{-1}, for example) then other processes, such as the conversion of Hg^{+2} to Hg^0, are involved. For example, higher E_a values (dark measurements) have been found for mercury contaminated sites where HgS is the predominant form of mercury (Lindberg et al. 1995). Our data (31 kcal·mol^{-1}) is more consistent with "background" soils (Gustin et al. 1997).

In the present work, we investigated the effect of soil temperature and solar radiation on mercury fluxes. As shown in Figure 24, a significant correlation (r^2=0.84; $p<0.05$) between Hg fluxes and soil temperature was observed over forest soil in warm season. The activation energy for Hg emission over forest soil was estimated to be 31.3 kcal·mol^{-1} using the Arrhenius equation. This result is comparable to other published soil Hg activation energies: 18.6-69.1 kcal·mol^{-1} (Feng et al. 2005) and 14.6-29.4 kcal·mol^{-1} (Zhang et al. 2001; Poissant et al. 2004)). The dependence of Hg flux on temperature was also evaluated under "dark" conditions, where agricultural soil was shaded and soil temperature monitored. Results show that Ea was estimated to be 46 kcal·mol^{-1} (Figure 25).

It has been proposed that there are at least two sources of Hg^0 emitted from soil, a natural "pool" of Hg^0 which is primarily adsorbed on surfaces, and Hg^{+2} which can be photo-chemically reduced to Hg^0 by sunlight (Gustin et al. 2003). This later process seems to be enhanced in soils with higher levels of organic matter (Gustin et al. 2003). Thus, under "dark" conditions the primary factor leading to emission of Hg from soils is likely related to the enthalpy of volatilization, whereas under "light" conditions emissions are related to both enthalpy of volatilization (warming soil) and photo-reduction processes.

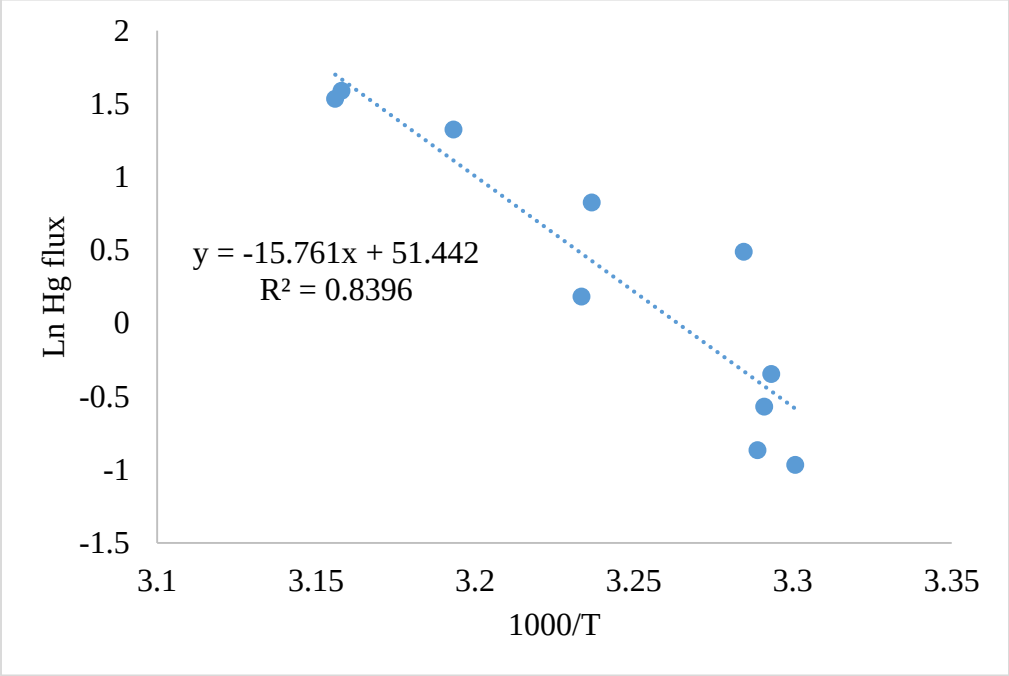

Figure 24. Arrhenius relationship between Hg flux and soil temperature over a loblolly pine forest floor during the warm season

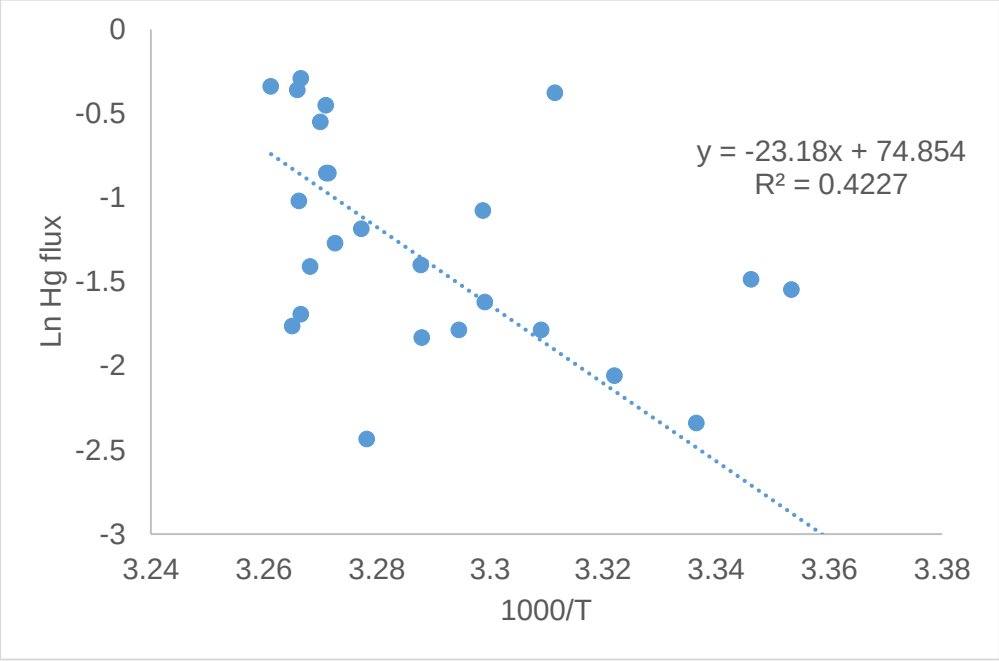

Figure 25. Arrhenius relationship between Hg flux and soil temperature over an agricultural soil under dark condition. Note: air temperature (measured inside the shaded box) was assumed to match soil temperature and may have contributed to variability in the data

To further explore the emission phenomena in our soils, we conducted a controlled experiment on the roof of Anderson Hall on the University of Mississippi campus (Figure 26). Two mercury analyzers were used. One (a Tekran 2537A, borrowed from Southern Research Institute) was used to measure atmospheric mercury concentrations, the other (a Tekran 2537B, our property) alternately measured concentrations over Delta Dundee soil using two identical dynamic flux chambers. One of the DFCs was covered with aluminum foil and represented dark conditions, the other was uncovered and represented light conditions.

Unfortunately, the Hg analyzer we borrowed was an older unit that came from use in a coal fired power plant, where Hg levels are much higher. Despite out efforts to clean the system (filter housing, tubing, etc.) to reduce background levels we could not get two instruments to match ambient air concentrations, although the data correlated well. Thus, ambient Hg levels measured by the older unit were adjusted by a factor of 0.30 to match ambient background levels established from a year-long data set (see chapter 2).

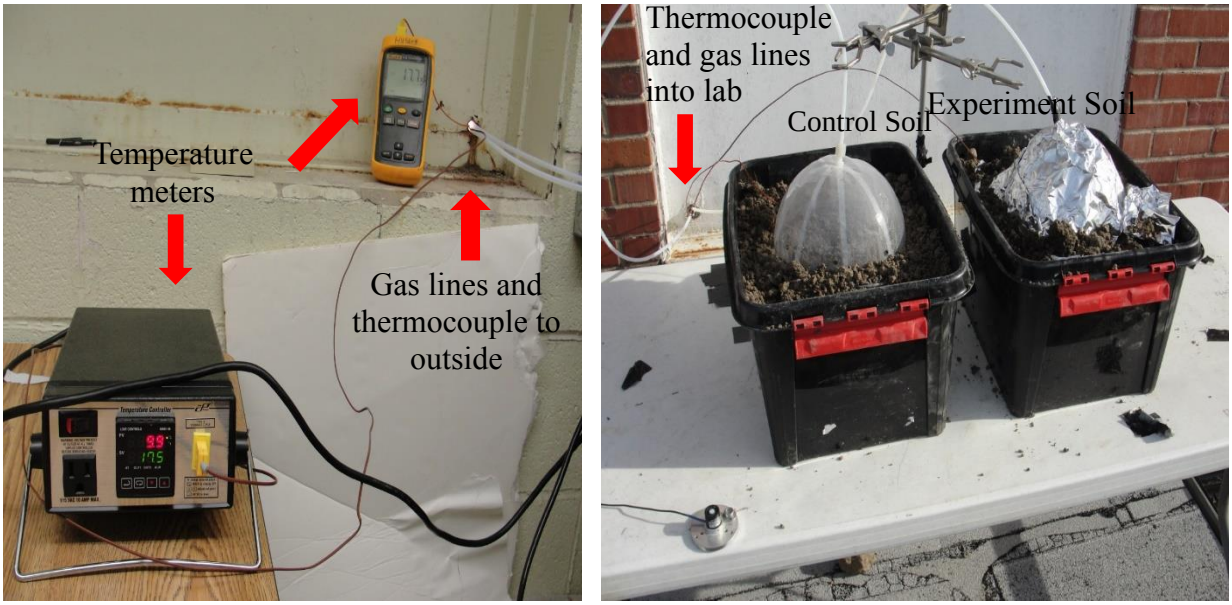

Figure 26. Experimental setup to simultaneously measure soil temperature and Hg flux for covered and uncovered soil. Temperature meters (left); soils with DFCs (right)

Fu et al (2008) reported that the activation energies at one agriculture sampling site showed a clear seasonal variation with higher activation energy in the winter sampling campaign. Kockman et al (2010) observed a decreasing trend of Ea with increasing THg concentration in soil. However, it depends on the form of mercury; significantly higher Ea values were found for mercury contaminated soils with relatively high levels of HgS by Bahlmann et al (2006).

In our study, strong correlations between Hg flux and soil temperature were observed for both uncovered (r^2=0.88) and covered (r^2=0.92) Delta Dundee soil (Figure 27), with the Ea of 18.1 kcal·mol^{-1} over uncovered soil and 94.0 kcal·mol^{-1} over covered soil. Both are higher than the mercury heat of vaporization of 14.5 kcal·mol^{-1} at 20 ºC (Carpi and Lindberg. 1997), indicating that Hg emissions from soils cannot be solely explained by the direct emission of elemental Hg from the soil surface. The higher activation energy over covered soil implies the importance of solar radiation, and the photoreduction from Hg^{+2} to Hg^0 may be a dominant factor.

At this point our data is too limited to elucidate mechanisms, and to determine the relationships between thermally-induced flux and light-induced flux. We planning a more systematic study using a single Hg vapor analyzer however this requires an additional switching valve for which funds are being sought.

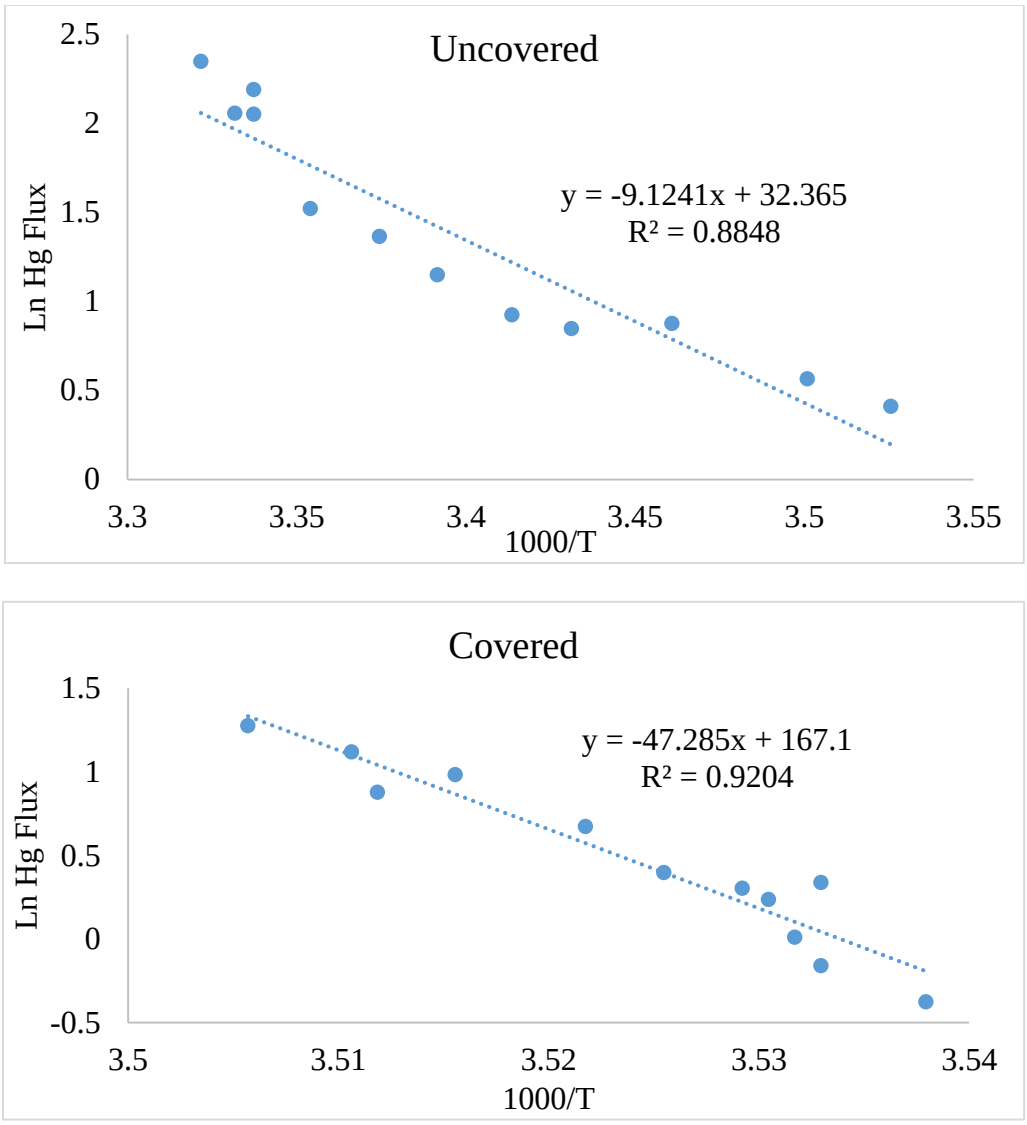

Figure 27. Arrhenius relationships between mercury flux and uncovered (top), covered (bottom) for Delta Dundee soil

3.4.10 Effect of soil moisture on fluxes

Soil moisture was identified as one of the key factors affecting the Hg air/soil flux (Carpi and Lindberg. 1998; Xin et al. 2007). In our study, its effect was investigated by comparing the relative Hg flux over the same soil (Delta Dundee) with varying moisture content (Figure 28). The soil was split into two bins. About a 0.5 liter of water was added uniformly to one bin and allowed to soak-in.

Figure 28. Experimental setup comparing mercury fluxes over dry and wet soils

Emission fluxes over wet and dry soils was evaluated. The relative concentrations (wet/dry) of mercury over the two soils is shown in Figure 29. Mercury fluxes over the wet soil initially decreased (for about 2 hours) but then returned to about the same level as the drier soil during the night. The decrease is agreement with other studies (Bahlmann et al. 2006; Kockman et al. 2010) and may stem from water impeding mercury desorption from soil (lowering diffusivity). Bahlmann et al (2006) also proposed that decreased Hg flux was due to a combination of soil moisture tension and soil moisture. In their study, after wetting the soil they allowed the water to percolate through the soil column. The soil moisture tension in the surface layer became weaker, resulting in less Hg enriched soil air being displaced and less Hg being desorbed from the soil surface.

In the present study, the ratio of the wet-to-dry Hg flux ratio increased the next day, starting with daylight. Presumably evaporation rates are higher from the wetted soil, allowing release of Hg^0. Moreover, the water percolated into the soils generates additional pores for Hg vapor to escape to the atmosphere.

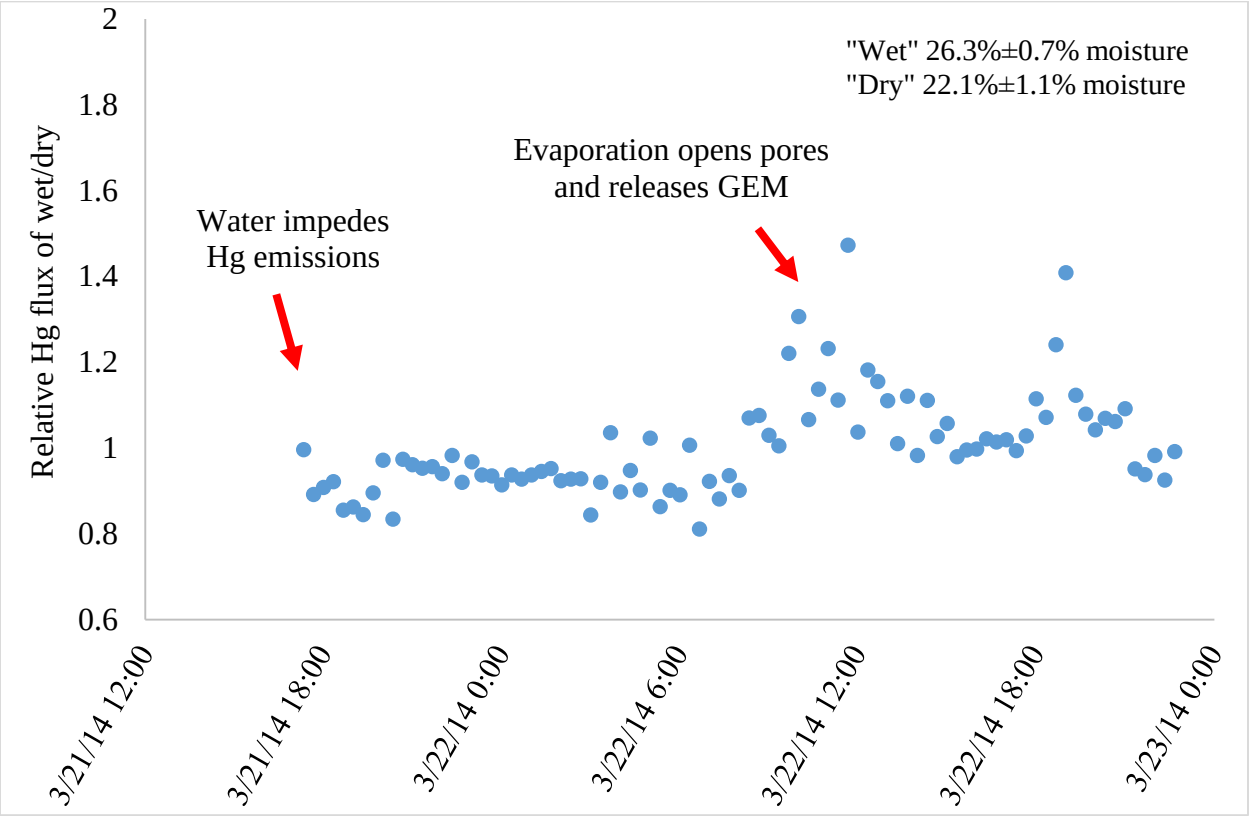

Figure 29. Effect of rain/moisture on TGM emissions from soils (Wet/Dry).

3.5 CONCLUSIONS

Soils selected for analysis came from major ecoregions in the mid-south US including the Mississippi Alluvial Plain (representative agricultural soils from the Mississippi Delta), and the Southeastern Coastal Plain (both forested and agricultural areas). Agricultural practices include turning-over soils which exposes new surface areas for exchange with the atmosphere. In addition, wetland sediment was selected because wetlands are widely considered hot-spots for mercury methylation. To date there have been no measurements of Hg emissions from soils in the mid-south US where agriculture is intensive and wetlands are numerous.

This work represents the first measurements of Hg fluxes (air-soil gas exchange) in the region. Fluxes exhibited both seasonal and diurnal patterns. Emission to the atmosphere was dominant in warm season, while deposition to surfaces was dominant in cold season. Mercury fluxes averaged 1.65 ± 1.58 ng·m-2·h-1 during the summer and -0.13 ± 0.14 ng·m-2·h-1 during the winter. Clear diurnal Hg flux patterns were also observed, especially during warm season, with the maximum flux at midday and the minimum flux at night. This diurnal variability was found to be related to solar radiation, temperature, and relative humidity. Other meteorological parameters (e.g. wind speed, pressure) were also monitored but had less influence flux rates. Overall, our measured flux rates are in the range that have been reported for background (non-contaminated) soils for similar landscapes outside the region (e.g. Ericksen et al. 2006; Schroeder et al. 2005).

Because there were significant positive correlations between total gaseous mercury and surface mercury emission fluxes, especially during the warm season, we conclude that the soils are indeed sources of mercury to the air. In contrast, there were significant negative correlations found during the winter, indicating the soils are serving primarily as sinks during that season.

Because summer emission rates exceed winter deposition rates, we suggest that overall soil is a net positive contributor to the global atmospheric budget. Moreover, with global warming one can expect that the emission rates from soil will rise, further increasing atmospheric levels.

Future work should focus on (1) seasonal (all seasons) variations of Hg fluxes over sampling soils; (2) lake studies that examine the relationship between dissolved gaseous mercury, and dissolved organic carbon and pH; (3) understanding of mechanisms controlling Hg exchange flux for a variety of variables, including soil temperature, soil moisture content, solar radiation, rain events, and vegetation cover.

3.6 ACKNOWLEDGMENTS

The authors thank L. Hawkins and E. Prestbo (Tekran Inc.) for advice on using the speciation system and for discussion of mercury flux measurement. The authors also greatly appreciate M. Gustin and A. Carpi for providing the dynamic flux chambers. The environmental data was obtained by Zhen Guo from Geology Department of University of Mississippi. Funding granted by U.S. Environmental Protection Agency (#CD-95450510-0).

3.7 LIST OF REFERENCES

Bahlmann, E., Ebinghaus, R., and Ruck, W. **2006**. Development and application of a laboratory flux measurement system (LFMS) for the investigation of the kinetics of mercury emissions from soils. *J. Environ. Manage*. 81, 114–125.

Carpi, A., Lindberg, S. E., **1997**. Sunlight-mediated emission of elemental mercury from soil amended with municipal sewage sludge. *Environ. Sci. Technol*. 31, 2085-2091.

Carpi, A., Lindberg, S. E., **1998**. Application of a TeflonTM dynamic flux chamber for quantifying soil mercury flux: tests and results over background soil. *Atmos. Environ*. 32, 873–882.

Choi, H., Holsen, M. T., **2009**. Gaseous mercury fluxes from the forest floor of the Adirondacks. *Environ. Pollut*. 157, 592-600.

Eckley, C. S., Gustin, M., Lin, C. J., Li, X., Miller, M. B., **2010**. The influence of dynamic chamber design and operating parameters on calculated surface-to-air mercury fluxes. *Atmos. Environ*. 44, 194-203.

Edwards, C. G., Howard, A. D., **2013**. Air-surface exchange measurements of gaseous elemental mercury over naturally enriched and background terrestrial landscapes in Australia. *Atmos. Chem. Phys.* 13, 5325-5336.

Engle, M. A., Gustin, M. S., Goff, F., Counce, D. A., Janik, C. J., Bergfeld, D., Rytuba, J. J., **2006**. Atmospheric mercury emissions from substrates and fumaroles associated with three hydrothermal systems in the western United States. *J. of Geophys. Res*. 111, D17304.

Ericksen, A. J., Gustin, M. S., Xin, M., Weisberg, J. P., Fernandez, G. C. J., **2006**. Air-soil exchange of mercury from background soils in the United States. *Sci. Total Environ*. 366, 851-863.

Estrade, N., Carignan, J., and Donard, F. X. O., **2011**. Tracing and Quantifying Anthropogenic Mercury Sources in Soils of Northern France Using Isotopic Signatures. *Environ. Sci*. Technol. 45(4), 1235–1242.

Feng, X., Tang, S., Li, Z., Wang, S., Liang, L., **2004**. Landfill is an important atmospheric mercury emission source. *Chinese Science Bulletin*. 49(19), 2068-2072.

Feng, X., Wang, F. S., Qiu, L. G., Hou, M. Y., and Tang, L. S., **2005**. Total gaseous mercury emissions from soil in Guiyang, Guizhou, China. *J. Geophys. Res*. 110, D14306, doi:10.1029/2004JD005643.

Fitzgerald, W. F., Engstrom, R. D., Mason, R., and Nater, A. E., **1998**. The case for atmospheric mercury contamination in remote areas. *Environs. Sci. Technol*. 32: 1-7.

Fleck, J., Aiken, G., Bergamaschi, B., Latch, D., **2007**. Mercury release from delta wetlands: facilitation and fluxes. An amendment to existing CALFED project #2000-G01. Annual final report.

Fu, X., Feng, X., Wang, S., **2008**. Exchange fluxes of Hg between surfaces and atmosphere in the eastern flank of Mount Gongga, Sichuan province, southwestern China. *J. Geophys. Res*. 113, D20306, doi: 10.1029/2008JD009814.

Fu, X., Feng, X., Zhang, H., Yu, B., Chen, L., **2012**. Mercury emissions from natural surfaces highly impacted by human activities in Guangzhou province, South China. *Atmos. Environ*. 54, 185-193.

Gustin, S., Coolbaugh, M., Engle, M., Fitzgerald, B., Keislar, R., Lindberg, S., Nacht, D., Quashnick, J., Rytuba, J., Sladek, C., Zhang, H., andZehner, R., **2003**. Atmospheric mercury emissions from mine wastes and surrounding geologically enriched terrains. *Environ. Geol.* 43, 339–351.

Gustin, M. S., J, A. Ericksen, D, E. Schorran., D, W. Johnson., S, E. Lindberg., and J, S. Coleman., **2004**. Application of controlled mesocosms for understanding mercury air-soil-plant exchange. *Environ. Sci. Technol*. 38, 6044–6050, doi:10.1021/es0487933.

Gustin, M. S., Kolker, A., Gardfeldt, K., **2008**. Transport and fate of mercury in the environment. *Appl. Geochem*. 23, 343-344.

Katriina, K., Hakola, H., Hellen, H., Korhonen, M., Verta, M., **2012**. Atmospheric Mercury Fluxes in a Southern Boreal Forest and Wetland. *Water Air Soil Poll*. 223, 1171-1182.

Lindberg, S. E., Price, J., **1999**. Airborne emissions of mercury from municipal landfill operations: a short-term measurement study in Florida. *J. Air Waste Manage. Assoc*. 49, 520–532.

Kuiken, T., Zhang, H., Gustin, M., Lindberg, S., **2008**. Mercury emission from terrestrial background surfaces in the eastern USA. Part I: Air/surfaces exchange of mercury within a southeastern deciduous forest (Tennessee) over one year. *Appl. Geochem*. 23, 345-355.

Kuiken, T., Zhang, H., Gustin, M., Lindberg, S., Sedinger, B., **2008**. Mercury emission from terrestrial background surfaces in the eastern USA. II: Air/surfaces exchange of mercury within forests from South Carolina to New England. *Appl. Geochem*. 23, 356-368.

Moore, C., and A, Carpi., **2005**. Mechanisms of the emission of mercury from soil: Role of UV radiation. *J. Geophys. Res*. 110, D24302, doi:10.1029/2004JD005567.

Nacht, D. M., Gustin, M. S., **2004**. Mercury emissions from background and altered geologic units throughout Nevada. *Water Air Soil Pollut*. 151, 179–193.

Pacynaa, G. E., Pacynaa, M. J., Sundsetha, K., Munthec, J., Kindbomc, K., Wilsond, S., Maxson, P. F., **2010**. Global emission of mercury to the atmosphere from anthropogenic sources in 2005 and projections to 2020. 44(20), 2487–2499.

Poissant, L., Casimir, A., **1998**. Water–air and soil–air exchange rate of total gaseous mercury measured at background sites. *Atmos. Environ*. 32, 883–893.

Poissant, L., Pilote, M., Constant, P., Beauvais, C., Zhang, H., Xu, X., **2004**. Mercury gas exchanges over selected bare soil and flooded sites in the bay St. Francois wetlands (Quebec, Canada). *Atmos. Environ*. 38, 4205-4214.

Schluter, K., **2000**. Review: Evaporation of mercury from soils. An integration and synthesis of current knowledge. *Environ. Geol.* 39, 249–271, doi:10.1007/s002540050005.

Schroeder, W. H., Munthe, J., **1998**. Atmospheric mercury – an overview. *Atmos. Environ*. 32, 809–822.

Schroeder, W. H., Beauchamp, S., Edwards, G., Poissant, L., Rasmussen, P., Tordon, R., Dias, G., Kemp, J., Van Heyst, B., and Banic, M. C., **2005**. Gaseous mercury emissions from natural sources in Canadian landscapes. *J. Geophys. Res*. 110, D18302.

Soil survey in Mississippi. **1953**. United States Department of Agriculture Soil Conservation Service in Cooperation with Mississippi Agriculture Experiment Station. Series 194, No. 9.

Spalding, M. G., Bjork, R. D., Powell, G. V. N., Sundlof, S. F., **1994**. Mercury and cause of death in great white herons. *J. Wildlife Manage*. 58, 735–739.

Streets, G. D., Hao, J., Wu, Y., Jiang, J., Chand, M., Tian, H., Feng, X., **2005**. Anthropogenic mercury emissions in China. *Atmos. Environ*. 39(40), 7789–7806.

Xiao, Z. F., Munthe, J., Schroeder, H. W., Lindqvist, O., **1991**. Vertical fluxes of volatile mercury over forest soil and lake surfaces in Sweden. *Tellus*, 43B, 267-279.

Xin, M., Gustin, M. S., Ladwig, K., Pflughoeft-Hassett, D. F., **2006**. Air-substrate mercury exchange associated with landfill disposal of coal combustion products. *J. Air Waste Manage. Assoc*. 56, 1167-1176.

Xin, M., Gustin, M., and Johnson, D., **2007**. Laboratory investigation of the potential for re-emission of atmospherically derived Hg from soils, *Environ. Sci. Technol*. 41, 4946–4951.

Zhang, H., Lindberg, E. S., Marsik, J. F., Keeler, J. G., **2001**. Mercury air/surface exchange kinetics of background soils of the Tahquamenon river watershed in the Michigan upper peninsula. *Water, Air, and Soil Pollut*. 126, 151-169.

CHAPTER FOUR

4. WET AND DRY DEPOSITION OF MERCURY TO THE YOCONA WATERSHED AND ENID LAKE

4.1 ABSTRACT

Atmospheric mercury speciation and deposition are critical in understanding the cycling of mercury in the environment. To estimate the wet and dry deposition of mercury in Yocona Watershed and Enid Lake, the concentrations of total mercury (THg) in atmospheric precipitation samples (January 2013-March 2013 and August 2013-December 2013) as well as deposition rate of gaseous oxidized mercury (GOM) to surrogate surfaces were measured in Oxford, MS. Mercury species data collected in 2011-2012 was also used to estimate the dry deposition rate by using inferential method.

The mean wet deposition rate of THg were 17.7 $\mu g \cdot m^{-2} \cdot y^{-1}$ by averaging the values from 8 months, with highest concentration in August and lowest value in February. This trend agrees very well with other measurements conducted at multiple locations in Eastern and Central North America. The wet deposition of THg contributed to Yocona Watershed and Enid Lake were estimated at 35 kg/yr and 1.52 kg/yr, respectively. The mean dry deposition rate of GOM measured by using surrogate surface was 4.35 ± 1.36 $\mu g \cdot m^{-2} \cdot y^{-1}$. Inferential method estimated the dry deposition rates of GEM, GOM, and PBM were 11.9 – 40.3 $\mu g \cdot m^{-2} \cdot y^{-1}$, 0.69 – 2.75 $\mu g \cdot m^{-2} \cdot y^{-1}$, and 0.112 – 0.308 $\mu g \cdot m^{-2} \cdot y^{-1}$, respectively. The modeled and measured deposition rates of GOM are at the same magnitude, indicating surrogate surface method could be reliable. GOM deposition rate is 5-10 times higher than PBM deposition, due to their different dry deposition velocities (V_d). Total dry deposition to Enid Lake ranged from 10.8 – 36.8 kg/yr and dry deposition contributes more than wet deposition to Enid Lake (5-10 times).

4.2 INTRODUCTION

Atmospheric mercury deposition is critical in understanding the cycling of mercury, global mercury mass balance estimates, and mercury sources (Lindberg et al. 2007; Selin et al. 2007). There are two types of mercury deposition mechanisms: wet deposition and dry deposition. Wet deposition is associated with precipitation events (e.g. rain, snow). Wet deposition of mercury can be measured directly by collecting precipitation on a daily, weekly, or event basis. The water that is collected is then analyzed for total mercury, or less often for specific forms of mercury. Dry deposition is Hg deposition in the absence of precipitation (Lindberg et al. 2007).

4.3 MATERIAL AND METHODS

4.3.1 Wet deposition of mercury

4.3.1.1 Precipitation sampling and sampling preparation

Precipitation was collected outside the Department of Chemistry and Biochemistry at the University of Mississippi along Science Row Street (latitude 34° 21' 57" N and longitude 89° 31' 31" W) using acid washed 2 liter polycarbonate bottles (Nalgene®) with a 11-in diameter low-density polyethylene funnel. The setup was secured on a ring stand and placed on the site for collection (Figure 30). The first ~100ml of rainwater was discarded and served to clean out the bottles before collection. Once collected, samples were transferred to 50ml polyethylene tubes and preserved to 0.4% HCl using 12N HCl.

Figure 30. Rainwater collection apparatus outside of Coulter Hall on the University of Mississippi campus

4.3.1.2 Total-Hg analysis

The rain samples were analyzed using a 2600 Mercury Analyzer (Tekran®, Toronto, CA) following EPA method 1631 “Mercury in Water by Oxidation, Purge and Trap, and Cold Vapor

Atomic Fluorescence Spectrometry" (USEPA, 2002). In short, bromine monochloride (BrCl) is used as an oxidizing agent to digest Hg species in the samples. The oxidizing agent is added to the filtered and unfiltered samples for digestion. The sample is reduced with hydroxylamine hydrochloride ($NH_2OH \cdot HCl$) to destroy free halogens. Stannous chloride ($SnCl_2$) reduces Hg^{2+} to Hg^0 for subsequent detection by a CVAFS photomultiplier tube.

Mercury standards (1 ng/L, 5 ng/L, 10 ng/L, 25 ng/L, and 50 ng/L) were used for calibration. The r^2 value for the calibration was > 0.99, and the recovery values for all calibration standards and references were between 80-122%.

4.3.2 Dry deposition of mercury

4.3.2.1 Direct measurement of dry deposition of Mercury

The use of surrogate surfaces to trap deposited mercury is increasing (Lyman et al. 2007). Surrogate surfaces include water surfaces, gold-coated quartz filters, and cation-exchange membranes. These surfaces are exposed to the atmosphere for a period of time, and the depositional rate can be determined. The cation-exchange membrane has been selected as the surrogate surface for this study; it is particularly efficient in capturing GOM. The concentration of GOM fluctuates diurnally (Figure 31) due to the photochemical conversion of GEM, which comprises more than 90% of atmospheric mercury. GOM is consistently deposited throughout the day; but during the night, no GEM is being converted to GOM; the concentration of GOM drops during the night and rises during the day. This GOM is of special interest because it is soluble in water and it is a source of mercuric ion which is converted to toxic methylmercury primarily by sulfate reducing bacteria in anoxic sediments.

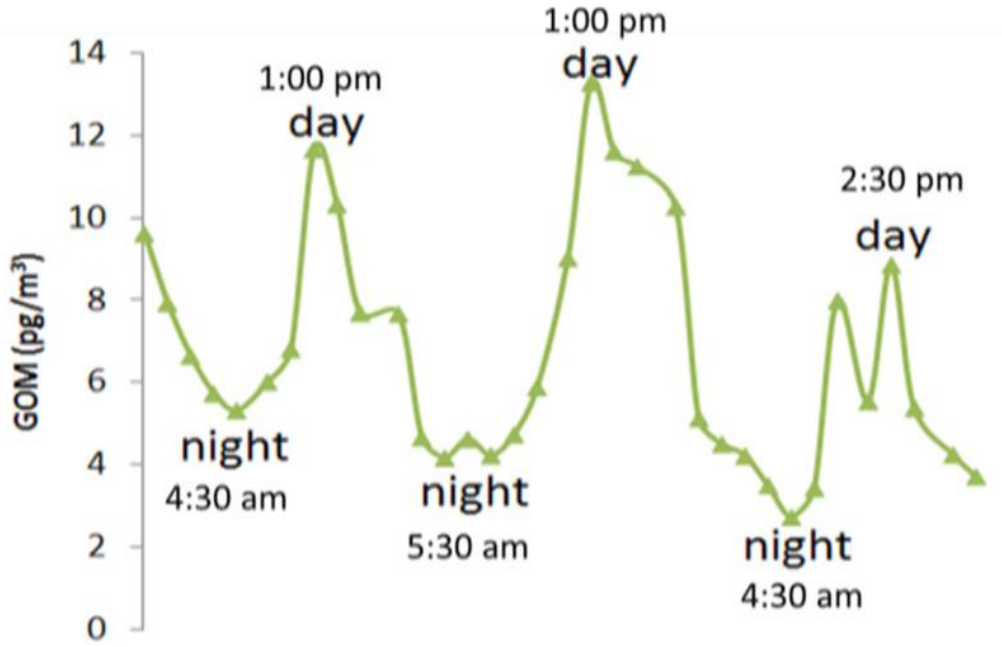

Figure 31. The diurnal fluctuations of GOM

The purpose of this study was to: 1) test a new membrane for capturing airborne GOM, 2) evaluate a new approach for determining mercury on surrogate surfaces, and 3) estimate dry deposition rates for Hg in Oxford, MS.

Cation-exchange membranes (Pall Corporation) were deployed as surrogate surfaces for the measurement of the dry deposition of GOM. The membrane is constructed of negatively-charged polyethersulfone, and is unsupported (bi-directional). The membranes were cut into 15 x 3.5 cm strips for deployment. The membrane strips were hang in the bottles by clamping them between two acrylic plates and inserting them into the neck of the bottles. The acrylic plates are designed so that the neck of the bottle holds them tight together. The sampling apparatus consists of two-liter polycarbonate bottles (Nalgene) (Figure 32). They were painted with opaque, light-colored paint to reduce evasion of deposited mercury in conditions of high solar radiation. Four 2cm holes in the bottoms allow for the exchange of air. Bottles with the holes covered were used

for blanks. The sample set consisted of three samples and three blanks. The bottles were then secured with Velcro to a rail on the top of Anderson Hall for a period of two weeks (Figure 32).

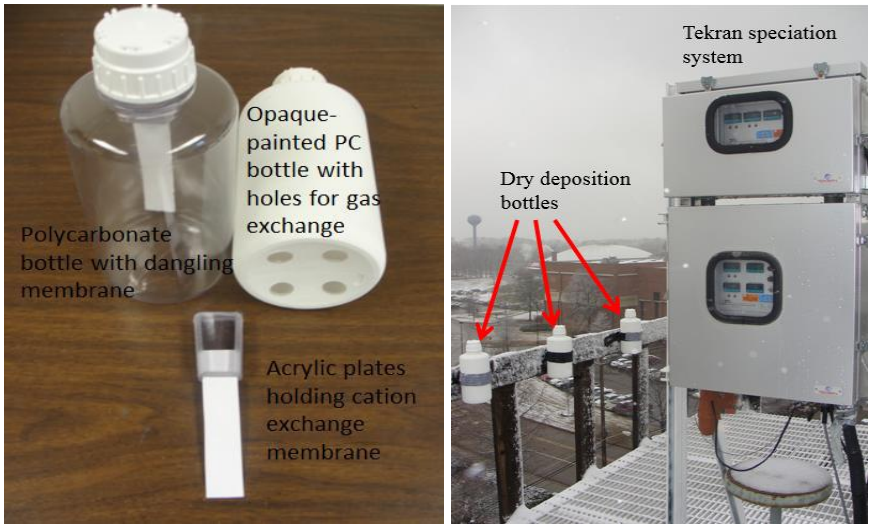

Figure 32. Setup of the deployment apparatus showing the bottle and acrylic plates (left) and the position of the bottles on top of Anderson Hall (right)

Upon retrieval of the bottles, the membranes were removed, and the 2 cm of the membranes that were between the acrylic plates were removed. They were then bisected to yield 6.5 x 3.5 cm sections. All handling of the membranes was performed in a HEPA-filtered laminar flow hood. The other halves were analyzed for total mercury using the Milestone Direct Mercury Analyzer (DMA), which is a combustion-AAS instrument. The DMA was calibrated by direct mercury vapor injection using the Tekran 2505 Mercury Vapor Primary Calibration Unit and a digital syringe.

The deposition rate of mercury can be determined by the equation:

$$D = [(S - B)/A]/T$$

Where D is the deposition rate in $ng \cdot m^{-2} h^{-1}$, S is the amount of mercury recovered from the sample, B is the average total mercury recovered from the blanks, A is the surface area of the membrane in m^2, and T is the deployment time in hr (Lyman et al. 2010).

4.3.2.2 Dry deposition schemes using ambient speciation data

Numerical models have been developed to study the atmospheric cycling of Hg on regional (Miller et al. 2005; Pan et al. 2008) and global scales (Selin et al. 2007; Storde et al. 2007). In these Hg transport models, dry deposition of GEM, GOM and PBM need to be evaluated. In this study, estimates of speciated and total Hg dry deposition at Oxford, MS were conducted. The results are expected to provide useful information for the atmospheric mercury community as well as to the estimation of dry deposition to the adjacent watersheds.

Speciated Hg concentrations for the year 2011-2012 were used for this study (Jiang Chapter 2). The inferential method, an atmospheric species' dry deposition flux (F) estimated as a product of its air concentration (C) and its dry deposition velocity (V_d), was employed to estimate F for the three fractions of Hg (GEM, GOM and PBM).

V_d for GEM and GOM were usually calculated using the big-leaf dry deposition model described by Zhang el al (2012):

$$Vd = \frac{1}{\mathrm{Ra} + \mathrm{Rb} + \mathrm{Rc}}$$

Where individual resistance terms include R_a as aerodynamic, R_b as quasi-laminar, and R_c as canopy resistance, respectively.

V_d for PBM was calculated using the size-segregated particle dry deposition model described in Zhang et al (2012):

$$Vd = \frac{1}{\mathrm{Ra}+\mathrm{Rs}} + \mathrm{V_g}$$

Where V_g is the gravitational setting velocity, and R_s is the surface resistance.

4.4 RESULTS AND DISCUSSION

4.4.1 Seasonal variations of mercury wet deposition

The concentrations of THg in the rainwater ranged from 4.1-47.5 ng/L and averaged of 11.8±14.9 ng/L (Figure 33). Concentrations of mercury were highest during the summer (August/September) and lower during the fall and winter. This observation is consistent with other studies in the southeast U.S. (Prestbo et al. 2009). One of the factors that impacts levels of Hg in rainfall is the nature of the storm. Large convective summer thunderstorms routinely occurring in the southeast U.S. reach relatively high levels in the atmosphere and scavenge a pool of gaseous oxidized mercury in the upper troposphere (Zhang et al. 2012; Selin et al. 2008). Thus, the maximum in Hg wet deposition in the southeast (see Figure. 2) may not associated with local sources (Driscoll et al. 2013). Moreover, summer storms may contribute more Hg to the watershed based on these higher levels.

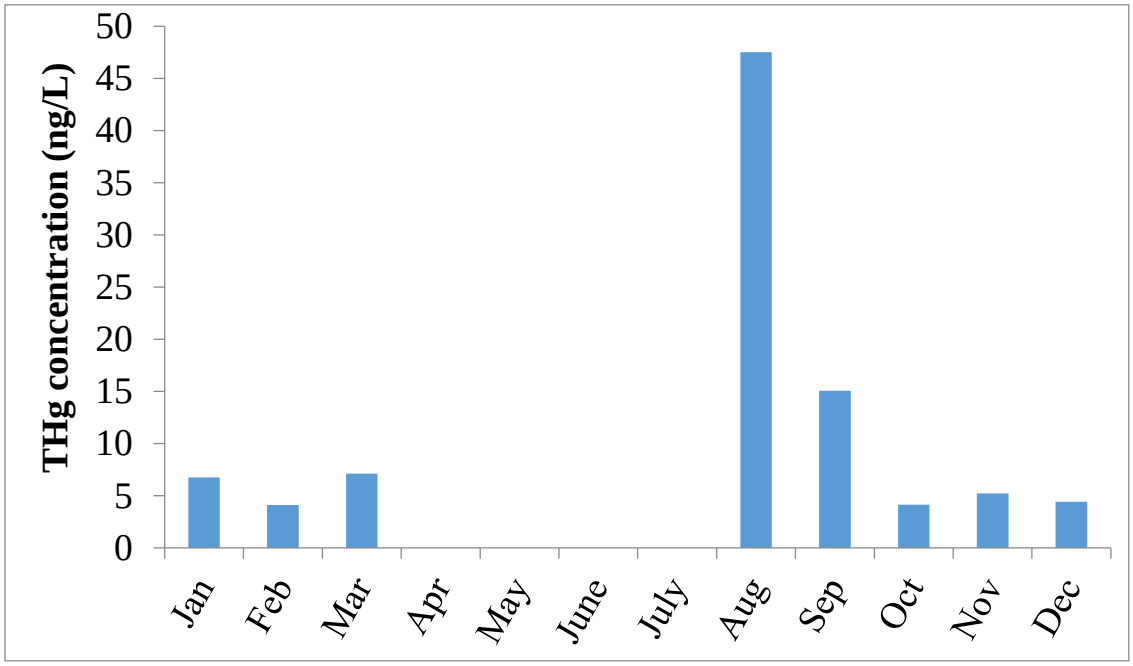

Figure 33. Total-Hg concentrations in rain in Oxford, MS during 2013. Note that during April-July, no samples were collected, but are planned in the future

4.4.2 Mercury loading to watershed via wet deposition

Mercury loading to the Yocona River Watershed Enid Lake was estimated based on the mean mercury concentration in the rain, the average annual precipitation to the region, and the watershed area. Direct THg deposition was determined by:

Hg Wet Deposition Rate ($\mu g \cdot m^{-2} \cdot y^{-1}$) = C_{Hg} x I / 1000

Where C_{Hg} = concentration of Hg in precipitation ($\mu g \cdot m^{-3}$) and I = precipitation intensity ($mm \cdot y^{-1}$). The mercury wet deposition rate around Oxford, MS is 17.7 $\mu g \cdot m^{-2} \cdot y^{-1}$. NADP estimated wet deposition rate of mercury in Northern Mississippi ranged from 12-14 $\mu g \cdot m^{-2} \cdot y^{-1}$. Our data is similar to the modeled data. The THg loadings to the Yocona River Watershed (area = 1949 km^2), through wet deposition, was 35 kg and the direct THg deposition to Enid Lake (area = 85km^2) was 1.52 kg. This data is being used in mass-balance model study. The vast majority of the Hg in the rainwater was inorganic Hg^{+2}. MeHg averaged <3% of the total-Hg.

4.4.3 Dry deposition rates of surrogate surface measurements

The average amount of mercury in the blanks was 0.11 ng. The results for the DMA analysis are highlighted in Table 18. The average dry deposition rate of GOM (4.35 ± 1.36 $\mu g \cdot m^{-2} \cdot y^{-1}$) is similar to those reported by Lyman, et al (2007, 2010), indicating the members could be accurately analyzed directly by combustion-AAS. Future work will include deployment of surrogate surfaces at Grenada Lake, Enid Lake and Sardis Lake, a gradient of GOM deposition rates (Grenada>Enid~=Sardis) are expected based on the geological distances between a CFPP and these lakes.

Table 18. Amount of mercury captured by surrogate surfaces deployed for about two weeks and the associated deposition rate

Deploy Date	Recovered Hg (ng)	Deposition rate ($\mu g \cdot m^{-2} \cdot y^{-1}$)	Average Deposition rate ($\mu g \cdot m^{-2} \cdot y^{-1}$)
March 6th-20th 2012	1.13	5.87	4.35 ± 1.36
	0.80	3.94	
	0.68	3.24	

4.4.4 Dry deposition rates using inferential method

Zhang et al (2012) estimated the annual average V_d (cm/s) of three airborne mercury species as follow: GOM: 0.5 to 2.0; PBM: 0.08 to 0.22; GEM: 0.024 to 0.081. Based on these estimated V_d for three mercury species, we estimated dry deposition fluxes in Table 19.

Table 19. Dry deposition rates in Oxford, MS estimated by using inferential method

Species	Mean concentration in air ($pg \cdot m^{-3}$)	V_d ($cm \cdot s^{-1}$)	F_d ($\mu g \cdot m^{-2} \cdot y^{-1}$)
GOM	4.36	0.5 - 2.0	0.69 - 2.75
PBM	4.45	0.08 - 0.22	0.112 - 0.308
GEM	1580	0.024 - 0.081	11.9 - 40.3

The estimated annual dry deposition of GOM + PBM ranged from 0.8 – 3.0 $\mu g \cdot m^{-2} \cdot y^{-1}$. GOM contributed 0.69 – 2.75 $\mu g \cdot m^{-2} \cdot y^{-1}$ to these fluxes, whereas PBM was relatively small, contributed only 0.112 – 0.308 $\mu g \cdot m^{-2} \cdot y^{-1}$. The estimated dry deposition rate of GOM calculated based on inferential method is comparable smaller than direct measurement, probably due to lower mean concentration of GOM used in calculation. The estimated annual GEM dry deposition was in the range of 11.9 – 40.3 $\mu g \cdot m^{-2} \cdot y^{-1}$. Note that V_d value used for GEM are thought to be conservative. The very high dry deposition fluxes of GEM is certainly due to the 2-3 orders of

magnitude higher concentration of GEM compared to those of GOM + PBM. The dry deposition rate of all three mercury species was estimated in the range of 12.7 – 43.3 $\mu g \cdot m^{-2} \cdot y^{-1}$, and loading mercury to the Enid Lake via dry deposition was estimated in the range of 10.8 – 36.8 $kg \cdot y^{-1}$ (Figure 34).

The data garnered here is to be included in a mass balance Hg budget for Enid Lake (described earlier). Eventually all known inputs, outputs and storage terms will be used to determine the sources and cycling of Hg in the impaired waterbody. Inputs include atmospheric deposition (wet and dry depositions), tributaries, and groundwater. Outputs include efflux (volatilization) to the atmosphere, outflow via the lower Yocona River, biota removal, and sediment storage. Early work on the Hg Enid Lake budget provided estimates for the Yocona River and other stream, flows, and outflows (Brown Jr., 2013). Here, we provide wet and dry deposition estimation. Moreover, the methodology has been developed to measure Hg fluxes from Enid Lake surface (see Chapter 3).

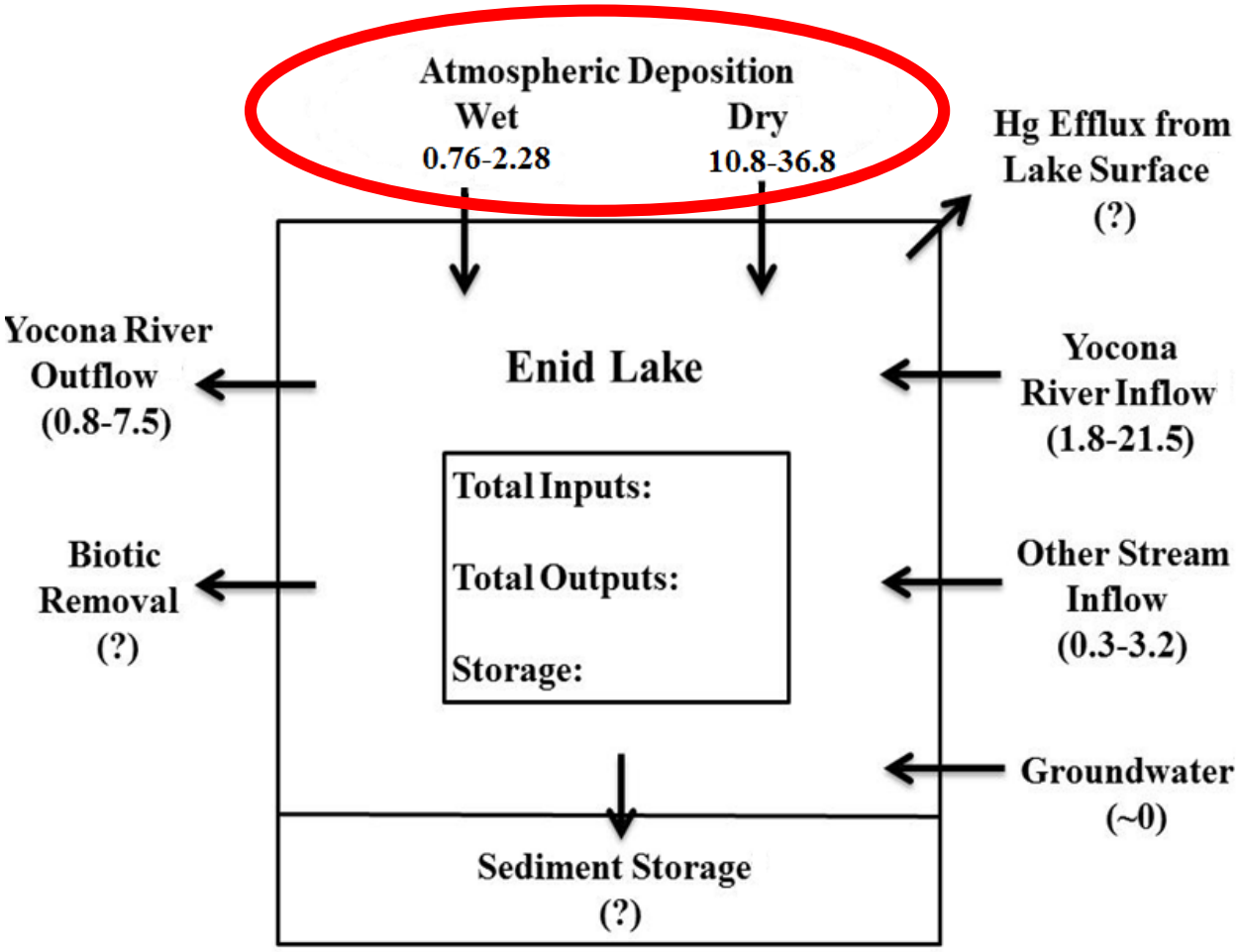

Figure 34. Estimated Hg mass balance (ky/yr) for Enid Lake with newly added wet and dry deposition

Dry deposition was estimated by using inferential method and annual mean concentrations of three mercury species in the year 2011-2012. The dry deposition to Enid Lake is in the range of 10.8 – 36.8 $kg \cdot y^{-1}$.

4.5 CONCLUSIONS AND FUTURE WORK

Wet deposition and dry deposition of mercury species to Enid Lake were investigated. Regarding wet deposition, concentrations of total-Hg was measured in rain collected for eight separate rainfall events in Oxford, MS. Wet deposition both directly and indirectly (through runoff, which has elevated Hg levels) is a significant source of Hg to Enid lakes. An estimated 35 kg of Hg is deposited annually via rainfall to the Yocona River (Enid) watersheds and 1.52 kg of Hg deposited directly to the Enid Lake. The range was obtained by using a factor of 0.5 (mean 1.52 kg/yr) to address dry and wet years. The annual range of wet deposition to Enid Lake is 0.76 – 2.28 kg/yr. The wet and dry deposition amounts are significant. Figure 34 depicts a preliminary Hg mass balance for Enid Lake. It can be seen that inputs from wet and dry deposition are ~11.5-39.0 kg/yr, whereas the total for other inputs is ~2.1-24.7 kg/yr. Thus from this perspective atmospheric deposition is likely the largest single source to the lake.

For dry deposition, despite the potential large uncertainties in concentration measurements and calculated deposition velocities, the estimated dry deposition of GOM agrees with limited surrogate surface dry deposition measurements. Mercury captured on a PES surrogate surfaces was well-above unexposed background membranes. The membranes can be accurately analyzed directly by combustion-AAS. This increases our confidence on estimate of dry deposition. Results from dry deposition modeling suggest that GEM contributes at least 5 times more than GOM+PBM to total dry deposition and dry deposition also contributes more than wet deposition to Enid Lake (5-10 times).

Zhang et al (2012) plotted Hg wet deposition rate and dry deposition rate in Eastern and Central North America (Figure 35). In the current study, the annual wet deposition rate around Oxford was estimated at ~18 $\mu g \cdot m^{-2}$, which is slightly higher than that predicted in Zhang's

model. Our data is similar to that shown for central Florida. For dry deposition (GOM+PBM), we estimate 0.8-3.0 $\mu g \cdot m^{-2}$ for north Mississippi, similar to values reported in the Northeast and Gulf Coast areas (Figure 35). Our estimated annual dry deposition of GEM ranged from 11.9-40.3 $\mu g \cdot m^{-2}$, higher than other sites. This difference may stem from our use of a general deposition velocity value obtained from the literature since specialized micrometeorological equipment is needed for site-specific measurements.

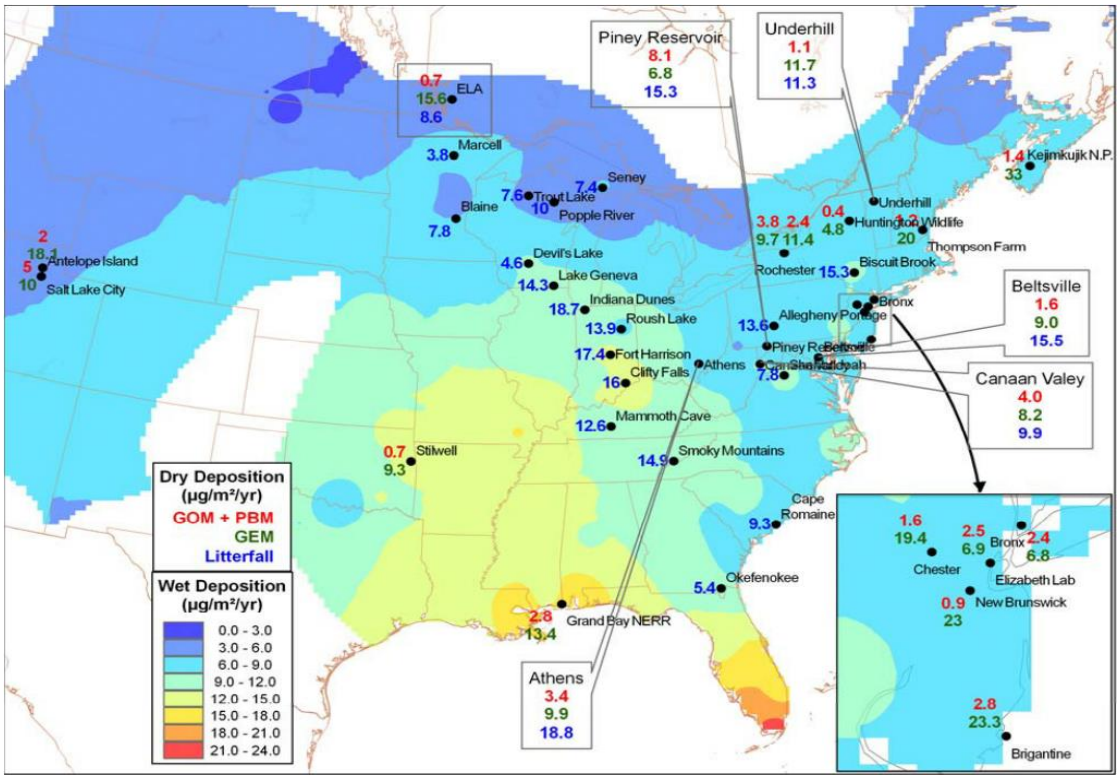

Figure 35. Comparisons of estimated dry deposition of GOM+PBM and GEM from 2008 and 2009 speciated concentrations with litterfall deposition collected during 2007-2009 and with wet deposition monitored during 2007-2009. (Zhang et al. 2012)

Our results suggest that wet and dry deposition is a major source of mercury to lakes in the region. Moreover, because the mercury that is being deposited is primarily in the oxidized form it can readily be converted to methylmercury in the aquatic environment. The more mercury that is deposited, the more that is converted to methylmercury, and the more that is

bioaccumulated and biomagnified in the ecosystem. The consequence is that atmospheric deposition is resulting in adverse effects on both wildlife and humans who consume contaminated fish. Brown (2013) measured total mercury levels in three species of fish from Enid Lake. A total of 46 fish were collected from Enid Lake, which included 16 white crappie (WC), 15 largemouth bass (LMB), and 15 channel catfish (CC). The average Hg concentrations in LMB were 289 ng/g and ranged between 108 ng/g to 954 ng/g. CC and WC concentrations averaged 147 ng/g and 214 ng/g with a range of 69 ng/g to 272 ng/g and 120 ng/g to 285 ng/g, respectively. A risk assessment was also calculated and found that LMB from Grenada had an adult Hazard Index (HI) >1 by seven different risk calculations, indicating a significant and increased potential for toxicity if the fish are consumed. Similarly, all fish species from all three lakes yielded HI>1 for children.

Future work should focus on deploying surrogate surfaces in different lakes including Grenada, Enid, and Sardis Lakes. Also Hg fluxes over Enid Lake surface (see Chapter 3), biotic removal, groundwater contribution, and storage in bed sediments should also be determined.

4.6 ACKNOWLEDGMENTS

The author thanks Theodore Watson for his contribution in the determination of GOM from surrogate surfaces. The author also greatly appreciates Garry Brown for helpful discussion. Instrumentation used in this study was obtained by Dr. Cizdziel on a USEPA grant (#CD-95450510-0).

4.7 LIST OF REFERENCES

Driscoll, T. C., Mason, P. R., Chan, H., Jacob, J. D., Pirrone, N., **2013**. Mercury as a global pollutant: sources, pathways, and effects. *Environ. Sci. Technol.* 47(10), 4967-4983.

Lindberg, S., Bullock, R., Ebinghaus, R., Engstrom, D., Feng, X., Fitzgerald, W., Pirrone, N., Prestbo, E., and Seigneur, C., **2007**. A Synthesis of Progress and Uncertainties in Attributing the Sources of Mercury in Deposition. *AMBIO: J. Human Environ*. 36, 19–33.

Lyman, N. Seth., et al. **2010**. A Passive Sampler for Ambient Gaseous Oxidized Mercury Concentrations. *Atmos. Environ*. 44, 246-252.

Miller, E. K., Vanarsdale, A., Keeler, G. J., Chalmers, A., Poissant, L., Kamman, N.C., Brulotte, R., **2005**. Estimation and mapping of wet and dry mercury deposition across northeastern North America. *Ecotoxicology*. 14, 53–70.

Pan, L., Carmichael, G. R., Adhikary, B., Tang, Y., Streets, D., Woo, J. H., Frieli, H. R., Radke, L. F., **2008**. A regional analysis of the fate and transport of mercury in East Asia and an assessment of major uncertainties. Atmos. Environ. 42, 1144-1159.

Selin, N. E., Jacob, D. J., Park, R. J., Yantosca, R. M., Strode, S., Jaegle, L., Jaffe, D., **2007**. Chemical cycling and deposition of atmospheric mercury: global constraints from observations. *J. Geophys. Res*. 112, D02308. doi:10.1029/2006JD007450.

Strode, S. A., Jaegle, L., Selin, N. E., Jacob, D. J., Park, R. J., Yantosca, R. M., Mason, R. P., Slemr, F., **2007**. Air–sea exchange in the global mercury cycle. *Global Biogeo-chemical Cycles* 21 (GB1017). doi:10.1029/2006GB002766.

USEPA. **2002**. Method 1631, Revision E, Mercury in water by oxidation, purge and trap, and cold vapor atomic fluorescence spectrometry. United States Environmental Protection Agency.

Zhang, L., Blanchard, P., Johnson, D., Dastoor, A., Ryzhkov, A., Lin, C.-J., Vijayaraghavan, K., Gay, D., Holsen, T. M., Huang, J., Graydon, J. A., St. Louis, V. L., Castro, M. S., Miller, E. K.,

Prestbo, M. Eric., Gay, A. D., **2009**. Wet deposition of mercury in the U.S. and Canada, 1996-2005: Results and analysis of the NADP mercury deposition network (MDN). *Atmos. Environ*. 43, 4223-4233.

Risch, M. R., Gay, D., Fowler, K., Keeler, G., Blanchard, P., Backus, S., Barres, J., and Dvonch, T., **2012b**. Spatial patterns and statistical trends in mercury concentrations, precipitation, and mercury wet deposition in the North American Great Lakes region, 2002–2008. *Environ. Pollut.* 161, 261–271.

Zhang, L., Blanchard, P., Gay, A. D., Prestbo, M. E., Risch, R. M., Johnson, D., Narayan, J., Zsolway, R., Holsen, M. T., Miller, K. E., Castro, S. M., Graydon, A. J., St. Louis, L. V., Dalziel, J., **2012**. Estimation of speciated and total mercury dry deposition at monitoring locations in Eastern and Central North America. *Atmos. Chem. Phsy. Discuss*. 12, 2783-2815.

Zhang, Y., Jaegle, L ., Donkelaar, A., Martin, R. V., Holmes, C. D., Amos, H. M., Wang, Q., Talbot, R., Artz, R., Brooks, S., Luke, W., Holsen, T. M., Felton, D., Miller, E. K., Perry, K. D., Schmeltz, D., Steffen, A., Tordon, R., Weiss-Penzias, P., Zsolway, R., **2012**. Nested-grid simulation of mercury over North America. *Atmos. Chem. Phys.* 12, 6095–6111. doi:10.5194/acp12-6095-2012

CHAPTER FIVE

5. CONCENTRATIONS OF GASEOUS ELEMENTAL MERCURY IN AMBIENT AIR WITHIN AN ACADEMIC CHEMISTRY BUILDING

Cizdziel J., Jiang Y. (2011) “Concentrations of Gaseous Elemental Mercury in Ambient Air within an Academic Chemistry Building”, Bull. Environmental Contamination and Toxicology, 86:419–422.

5.1 ABSTRACT

Gaseous elemental mercury (GEM) concentrations were determined within an academic chemistry building by cold vapor atomic fluorescence spectrometry. Concentrations varied depending on the room activity, with night time and weekend levels the lowest and most stable (typically between 10 and 20 ng/m^3), and daytime weekday levels the highest (averaging about 3 to 5 times higher). Laboratory air exhibited daytime concentration spikes as high as 1600 ng/m^3. Office levels were similar to weekend laboratory concentrations, suggesting a general building-wide mercury background. However, concentration spikes suggest GEM levels may be exacerbated by foot traffic which may cause motion-induced wafting from higher concentration areas. Based on current regulations the GEM levels do not present a health hazard.

Keywords: mercury, gaseous elemental mercury, cold vapor, atomic fluorescence spectrometry, indoor air

5.2 INTRODUCTION

For decades elemental mercury has been widely used in academic chemistry laboratories for a variety of purposes, most notably barometers, thermometers, electrical switches, and atomic line lamps. The element is the only metal that is a liquid at standard conditions (0°C, 100 kPa). It is also dense (13.55 g/ml at 20°C) and has a relatively high vapor pressure (0.17 Pa at 20°C) (CRC. 2007). Other useful properties include a capability to conduct electricity and to form an amalgam with gold.

It is well known that mercury is a heavy metal pollutant that can damage the central nervous system, affecting the brain and causing developmental disorders in children. Exposure to elemental mercury vapor occurs primarily by direct transport across the lungs where it can enter the blood stream and be distributed throughout the body, including the brain; the respiratory and toxicological consequences of mercury vapor are detailed elsewhere (Lein et al. 1983). Possible symptoms from a large acute exposure include nausea, vomiting, abdominal pain, kidney damage, and death. Potential symptoms from a chronic exposure include inflammation of the mouth and gums, kidney damage, muscle tremors, spasms of the extremities, personality changes, depression, irritability, and nervousness (OSHA 1991). Due to its high vapor pressure, even small amounts of metallic mercury released into unventilated areas can raise air concentrations to harmful levels. The current environmental and occupational health standards (risk assessment and action levels) for mercury vapor are summarized in Table 20.

Table 20. Environmental and occupational health standards for mercury vapor

Agency	Concentration (ng/m^3)
OSHA ceiling exposure limit[a]	100,000
NIOSH recommended exposure limit[b]	50,000
ACGIH threshold limit value[b]	25,000
EPA reference concentration[c]	300
ATSDR minimal risk level[d]	200

[a]The concentration can not exceed this value at any time. [b]Time-weighted average for an 8 hour day. [c]Used primarily as a screening tool; adverse health effects do not necessarily result from exposure at or near these levels. [d]Estimate of daily exposure which is to be without appreciable risk of adverse heath effects. Occupational Safety and Health Administration (OSHA), National Institute for Occupational Safety and Health (NIOSH); American Conference of Governmental Industrial Hygienists (ACGIH); Agency for Toxic Substances and Disease Registry (ATSDR); U.S. Environmental Protection Agency (EPA).

Whereas many colleges and universities are moving away from using the toxic element, undoubtedly the liquid metal has been spilled inside laboratories over the years, especially in general chemistry laboratories where thermometers are routinely broken. As a liquid, the metal will pool in low areas and may be hidden or difficult to access (e.g., in drains, underneath tiles, floor cracks, etc.), thus some of the element may be left behind even after "cleanup" procedures are used. Also, old latex paint can contain high levels of mercury and expel gaseous mercury (Beursterian et al. 1991).

Gaseous elemental mercury as an indoor air pollutant has been the subject of a number of studies (e.g., Smart. 1986; Carpi and Chen et al. 2001; Riley et al. 2001; Liu et al. 2009). After fish consumption indoor air may be the next biggest source of mercury exposure (Carpi and Chen et al. 2001). Occupations which handle mercury (e.g., dental and gold trade shops that prepare or heat amalgams containing mercury) have much higher ambient air mercury concentrations than residential houses (Stone et al. 2007; Bastos et al. 2004).

In this study, we measured gaseous elemental mercury (GEM) in several laboratories and an office located in the Department of Chemistry and Biochemistry at the University of Mississippi. The building was first occupied in 1977 and has recently undergone an extensive renovation, including its ventilation system. The purpose of the study was to monitor GEM in the ambient air within the building under various use scenarios. Levels were compared to occupational safety permissible and recommended exposure limits.

5.3 MATERIAL AND METHODS

A mercury vapor analyzer based on cold vapor atomic fluorescence spectrometry (CVAFS) was used to measure GEM (Model 2537B; Tekran Inc., Toronto, Canada). A flow diagram for the system is shown in Figure 36. Air was sampled through a Teflon inlet tube which was placed about 1.5 m above the ground, at about the breathing zone of a typical standing adult. The automated system employs dual gold traps which effectively remove (capture) elemental mercury vapor from ambient air pulled through the cartridges. The instrument cycles such that while one gold cartridge is capturing (pre-concentrating) mercury, the other is rapidly heated, desorbing its captured mercury. The released mercury is then carried by a flow of ultra-high purity argon into a fluorescence cell for measurement. Inside the cell, atomic mercury is excited by 253.7 nm photons emitted from a sealed mercury lamp. As the excited mercury atoms relax back to the ground state, light of the same wavelength is re-emitted, some of which is detected by a photomultiplier tube situated at 90° to the excitation source. The combination of a low background and the detector's high amplification yields one of the most sensitive analytical techniques for mercury. The automated dual trap system allows GEM readings every five minutes and unattended operation for extended periods (weeks). Additional details of the instrument can be obtained from the manufacturer.

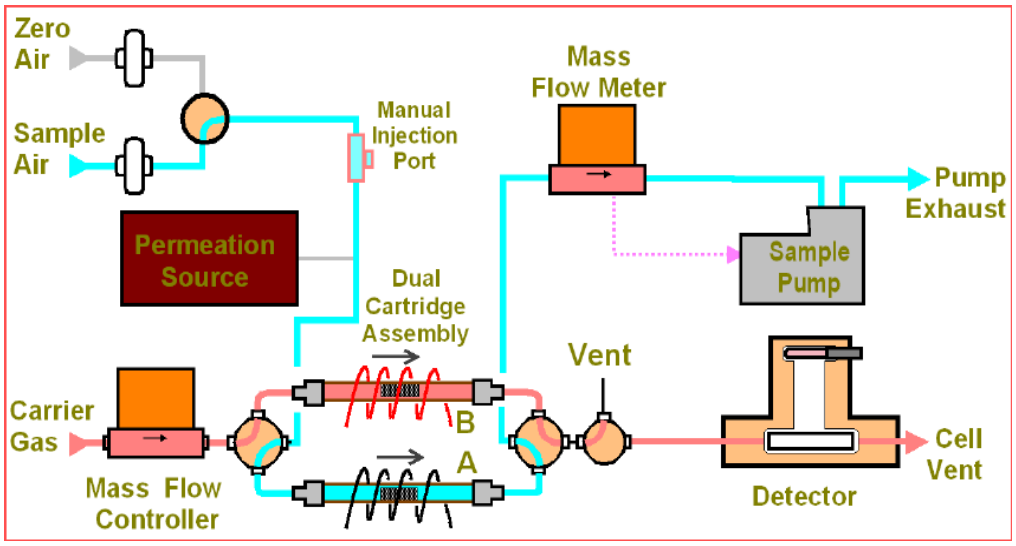

Figure 36. Flow diagram for the 2537 mercury analyzer

In this study, the instrument was calibrated nightly using an internal permeation source. There was good agreement between calibration peak areas for the two cartridges; the average relative difference was 0.6%. Instrument sensitivity was high, averaging 2.3 millivolts per picogram of Hg. Blank levels (measured daily using a canister that scrubs mercury from the air) were negligible, averaging less than 3% of the minimum GEM levels found for that day. As noted earlier, the instrument uses two gold cartridges which yield alternating data points. This provides the advantage of comparing the average of the two concentration values over long periods of stable concentration to check for trap bias that may be caused by passivation or leaks. This is important because some laboratories may have very high levels of acid and/or organic vapors present that may passivate the pure-gold cartridges over an extended period of time, depending on the concentrations levels. For this experiment, gold cartridge passivation was not observed (A/B cartridge bias was less than 1%, n=35; data from a stable overnight period). Moreover, we used a relatively small sample volume (7.5 liters) and a short monitoring time period (5 min). The cartridges are also heated slightly during collection to minimize adsorption of organic molecules.

A detection limit of 0.1 ng/m^3 was estimated by repeated analysis of a low level standard and using the volume of air in a typical analysis.

5.4 RESULTS AND DICUSSION

The concentrations of GEM varied with the room type (i.e., purpose) and usage (i.e., occupancy). This is shown in a series of Figures (Figure 37, 38). Each data point in the plots corresponds to a 5 minute integrated average. Mercury concentrations ranged from 9 to 1600 ng/m^3 and averaged 66 ng/m^3. This is comparable to an indoor air study that found an average of 69 ng/m^3 of mercury at 12 different sites chosen to represent a cross section of building types (Carpi and Chen. 2001).

In this study, despite numerous potential sources of mercury with the building, the levels (in all cases) were below the permissible and recommended exposure limits defined by OSHA, NIOSH and ACGIH (see introduction). Also, given the short duration of the concentration spikes, the levels would not exceed the ATSDR minimum risk level even when focusing only on daytime hours. This may be partly due to continuous air exchange (turnover) within the building from operation of a large number of fume hoods; the building's ventilation system was recently overhauled from re-use to single pass air.

The highest concentrations were found for a common area that is located between four laboratories (Figure 37). It is noteworthy that this area is smaller than the labs and does not have a fume hood. Spikes in the concentration of GEM, the highest of which reached 1600 ng/m^3, corresponded to activity in the adjacent room (e.g., morning and afternoon lab sessions); doors are kept open between these rooms. There was no laboratory session on Friday and the concentration returned to an apparent background level of < 50 ng/m^3. It is suspected that disturbances to air flow patterns (turbulence) in the room during class sessions from foot traffic redistributes mercury vapor from areas or pockets containing relatively higher levels, presumably in proximity to mercury sources, to the larger room volume. Scuffing of dust from the floor by

foot traffic should not be an issue as it is filtered out prior to analysis. Humans can also be sources of mercury vapor, especially those with tooth fillings containing mercury amalgams. Cosmetics can also contain mercury (MMWR 1996). However, if humans were the only source of mercury, one might expect the room to gradually increase as mercury is exhaled or effluxed rather than exhibit large and inconsistent spikes in concentration with time.

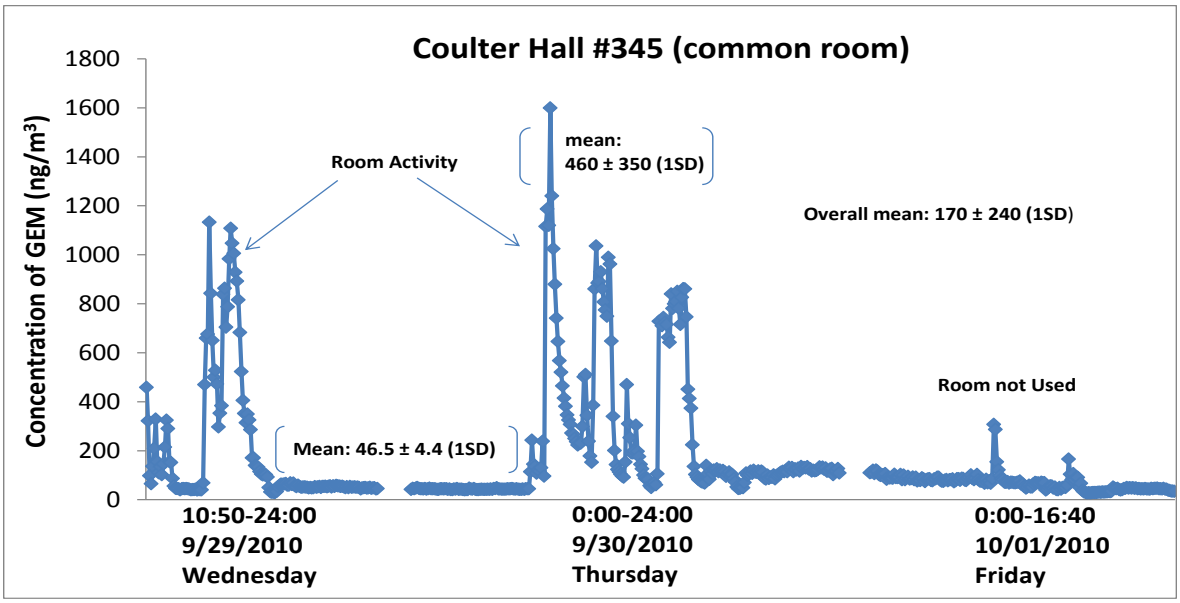

Figure 37. Temporal fluctuations in gaseous elemental mercury in a common room between general chemistry laboratories. Each data point corresponds to a 5 minute integrated concentration. The gaps in the baseline are inserted to delineate individual days. SD = standard deviation

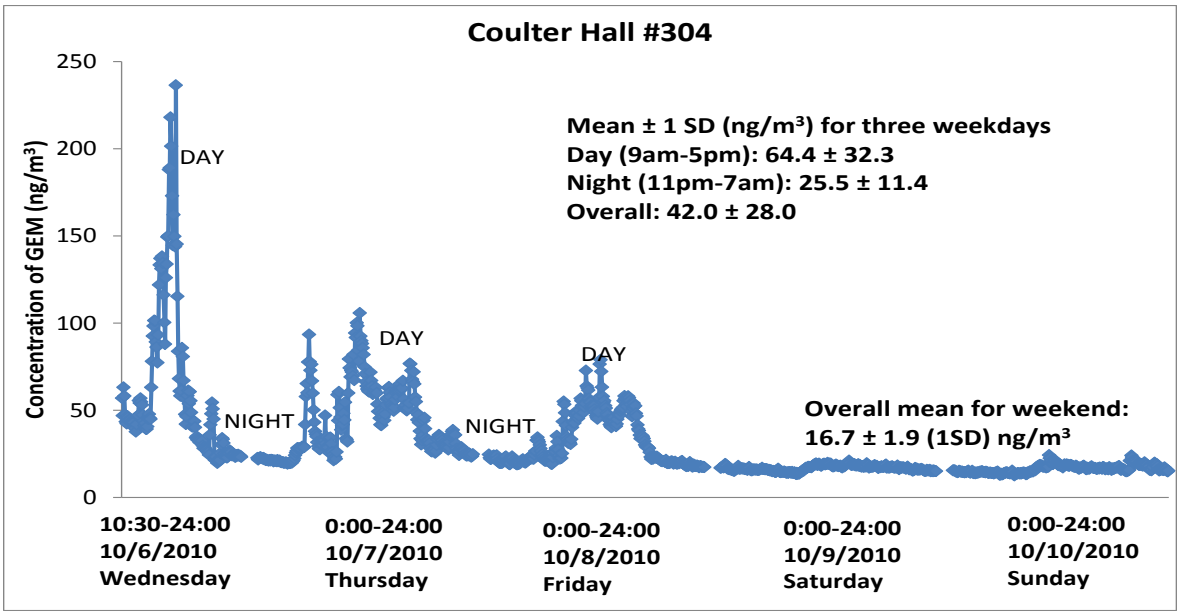

Figure 38. Gaseous elemental mercury in a laboratory over the course of five days. Note the relatively low and stable concentrations during the weekend. The gaps in the baseline are inserted to delineate individual days. SD = standard deviation

Figure 38 corresponds to an instrumental laboratory. Again, there is a clear difference between concentrations during the day, when the room is being used, and during the night, when activity ceases. The figure also shows that the weekend achieves a steady background state (16.7 ± 1.9 ng/m^3), significantly below the work-week daytime concentrations (64 ± 32 ng/m^3).

GEM in a faculty office adjacent to the general chemistry laboratories was similar to levels found in the laboratories weekends (date not shown). As noted, the building's ventilation system was recently overhauled. It plausible that there is a consistent ambient background level similar throughout the building, which can be exacerbated in areas by wafting from additional mercury sources resulting in the observed concentration spikes.

In summary, this study shows that the concentration of mercury in ambient air within a chemistry building fluctuates during the day depending on room activity and usage. Whereas

GEM levels are significantly higher than outdoor air, the concentrations did not exceed the permissible and recommended exposure limits.

5.5 ACKNOWLEDGMENTS

We thank E. Prestbo and L. Hawkins (Tekran Inc.) for advice on using the 2537 instrument and for discussion of ambient mercury measurements. The equipment was purchased through a grant from the U.S. Environmental Protection Agency (#CD-95450510-0).

5.6 LIST OF REFERENCES

Bastos, W. R., Fonseca, M. F., Pinto, F. N., Rebelo, M. F., Santos, S. S., Silveira, E. G, Torres, J. P. M., Malm, O., Pfeiffer, W.C., **2004**. Mercury persistence in indoor environments in the Amazon Region, Brazil. *Environ. Res*. 96, 235–238.

Beusterien, K. M., Etze1, R. A., Agocs, M. M., Egeland, G. M., Socie, E. M., Rouse, M. A., Mortensen, B. K., **1991**. Indoor Air Mercury Concentrations Following Application of Interior Latex Paint. Arch. Environ. *Contain. Toxicol*. 21, 62-64.

Carpi, A, Chen, Y. F., **2001**. Gaseous elemental mercury as an indoor air pollutant. *Environ Sci Tech.* 35, 4170-4173.

CRC. **2007**. Handbook of Chemistry and Physics, 2009-2010, 87th ed. CRC Press: Boca Raton, FL. ISBN 978-1-4200-9084-0.

Lien, D. C., Todoruk, D. N., Rajani, H. R., Cook, D. A., Herbert, F. A., **1983**. Accidental inhalation of mercury vapour: respiratory and toxicologic consequences. *Can Med Assoc J.* 129(6), 591–595.

Liu, Y., Zhan, Z., Dua, F., Kong, S., Liu, Y., **2009**. Indoor air concentrations of mercury species in incineration plants for municipal solid waste (MSW) and hospital waste (HW). *Chemosphere.* 75, 266–271.

MMWR. **1996**. Update: mercury poisoning associated with beauty cream-Arizona, California, New Mexico, and Texas. MMWR Morb Mortal Wkly Rep, 45:633-5.

OSHA. **1991**. Mercury vapors workplace atmospheres. United States Occupational Safety and Health Administration, T-ID140-FV-01-9106-M, p.1-13.

Riley, D. M., Newby, A., Leal-Almeraz, T. O., Thomas, V. M., **2001**. Assessing elemental mercury vapor exposures from cultural and religious practices. *Environ. Health Perspect.* 109, 779-784.

Smart, E. R., **1986**. Mercury vapor levels in a domestic environment following breakage of a clinical thermometer. *Sci. Total Environ*. 57,99-103.

Stone, M. E., Cohen, M. E., Debban, B. A., **2007**. Mercury vapor levels in exhaust air from dental vacuum systems. *Dent. Mater*. 23:527–533.

VITA

Yi Jiang

420 Saddle Creek Dr., Oxford, MS 38655 || 662-202-6323 || jiangyi2010@hotmail.com

Summary

An enthusiastic self-starter with strong leadership and communications skills. Proven academic and curricular achievements. Possesses the analytical and soft skills required to achieve objectives in team environment.

Education

Ph.D. Analytical/Environmental Chemistry — University of Mississippi
Expected Graduation Date: August, 2014
Dissertation: Atmospheric Mercury Species in Northern Mississippi: Concentrations, Sources, Temporal Patterns, and Soil-Air Exchange

BS Pharmaceutical Engineering, 2009 — Beijing Institute of Technology
Thesis: Dynamics between Proteins and Water-soluble Fullerene or Single Wall Carbon Nanotubes

Professional Experience

Research Assistant — January 2010 to Current
The University of Mississippi — Oxford, MS

Major Accomplishments:

- Initiated a series of Hg-related projects. Implemented the first atmospheric Hg speciation monitoring site in Northern Mississippi, which enhanced the understanding of Hg transport and airborne cycling.
- Investigated the trapping efficiency of gold coated nano-particles by using ICP-MS and Tekran 2600.
- Examined the characteristics of Hg gas exchange over background soils in the mid-south region, facilitating the modelling and scale-up needs.
- Investigated wet and dry deposition of mercury that contributed to Hg mass balance in the region, familiar with EPA method 1640.

- Performed instrument maintenance and troubleshooting for a wide range of Hg instrumentation, prepared results and reports for supervisor and quality control inspections.
- Supervised and mentored 1 graduate student and 3 undergraduate students, advised them on academic, curricula, and career issues.

Undergraduate Research Assistant January 2009 to June 2009

China Academic of Science Beijing, China

Major Accomplishments:

- Analyzed the toxicology of water-soluble fullerene or single wall carbon nanotubes, which improved the awareness about their safety and environmental impact by using PCR.
- Investigated the dynamics between several proteins and water-soluble fullerene or single wall carbon nanotubes, promoted the potential uses in the fields of biomaterials, drug delivery, and nanotoxicology.
- Organized and planned the daily activities of the laboratory setting, managed the chemicals placement and waste disposal.

Awards & Honors

Celebration of Achievement Metal (2014)
University of Mississippi – awarded to excellent performance on research and curriculum study.

Dissertation Fellowship (2014)
University of Mississippi – a select few graduate students with high-impact dissertations.

Graduate Student Council Research Grant - $1000 (2013)
University of Mississippi – awarded to examine mercury flux rates and associated mechanisms for a variety of important soils and water surfaces.

Best Undergraduate Paper Award (2009)
Beijing Institute of Technology – awarded to excellent writing on thesis entitled "Dynamics between Proteins and Water-soluble Fullerene or Single Wall Carbon Nanotubes".

Second Prize in Undergraduate Mathematical contests in Modeling in Beijing District (2008)
China Ministry of Education – awarded to competitive performance on analyzing problems, proposing possible solutions, and programming.

Teaching Experience

Teaching Assistant in General Chemistry I & II – University of Mississippi (2010-2013)
Major Accomplishments: Taught freshman chemistry laboratory courses. The courses introduce fundamental concepts, theories, and laws of chemistry. Student learned chemistry the hands-on way with lab experiments.

Teaching Assistant in Quantitative Analysis – University of Mississippi (2009)
Major Accomplishments: Co-drafted (w/Samantha Reilly) the laboratory manual, planned, evaluated, and explained lab procedures, course content, and course materials.

Publications

- Lu D., Cizdziel J., Jiang Y., White L., Reddy R. (2014) "Numerical Simulation of Atmospheric mercury in Northern Mississippi", *Air Quality, Atmosphere and Health*. (online 28th March 2014)
- Jiang Y., Cizdziel J., Lu D. (2013) "Temporal patterns of atmospheric mercury species in Northern Mississippi during 2011-2012: influence of sudden population swings", *Chemosphere*, 93(9): 1694-1700.
- Cizdziel J., Jiang Y. (2011) "Concentrations of Gaseous Elemental Mercury in Ambient Air within an Academic Chemistry Building", *Bull. Environmental Contamination and Toxicology*, 86:419–422.
- Jiang Y., Cizdziel J. (In preparation) "Air-soil exchange of mercury from background soils in Northern Mississippi".

Presentations & Posters

Cizdziel J., Jiang Y., Nallamothu D., Brown G. "Distribution and cycling of mercury species in Wetlands and reservoirs in North Mississippi" 2014 Mississippi Water Resources Conference, Jackson, Mississippi, 1th-2th April 2014.

Cizdziel J., Jiang Y. "Mercury gas exchange over bare soils and other landforms in Mississippi" Mississippi Academy of Sciences 78th annual meeting, Hattiesburg, Mississippi, 6th-7th March 2014.

Jiang Y., Cizdziel J. "Atmospheric mercury species (GEM, GOM, PBM) in North Mississippi during 2011-2012: Influence of sudden population swings" 11th International Conference on Mercury as a Global Pollutant, Edinburgh, Scotland, 28th July – 2nd August 2013.

Jiang Y., Cizdziel J. "Atmospheric mercury species in Northern Mississippi during 2011-2012" National Center for Natural Production Research 2012 Internal Poster Session, Oxford, Mississippi, 8th November 2012.

Cizdziel J., Jiang Y., Brown G., Chakravarty P. "Mercury in Northern Mississippi, USA: atmospheric speciation, historical deposition, and concentrations of methylmercury in natural waters" 10th International Conference on Mercury as a Global Pollutant, Halifax, Nova Scotia, Canada, 24th-29th July 2011.

Jiang Y., Cizdziel J. "Atmospheric speciation of mercury in Northern Mississippi: Preliminary Results" University of Mississippi Graduate Student Council Research Day, Oxford, Mississippi 8th April, 2011.

Other Activities

Analytical Skills: CVAFS, ICP-MS, GC-MS, HPLC

Language: Mandarin/English

Other: Outdoor enthusiast, Fishing, Sports lover, Pet fan, 2 years self-study of Java, Python, JavaScript, HTML, CSS.